AL/OE-TR-1997-0130

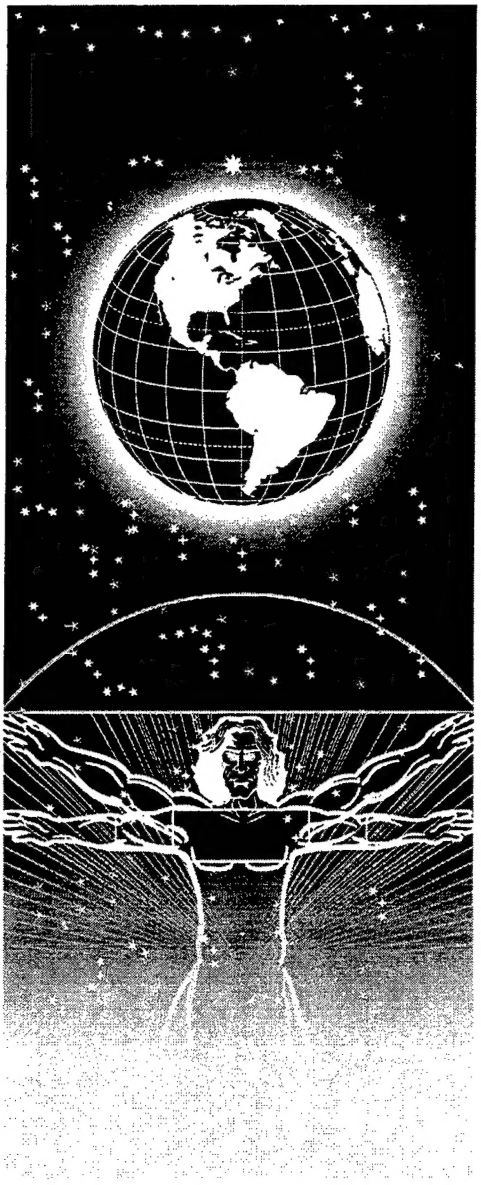

UNITED STATES AIR FORCE ARMSTRONG LABORATORY

PHYSIOLOGICALLY BASED PHARMACODYNAMIC MODELING OF CHEMICALLY INDUCED OXIDATIVE STRESS

J.Z. Byczkowski
C.D. Flemming

MANTECHGEO-CENTERS JOINT VENTURE
P.O. BOX 31009
DAYTON, OH 45437

M.A. Curran
C.R. Miller
W.J. Schmidt
A.P. Moghaddam
S.R. Channel

TOXICOLOGY DIVISION
OCCUPATIONAL & ENVIRONMENTAL HEALTH DIRECTORATE
2856 G STREET, BLDG 79
WRIGHT-PATTERSON AFB, OH 45433-7400

September 1997

Occupational and Environmental Health Directorate
Toxicology Division
2856 G Street
Wright-Patterson AFB OH 45433-7400

NOTICES

When US Government drawings, specifications or other data are used for any purpose other than a definitely related Government procurement operation, the Government thereby incurs no responsibility nor any obligation whatsoever, and the fact that the Government may have formulated, furnished, or in any way supplied the said drawings, specifications, or other data is not to be regarded by implication or otherwise, as in any manner licensing the holder or any other person or corporation, or conveying any rights or permission to manufacture, use, or sell any patented invention that may in any way be related thereto.

Please do not request copies of this report from the Air Force Research Laboratory. Additional copies may be purchased from:

National Technical Information Service
5285 Port Royal Road
Springfield, Virginia 22161

Federal Government agencies and their contractors registered with the Defense Technical Information Center should direct requests for copies of this report to:

Defense Technical Information Service
8725 John J. Kingman Rd., Ste 0944
Ft. Belvoir, Virginia 22060-6218

DISCLAIMER

This Technical Report is published as received and has not
been edited by the Technical Editing Staff of the Air Force Armstrong Laboratory.

TECHNICAL REVIEW AND APPROVAL

AL/OE-TR-1997-0145

The animal use described in this study was conducted in accordance with the principles stated in the "Guide for the Care and Use of Laboratory Animals", National Research Council, 1996, and the Animal Welfare Act of 1966, as amended.

This report has been reviewed by the Office of Public Affairs (PA) and is releasable to the National Technical Information Service (NTIS). At NTIS, it will be available to the general public, including foreign nations.

This technical report has been reviewed and is approved for publication.

FOR THE DIRECTOR

STEPHEN R. CHANNEL, Maj, USAF, BSC
Branch Chief, Operational Toxicology Branch
Air Force Research Laboratory

REPORT DOCUMENTATION PAGE	Form Approved OMB No. 0704-0188

1. AGENCY USE ONLY *(Leave blank)*	2. REPORT DATE	3. REPORT TYPE AND DATES COVERED
	September 1997	Interim Report - December 1994-May 1997

4. TITLE AND SUBTITLE
Physiologically Based Pharmacodynamic Modeling of Chemically Induced Oxidative Stress

5. FUNDING NUMBERS
Contract F41624-96-C-9010
PE 61102F
PR 2312
TA 2312A2
WU 2312A202

6. AUTHOR(S)
J.Z. Byczkowski, C.D. Flemming, M.A. Curran, C.R. Miller, W. J. Schmidt, A.P. Moghaddam, and S.R. Channel

7. PERFORMING ORGANIZATION NAME(S) AND ADDRESS(ES)
ManTech Geo-Centers Joint Venture
P.O. Box 31009
Dayton, OH 45437-0009

8. PERFORMING ORGANIZATION REPORT NUMBER

9. SPONSORING/MONITORING AGENCY NAME(S) AND ADDRESS(ES)
Armstrong Laboratory, Occupational and Environmental Health Directorate
Toxicology Division, Human Systems Center
Air Force Materiel Command
Wright-Patterson AFB, OH 45433-7400

10. SPONSORING/MONITORING AGENCY REPORT NUMBER
AL/OE-TR-1997-0130

11. SUPPLEMENTARY NOTES

12a. DISTRIBUTION AVAILABILITY STATEMENT
Approved for public release; distribution is unlimited.

12b. DISTRIBUTION CODE

13. ABSTRACT *(Maximum 200 words)*

Health risk from chemicals depends on both the extent of exposure and a dose-response relationship, which is reflecting, in turn, the mode of action of chemicals. For quantitative modeling of the mode of action it is necessary to determine the exact chain of events of the chemical interaction with the biological system. To provide a tool potentially useful for risk characterization of pro-oxidant chemicals, a quantitative mathematical model (physiologically based pharmacodynamic or PBPD model) describing biological effects within the target organ was constructed in a way compatible with traditional pharmacokinetic (PBPK) models which describe the internal, local dose of a chemical. Based on the available literature and our own experimental data, the three basic modes of action of pro-oxidant chemicals were modeled and simulated *in silico*: i. lipid peroxidation (expressed by the formation of thiobarbituric acid reactive substance (TBARS) and the exhalation of ethane); ii. specific interaction of free radicals with homogenous cellular targets; and iii. random interaction of free radicals with multiple cellular targets. Based on the dose-response characteristic verified *in vitro*, a PBPD model of chemically initiated oxidative stress was developed and calibrated in B6C3F1 mice. The model consisted of three major modules. At first, a biologically based module for chemically induced lipid peroxidation was developed and calibrated *in vitro* using precision cut mouse liver slices. Next, the parameters describing the mechanism of action of pro-oxidant chemicals were applied to the physiologically based pharmacodynamic module describing chemically induced lipid peroxidation in mice *in vivo*.

14. SUBJECT TERMS	15. NUMBER OF PAGES
	110
	16. PRICE CODE

17. SECURITY CLASSIFICATION OF REPORT	18. SECURITY CLASSIFICATION OF THIS PAGE	19. SECURITY CLASSIFICATION OF ABSTRACT	20. LIMITATION OF ABSTRACT
UNCLASSIFIED	UNCLASSIFIED	UNCLASSIFIED	UL

THIS PAGE INTENTIONALLY LEFT BLANK.

PREFACE

This report describes the results of the development, experimental calibration and predictions of a physiologically based pharmacodynamic model simulating biological effects of oxidative stress induced by chemicals *in vitro* and *in vivo*. This is one of a series of technical reports and publications describing results of a collaborative effort conducted by ManTech Environmental Technology, Inc., Toxic Hazards Research Unit, located at Wright-Patterson Air Force Base, and by Occupational and Environmental Health Directorate, Toxicology Division, and aimed at pharmacodynamic description of biological effects.

The animals used in this study were handled in accordance with the principles stated in the *Guide for the Care and Use of Laboratory Animals* prepared by the Committee on Care and Use of Laboratory Animals of the Institute of Laboratory Animal Resources, National Research Council, National Academy Press 1996, and the Animal Welfare Act of 1966, as amended.

Research performed by ManTech Environmental Technology was conducted under Department of the Air Force Contract No. F41624-96-C-9010. Lt Col Terry A. Childress, Director of the Toxicology Division, served as Contract Technical Monitor.

TABLE OF CONTENTS

LIST OF TABLES AND FIGURES

TABLE **PAGE**

LIST OF FIGURES

FIGURE **PAGE**

ABBREVIATIONS

ACSL	Advanced continuous simulation language
AUC	Area under the concentration curve
BBDR	Biologically based dose response
BHT	Butylated hydroxytoluene
$BrCCl_3$	Bromotrichloromethane
CCl_4	Carbon tetrachloride
CYP	Cytochrome P450
DMNQ	2,3-dimethoxy-1,4-naphtoquinone
EPR	Electron paramagnetic resonance
GC	Gas chromatography
GSH	Glutathione
h	Hour
i.p.	Intraperitoneal
L	Liter
MAPK	Mitogen activated protein kinase
min	Minute
MTT	3(4,5-dimethylthiazol-2-yl)-2,5-diphenyltetrazolium bromide
$O_2^{\bullet-}$	Superoxide anion radical
PBN	N-tert-butyl-α-nitrone
PBPD	Physiologically based pharmacodynamics
PBPK	Physiologically based pharmacokinetics
PD	Pharmacodynamic
PK	Pharmacokinetic
ppm	Parts *per* million
SD	Standard deviation
SOD	Superoxide dismutase
TBARS	Thiobarbituric reactive substance
TBOOH	tert-Butyl hydroperoxide
TCE	Trichloroethylene

INTRODUCTION

CHEMICALLY INDUCED OXIDATIVE STRESS

Pro-oxidant chemicals are those compounds that may bring about a state of excess one-electron oxidations, either directly or indirectly *via* metabolic breakdown. Oxidative stress is a pathophysiological process in which the balance between pro-oxidants and antioxidants in tissue is shifted towards pro-oxidants (Figure 1; Byczkowski and Channel, 1996). Pro-oxidant chemicals may be provided by environmental, occupational, or therapeutic exposure to xenobiotics (Kehrer, 1993), may arise from dietary polyunsaturated fat (Gower, 1988; Finley and Otterburn, 1993; Haegele et al., 1994), or may be produced endogenously during physiological function of aerobic cells (Byczkowski and Gessner, 1988). From the primary pro-oxidant chemical, further metabolic reactions generate free radicals (defined as molecules or groups of atoms with one unpaired electron), and then, an avalanche-type process (e.g., lipid peroxidation) may release secondary and tertiary free radicals (Figure 2; for review see Roberfroid and Calderon, 1994). Additional factors, such as aging (Stadtman et al., 1993) or dietary deficiencies, may augment the oxidative stress status. Depletion of cellular antioxidants, as well as defective enzymatic scavenging systems, further increase oxidative stress and may enhance damage to cellular components. Oxidative stress can be reversed by natural and synthetic antioxidants (Williams, 1993; Papas, 1993; Pratt, 1993). Possible definitions and implications of oxidative stress and the basic literature on its measurement were reviewed in a recent publication by Byczkowski and Channel (1996).

Several chemicals can cause an oxidative stress directly (e.g., by generating free radicals during metabolism by cytochrome P450 (CYP) or during redox cycling; Kappus, 1986) or indirectly (e.g., by stimulating a respiratory burst in inflammatory cells; Kulkarni and Byczkowski, 1994a). In addition, several natural and synthetic peroxides (e.g., tumor-promoting organic hydroperoxides; Taffe et al., 1987; Timmins and Davies, 1993) can be cleaved by trace amounts of the transition metals, directly producing highly reactive free radicals without involvement of enzymatic metabolic pathways (Kulkarni and Byczkowski, 1994b). Chemically induced oxidative stress causes derangement of antioxidant mechanisms in tissues (Videla et al., 1990), may lead to lipid peroxidation (Comporti, 1985), inhibition of cellular enzymatic activities (e.g., CYP activity; Willis, 1980) and may result in cell injury (de Groot and Littauer, 1989). It has been demonstrated that lipid peroxidation may cause necrotic tissue damage rather than be an effect of necrosis (Biasi et al., 1995).

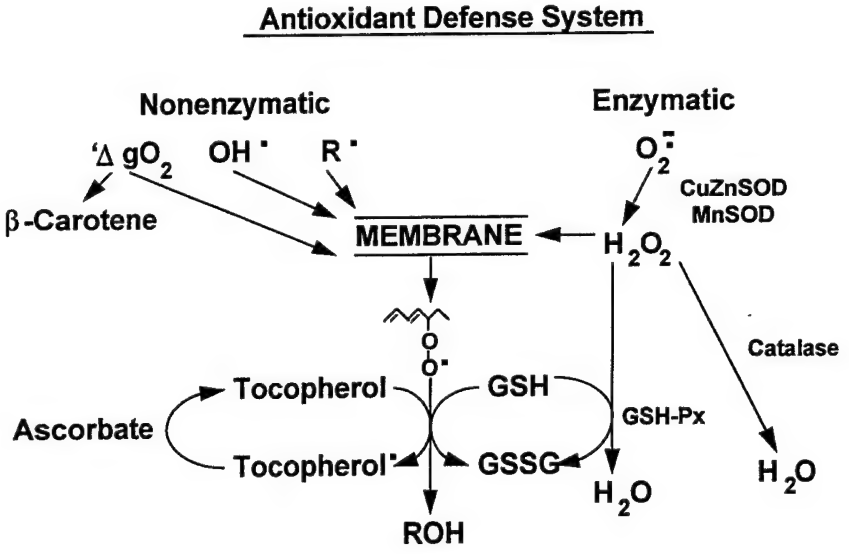

Figure 1. Cellular balance between pro-oxidants capable of inducing oxidative stress ('ΔgO_2 - singlet oxygen; OH• - hydroxyl radical; R• - carbon-, nitrogen- or oxygen-centered free radical; $O_2^{\bullet-}$- superoxide anion radical; -O-O• - peroxyl radical; H_2O_2- hydrogen peroxide), and intracellular antioxidants (SOD - superoxide dismutase; Catalase; GSH-Px - glutathione peroxidase; GSH - glutathione; Tocopherol - vitamin E; Ascorbate - vitamin C; β-Carotene; modified from Byczkowski and Channel, 1996; according to Bray and Betteger, 1990).

LIPID PEROXIDATION

Lipid peroxidation is a pathological process leading to a unique form of hepatocellular injury implicated in the genesis of liver necrosis evoked by several pro-oxidant chemical hepatotoxicants (e.g., carbon tetrachloride - CCl_4, yellow phosphorous, ethanol, etc.; Kulkarni and Byczkowski, 1994a), and it may be linked with carcinogenicity (Byczkowski and Channel, 1996). Lipid peroxidation is characterized by the formation of conjugated dienes, formation of thiobarbituric acid reactive substance (TBARS; mainly malondialdehyde), and the exhalation of alkanes (e.g., ethane). TBARS and ethane are generated, among other stable products, during the propagation and termination of lipid peroxidation process (Figure 3). The alkanes are formed in biological systems through peroxidation of the omega-3 (ethane) or omega-6 (pentane) fatty acids and the subsequent beta-scission decomposition of the intermediate hydroperoxides (Gardner, 1989).

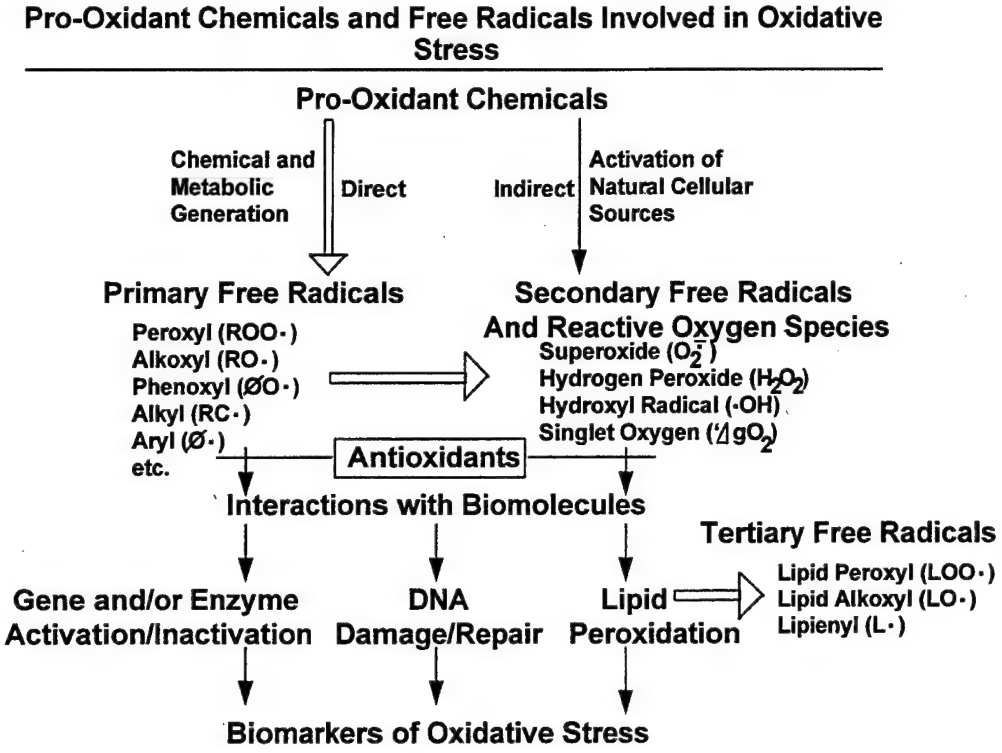

Figure 2. Free radicals and reactive oxygen species involved in the chemically induced oxidative stress (modified from Byczkowski and Channel, 1996, according to Trush and Kensler, 1991).

BIOMARKERS OF LIPID PEROXIDATION

Based on the findings of Riely et al. (1974) that mice treated with carbon tetrachloride have an increased amount of the exhaled ethane *in vivo*, numerous studies have been conducted in which ethane and/or pentane were measured as indices of lipid peroxidation or surrogate biomarkers of tissue damage by oxidative stress. Increased ethane exhalation was also found by Cojocel et al. (1989) as a consequence of lipid peroxidation in mice treated with trichloroethylene (TCE). Consequently, volatile alkane (ethane and/or pentane) detection in expired air has been used for some time as a non-invasive technique to measure lipid peroxidation in whole animals or human subjects (Refat et al., 1991; Kazui et al., 1992; Arterbery et al., 1994; Guilbaud et al., 1994). Ethane exhalation is more reliable as an index of lipid peroxidation than pentane, because CYP-mediated metabolism of ethane is substantially slower than that of pentane (Smith, 1991).

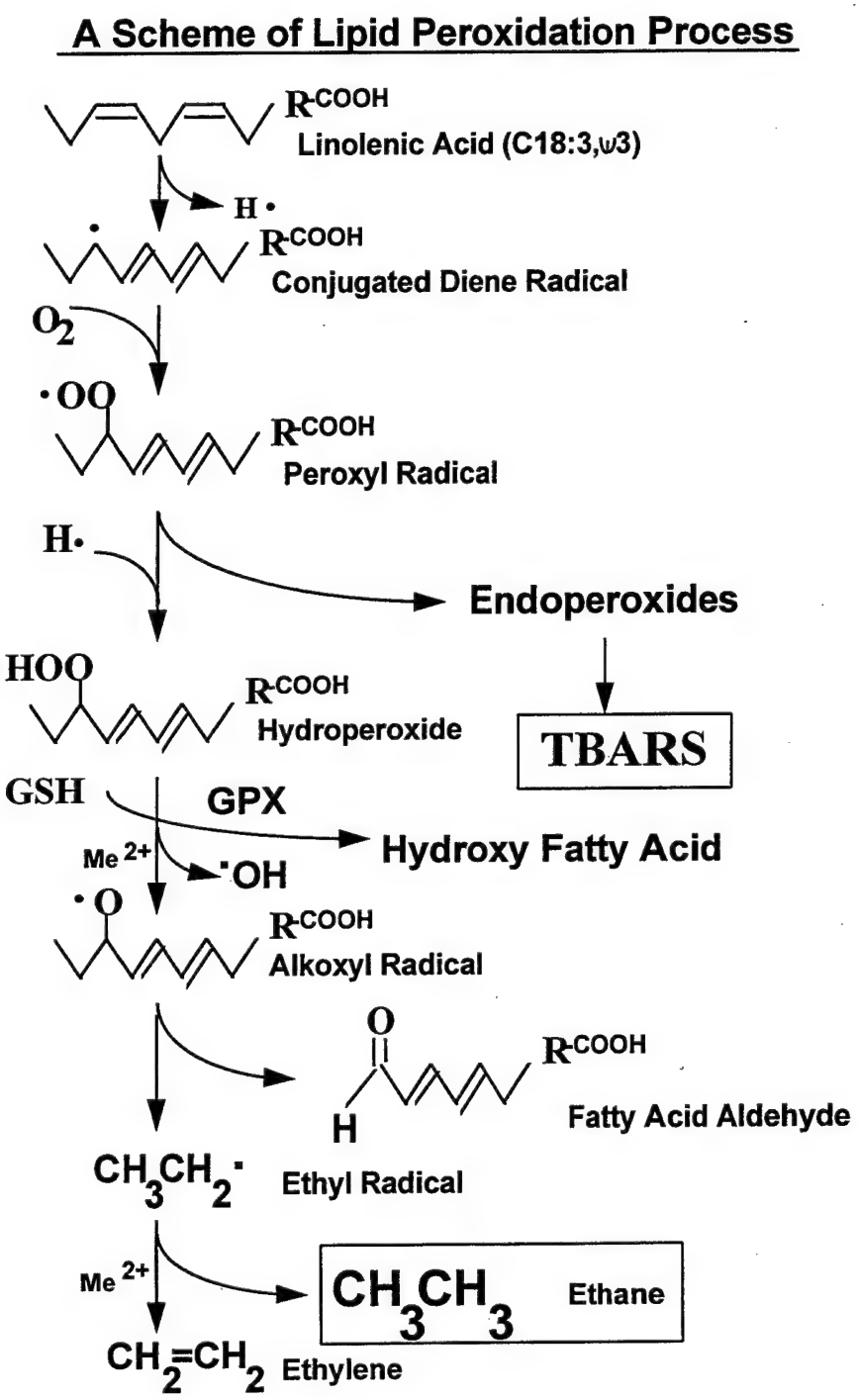

Figure 3. A simplified scheme of lipid peroxidation reactions which lead to production of thiobarbituric acid reactive substances (TBARS) and to generation of ethane (according to Sagai and Ichinose, 1980). Me^{2+} - transition metal cation.

Typically, in the assay, exhaled air is probed for ethane by gas chromatography using flame ionization, photoionization, or ion trap detectors (Kneepkens et al., 1994). Because of its direct

relation to lipid peroxidation (Jeejeebhoy, 1991; Figure 3), we chose ethane exhalation assay as an end point for development of the computer-aided PBPD model for simulation of the biological effects caused by CCl_4, TCE, and other pro-oxidant chemicals (tert-butyl hydroperoxide and bromotrichloromethane, $BrCCl_3$).

The measurement of rates of TBARS generation *in vitro* was used previously for calibration of the biologically based pharmacodynamic model (BBPD) of lipid peroxidation induced by tert-butyl hydroperoxide and $BrCCl_3$ in mouse liver slices, described elsewhere by Byczkowski et al. (1995; 1996). In the present report, a physiologically based pharmacodynamic (PBPD) model of lipid peroxidation is described which employs ethane exhalation as a measurable end point *in vivo* and incorporates the previously developed *in vitro* model as a mechanistic module. The developed PBPD model has been linked with a PBPK sub-model that describes the local concentrations of CCl_4 and TCE in the liver. The resultant hybrid PBPD model may be used for a pharmacodynamic description of oxidative stress, dose-response characterization, and risk characterization of pro-oxidant chemicals.

RISK CHARACTERIZATION OF PRO-OXIDANT CHEMICALS BASED ON THEIR MODE OF ACTION

Health risk from chemicals depends on both the extent of exposure and a dose-response relationship, which reflects, in turn, the mode of action of chemicals (Figure 4).

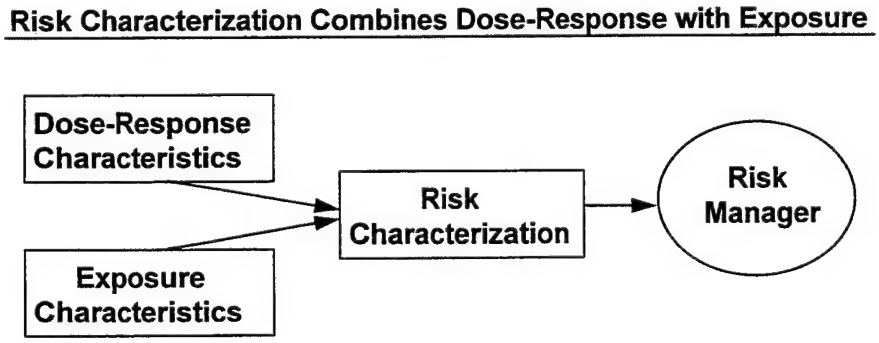

Figure 4. A paradigm for risk characterization.

Because biological responses of tissues and organs are mechanistically linked to local concentration of the active form of xenobiotic, the internal dose of chemical that reaches a particular physiological compartment must be used for any meaningful risk characterization.

Without understanding "what the particular dose of a chemical can do to the organism" the whole process of risk characterization is useless to a risk manager (Figure 4).

In addition to the question about the direct biological effect of the delivered concentration of an activated (free radical) form of the pro-oxidant chemical, other important questions are: i. "How is the target organ protected against free radical insult?"; ii. "How fast are normal (physiological) processes of autooxidation?"; and iii. "How fast do the activating enzymes (CYP) degrade?"

For quantitative characterization and modeling of the dose-response for pro-oxidant chemicals (e.g., CCl_4, $BrCCl_3$, or TCE) it was necessary not only to answer these questions, but also to include the mode of action and to determine the exact chain of events in the chemical interaction with the biological system (Figure 5).

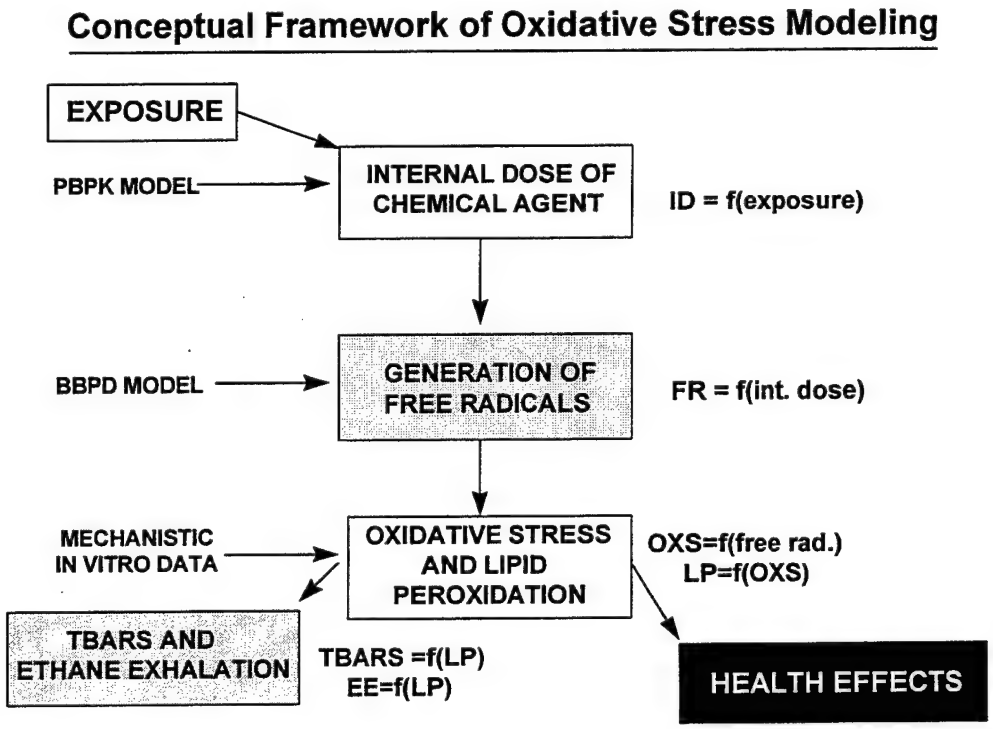

Figure 5. A conceptual framework for quantitative modeling and dose-response characterization of the chemically induced oxidative stress.

At first, the internal delivered dose of pro-oxidant chemical has been described as a function of exposure with an appropriate pharmacokinetic (PK and/or PBPK) model. Then, the local concentration of free radicals, generated by the pro-oxidant chemical, has been described as a function of the local dose of the chemical with an appropriate BBPD model. Next, using

mechanistic information, oxidative stress and lipid peroxidation have been described as functions of free radical concentration. Finally, the health effects may be quantitatively described by biologically based dose-response (BBDR) sub-model as continuous or discrete phenomena, depending on the magnitude of oxidative stress. The dependence may be either deterministic or stochastic in nature. These considerations, based on the available literature and experiments conducted in our laboratory, led to the development, calibration, and partial verification of the hybrid PBPD model for chemically induced oxidative stress. The resultant computer-assisted simulation model described in this report may be useful for risk characterization of pro-oxidant chemicals.

MATERIALS AND METHODS

CHEMICALS

All chemicals used in this study were of analytical grade. N-tert-butyl-α-nitrone (PBN) and 2,2,5,5,-tetramethyl-1-pyrrolidinyloxyl-3-carboxyamide (3-CAR) were purchased from Aldrich Chemical Co., Inc., Milwaukee, WI. Dimethyl sulfoxide (DMSO), BHT, CCl_4, $BrCCl_3$, TCE, and TBOOH were from Sigma Chemical Co., St. Louis, MO.

Dosage

The pro-oxidant chemicals tested: carbon tetrachloride (CCl_4), bromotrichloromethane ($BrCCl_3$), trichloroethylene (TCE), and tert-butyl hydroperoxide (TBOOH) were used *in vitro* or *in vivo* in the following concentrations or doses:

Liver slices *in vitro* (recalculated as final concentrations in the medium):

CCl_4 - 0.1, 0.5, 1.0, and 1.5 mM

$BrCCl_3$ - 0.1, 0.5, 1.0, and 1.5 mM

TCE - 0.1, 0.5, 1.0, and 1.5 mM

TBOOH - 0.1, 0.5, 1.0, 1.5 mM

Mice *in vivo* (single i.p. doses expressed per body weight):

CCl_4 - 0.075, 0.15, 0.3, and 1.5 g/kg

$BrCCl_3$ - 0.025, 0.05, 0.1, and 1.0 g/kg

TCE - 0.26, 1.0, and 2.6 g/kg

TBOOH - 0.025, 0.05, 0.1, and 0.225 g/kg

ANIMALS

The B6C3F1 male mice (Charles River Breeding Laboratories, Kingston, NY), 25 - 38 g body weight were used throughout the study. Routinely, the mice were provided with Purina Formulab 5008 standard diet and *Pseudomonas*-free softened water *ad libitum*. One week before experiment, the diet was switched to the vitamin A- and E- deficient, purified diet Purina 5827C-1.

MEASUREMENT OF LIPID PEROXIDATION *IN VITRO*

Precision-cut slices were prepared from livers of B6C3F1 male mice and maintained using the dynamic roller culture method (Sipes, et al., 1987; Brendel et al., 1993). The mice were euthanized with CO_2, their livers were removed and placed in ice-cold Sacks buffer (containing: KH_2PO_4 0.75 g/L, K_2HPO_4 9.5 g/L, $NaHCO_3$ 1.2 g/L, $KHCO_3$ 0.6 g/L, mannitol 37.5 g/L, and $MgCl_2$; pH 7.4).

Liver cores, 8 mm diameter, were prepared and sliced in ice-cold Sacks buffer using a Krumdieck tissue slicer (Alabama Research and Development, Munford, AL; Brendel et al., 1987; Krumdieck et al., 1980). The slices were loaded on rollers (two slices per roller) in ice-cold Sacks buffer. The rollers were then placed in scintillation vials containing 1.7 mL of Waymouths MB 752/1 media at 37 °C (Formula 78-5107EC, without phenol red, pH 7.4, Gibco BRL, Grand Island, NY), supplemented with $NaHCO_3$ 1.3 g/L, HEPES 2.38 g/L, NaCl 0.292 g/L, l-glutamine 0.35 g/L, gentamycin sulfate 50 mg/L, and 10% fetal bovine serum (Hyclone, Logan, UT), and capped with a scintillation vial cap with 1/4" hole for gas exchange. The vials were placed in a Dynamic Roller Culture Incubator (Vitron, Tucson, AZ) and gassed with 95% O_2/5% CO_2 for a 2-h preincubation period.

After a 2-h preincubation period, the rollers were removed from the vials, placed into prewarmed, sealed vials containing fresh media (pH 7.4), and dosed through the septa with either vapors (for volatile chlorinated hydrocarbons: CCl_4, $BrCCl_3$, TCE) or an appropriate dilution (for water-soluble compound, TBOOH) of pro-oxidant chemical at the desired final concentration. The dosed vials containing rollers were then returned to the roller culture incubator. Final concentrations of volatile pro-oxidant chemicals in the media were calculated using partition coefficients, determined for the equilibrated medium/air system at 37 °C (for CCl_4 0.666 [$\pm$ 0.05 S.D., n=15], for $BrCCl_3$ 1.97 [$\pm$ 0.23 S.D., n=18], for TCE 1.94 [$\pm$ 0.17 S.D., n=18]). Zero time controls were processed immediately. Then, the vials were removed at intervals over a 2-h incubation and slices were weighed and sonicated in their own media. Finally, aliquots of each sonicated sample were removed for TBARS assay and protein content measurements. Samples for TBARS assay were added to ice-cold D-PBS/GSH/EDTA buffer (pH 7.4) containing 20 mg reduced GSH and 48 mg EDTA in 100 mL D-PBS (Dulbeco's buffer; Gibco BRL, Grand Island, NY). Incubations were repeated several times with different liver preparation (typically, n=4).

Lipid peroxidation was measured by the formation of TBARS, employing the fluorescence spectrophotometry of solvent tissue extracts (Janero, 1990). Essentially, in this assay, the aldehyde products generated by splitting the endoperoxide alkoxyl radicals (formed during the peroxidation of unsaturated fatty acids; mostly malondialdehyde, MDA) reacted with thiobarbituric acid (TBA) to yield a 1:2 MDA:TBA red, fluorescent, complex (Janero, 1990). Incubation of liver slices without chemical inducer did not significantly increase the fluorescence for up to 2 hours. Since the control values for liver slices at time zero were subtracted from the results, under conditions of the assay, the determined amount of MDA:TBA complex reflected the extra amount of lipid hydroperoxides produced in addition to the normal physiological background.

At 1 hour and 2 hours of incubation, the samples of liver slices (control and treated) were removed for viability analysis. The viability was assessed from lactate dehydrogenase (LDH), aspartate aminotransferase (AST), and alanine aminotransferase (ALT) leakage, and intracellular potassium content. The enzyme leakage was determined using a Kodak Ektachem Analyzer (model 700XR) for aminotransferase activities and DuPont acaV for dehydrogenase activity. An acceptable enzyme leakage level for precision-cut liver slices was assumed to be less than 20% of the total content of enzymatic activity. Potassium content in sonicated tissue samples was determined using an AVL 982-S Electrolyte Analyzer (Roswell, GA). The acceptable level of intracellular potassium content in precision-cut liver slices was assumed to be greater than 35 mM K^+/g wet weight. If the average viability tests of either control or treated liver samples did not meet the above acceptable levels, the experimental results were discarded.

Free Radical Measurement

Known amounts of a spin label (N-tert-butyl-α-nitrone, PBN) were added to liver slices in Waymouth's media and incubated with or without addition of appropriate pro-oxidant chemical (1 mM CCl_4, $BrCCl_3$, TCE, TBOOH, for 60 min.). The radicals generated by these chemicals formed adducts with PBN which were detected by the electron paramagnetic resonance (EPR) spectroscopy (Buettner, 1987). The total radicals in the lyophilized samples of liver slices were measured using a Bruker EMS 104 EPR analyzer. The machine parameters for the EPR analyzer were: microwave power, 25 mW; sweep width, 100 G; modulation amplitude, 4.02 G; sweep time, 10.49 s; filter time constant, 20.48 ms; receiver gain, 60. The spectra were measured by peak height directly from the EMS 104 EPR analyzer and by double integration with normalization for receiver gain using the EPR program (Bruker, Billerica, MS).

All results were recalculated per liver dry weight and analyzed by one-way and two-factorial analysis of variance using the statistics package Design Ease®. The factors were concentration and time. Standard deviations and regression correlation were performed using Sigma Plot®.

ANIMAL TREATMENT AND MEASUREMENT OF LIPID PEROXIDATION *IN VIVO*

Animal Treatment

Male B6C3F1 mice (body weight 29 - 32 g), fed for one week the vitamin A- and E- deficient diet, were used to conduct the exhalation experiments and partition coefficient determinations. Animals were treated intraperitoneally (i.p.) with pro-oxidant chemicals at appropriate doses (calculated in g/kg body weight), dissolved in 0.2 mL of mineral oil. Immediately after treatment,

ethane production was monitored using a closed gas uptake system (Gargas et al., 1986). Four or five mice were placed simultaneously in a 0.75 L chamber containing 50 grams of soda lime that absorbs CO_2 and H_2O. Chamber oxygen concentration was monitored (MDA oxygen analyzer, MDA Scientific, Lincolnshire, IL) and kept at a range of 20-21.5% throughout the exposure. Ethane exhalation measurements were repeated several times with different groups of mice before and after the treatment (typically, n=4).

Air Sample Analysis

Samples were collected using an automatic sampling valve (1 mL sample loop) connected to a Hewlett Packard 5890 GC. Ethane was separated from other respiratory gases by a 6' x 1/8" stainless steel column packed with Chromosorb 102, 80-100 mesh (Alltech, Deerfield, IL). The column temperature was 50 °C, and the injector and flame ionization detector temperatures were 125 °C and 200 °C, respectively. A carrier gas (nitrogen) flow rate was set at 20 mL/min and the air *plus* hydrogen flow rate was 405 mL/min. The retention time was 2.1 min after the valve opened. A Hewlett-Packard 3396 Integrator was used to measure peak heights; and ethane concentrations were calculated using a calibration curve prepared with ethane standards.

A background noise at low levels of ethane as well as the ethane detection threshold and peak integration by GC and data-processing software were responsible for a quantification threshold, below which any measurement of ethane concentration was uncertain. Due to this uncertainty, a reliable ethane quantification level by the method used was above approximately 0.025 ppm. (minimum ethane concentration integrated as a peak by GC + 2 SD).

Partition Coefficients

Partition coefficients for ethane were determined in our laboratory (Seckel and Byczkowski, 1996) using a modified vial-equilibration method *in vitro*, described by Gargas et al. (1989). Tissues from five B6C3F1 mice were pooled, homogenized, and aliquoted into 12.4 mL headspace analyzer vials. Tissues analyzed included: blood, liver, fat, kidney, and muscle. Each tissue sample weighed 1 gram. To inhibit spontaneous lipid peroxidation, butylated hydroxytoluene (BHT; Sigma Chemical, St. Louis, MO) was added in the amount of 5 mg/g tissue. A 15 ppm concentration of ethane gas was added to the headspace of each vial. The vials with constituents were vortexed for 3 h at 37 °C. A sample was removed from the headspace of each vial *via* a Hewlett Packard 19395A autosampler. A Hewlett Packard 5890 GC was used to analyze samples with data handled by a P. E. Nelson Data Aquisition System equipped with Turbochrom (version 4.0) software. A Poraplot Q, 25 m x 0.53 mm (Chrompak, The Netherlands), was used for chemical separation along with the following GC conditions: oven temperature 100 °C, injector temperature 100 °C, flame ionization

detector 250 °C, and N_2 carrier flow through column and headspace sampler 5.3 cc/min. Ethane retention time was determined at 1.58 min.

MATHEMATICAL MODELING AND COMPUTER-ASSISTED SIMULATIONS

Ethane metabolism parameters (V_{max} and K_m) were estimated, fitted, and optimized with the PBPD model which was based on our *in vivo* experimental measurements of ethane uptake in a closed chamber, using the method for volatile chemicals essentially as described by Gargas et al. (1986). Partition coefficients were determined using the method of Gargas et al. (1989), as described above. The PBPD model was written in Advanced Continuous Simulation Language (ACSL; Mitchell and Gauthier Associates, Inc. 1993) with a sub-routine written in FORTRAN. The simulations were performed using SIMUSOLV® software with optimization capabilities (Steiner et al., 1990) on a VAX/VMS minicomputer. Parameters were optimized by SIMUSOLV®, which uses the log likelihood function as the criterion. Either the generalized reduced gradient method for single parameter optimization or the Nelder-Mead search method for multiple parameters optimization was used to adjust the values (Steiner et al., 1990).

RESULTS

MODEL STRUCTURE

Modules

The PBPD model for chemically induced oxidative stress was composed of several modules, interlinked to form integral sub-models (Figure 6). Each sub-model was calibrated and verified individually with experimental data from our laboratory and/or from the available literature.

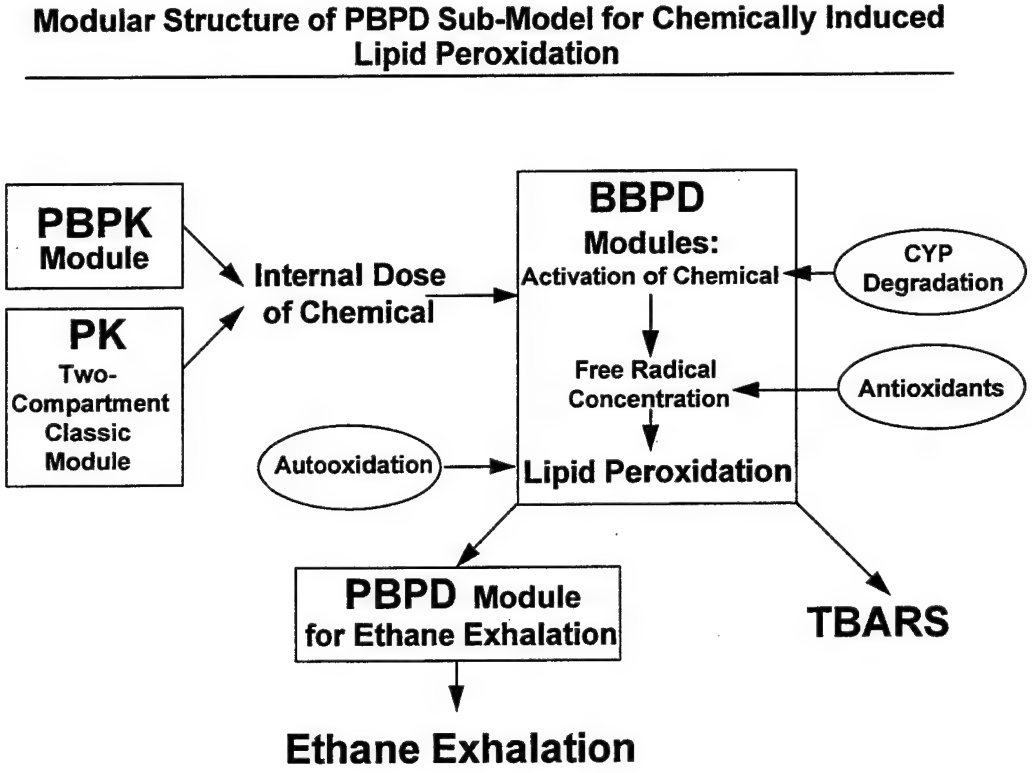

Figure 6. A simplified scheme of physiologically based pharmacodynamic (PBPD) sub-model for chemically induced lipid peroxidation.

The model, describing biological effects within the target organ, was constructed in a way compatible with physiologically based pharmacokinetic (PBPK) module and/or classic compartmental pharmacokinetic (PK) module which estimated the internal dose of a chemical. The biologically based pharmacodynamic (BBPD) module described bioactivation of a chemical (decreased by cytochrome P450 (CYP) degradation and suicidal inhibition), production of free radicals (quenched by antioxidants), and lipid peroxidation (enhanced by autooxidation) accompanied by TBARS and ethane generation. The PBPD module described distribution and exhalation of ethane.

PBPK Sub-Model for Internal Dose of Pro-Oxidant Chemical

The PBPK sub-model for internal dose of pro-oxidant chemicals was constructed as a traditional, flow-limited PBPK mathematical description of volatile compounds (Gargas et al., 1986; Yang and Andersen, 1994). A separate input compartment, parallel to the gastrointestinal tract, was added to this sub-model to estimate intraperitoneal exposure. The rate of change in the amount of chemical absorbed from the peritoneal cavity (RA_{ip} [mg/h]) was described as a product of the rate constant of absorption (KA_{ip} [1/h]) and the mass of chemical remaining in the peritoneal cavity (MR_{ip} [mg]):

$$RA_{ip} = KA_{ip} * MR_{ip}$$

and

$$MR_{ip} = D_{ip} + \int_0^t RMR_{ip} * dt$$

where D_{ip} [mg/animal] is the actual dose of the chemical injected i.p., RMR_{ip} [mg/h] is the rate of change of the chemical remaining in the peritoneal cavity (disappearance), and t [h] is time.

It was estimated that only a small fraction of the lipophilic pro-oxidant chemical may diffuse directly to the abdominal mesenteric fat, whereas about 99% of the chemical is being absorbed to venous circulation (blood absorption ratio, $B_{ab} = 0.99$ [ratio]) and eventually drained to the portal blood and delivered to the liver. Therefore, the product of $B_{ab} * RA_{ip}$ was added to the liver compartment.

The PBPK sub-model parameters for CCl_4, based on Paustenbach et al. (1988) and Gallo et al. (1993), were scaled allometrically to B6C3F1 mice and calibrated with data from the literature (Seckel and Byczkowski, 1996). Similarly, the PBPK sub-model parameters for TCE, based on Fisher et al. (1991), were scaled allometrically to B6C3F1 mice and calibrated with data from the literature (Das et al., 1994). The PBPK sub-model parameters for $BrCCl_3$ and TBOOH were not verified experimentally.

Classic PK Module for Intraperitoneal Dosing of Pro-Oxidant Chemicals

For many chemical compounds the PBPK sub-model parameters are not immediately available, whereas, their classic pharmacokinetic micro- and macro-constants may occasionally be found in the literature. To utilize this kind of data, an additional classic PK module was included in the pharmacokinetic sub-model and connected directly to the liver compartment. The classic PK module was based on a multiexponential equation for two-compartment system:

$$C_L = C_{L0} * k_{1,0} * (\exp(-\beta * t) - \exp(-\alpha * t))/(\alpha - \beta)$$

where C_L is local concentration of pro-oxidant chemical [mg/kg]; C_{L0} is estimate of initial concentration of the chemical [mg/kg]; $k_{1,0}$ is pharmacokinetic transfer micro-constant [1/h]; α is pharmacokinetic macro-constant [1/hr]; and β is pharmacokinetic macro-constant [1/h]. The pharmacokinetic constants were recalculated from the literature (e.g., for CCl_4 as presented by Seckel and Byczkowski, 1996).

BBPD Module for Activation of Pro-Oxidant Chemical and Free Radical Concentration

Production of free radicals and the local concentration of pro-oxidant chemical-derived free radicals were estimated by the square root algorithm presented previously (Byczkowski and Flemming, 1996) and verified with TCE (Byczkowski et al., 1996; Channel et al., 1997). For the bioactivation and free radical quenching reactions:

$$\text{Pro-oxidant chemical} \xrightarrow{k_i} FR_{ad} + FR_{ad} \xrightarrow{k_t} \text{Nonradical products}$$

it was assumed that: $dFR/dt = k_i * C_{LM} - k_t * FR_{ad} * FR_{ad} = 0$.

Therefore:

$$FR_{ad} = \sqrt{k_i * C_{LM}/k_t}$$

where FR_{ad} is a steady state concentration of pro-oxidant chemical-derived free radicals [µmol/0.1 g liver]; C_{LM} is local pro-oxidant chemical concentration [µmol/0.1 g liver]; k_i is a rate constant of free radical formation from the pro-oxidant chemical [1/h]; and k_t is the lumped rate constant of free radical recombination and quenching by the biological system [1/h].

Algorithm for CYP degradation and suicidal inhibition by activated pro-oxidant chemical was based on deterministic one-hit mechanism according to the reaction (presented previously by Byczkowski and Flemming, 1996):

$$FR_{ad} + CYP \xrightarrow{ACR} \text{INACTIVE CYP}$$

it was assumed that different kinds of CYP taking part in the bioactivation of pro-oxidant chemical have uniform sensitivity to FR_{ad}.

Therefore:

$$AC_{trem} = AC * \exp(-ACR * FR_{ad} * t)$$

where AC_{trem} is concentration of active CYP remaining over time [μmol/0.1 g liver]; AC is the initial concentration of active CYP [μmol/0.1 g liver]; ACR is the rate constant of CYP inactivation by free radicals [1/h]; t is time of incubation with free radicals [h]; and FR_{ad} is a steady-state concentration of pro-oxidant chemical-derived free radicals [μmol/0.1 g liver].

BBPD Sub-Model for Lipid Peroxidation

The BBPD sub-model estimated activity of lipid peroxidation expressed as TBARS production and ethane generation (Figure 7). The BBPD module for lipid peroxidation in the liver (calibrated with TBARS production), confirmed with experimental data for TBOOH and $BrCCl_3$ in precision-cut mouse liver slices, was published elsewhere by Byczkowski et al. (1996). A simplified scheme of this module is shown in Figure 7 (depicted by ovals). The source codes of *.CSL and *.CMD files for this module are archived in PBPK-L Public Domain Source Library and are accessible through the World Wide Web at the following URL: http://www.navy.al.wpafb.af.mil/new.htm

The PBPD module for ethane exhalation (depicted by rectangles in Figure 7) was calibrated with experimental data from our laboratory (presented previously by Seckel and Byczkowski, 1996). The PBPD module estimated rates of metabolism, distribution, and exhalation of ethane generated in the liver. On a molecular basis, about 0.1% of hydroperoxides derived from natural lipids will decompose to yield ethane (efficiency of ethane generation from fat, $EF_{fe} \leq 0.001$ [molar ratio]; Gardner, 1989; Janero, 1990).

BBDR Sub-Model for Cellular Target Inhibition

An inhibition of activities of cellular targets, caused by free radicals, was estimated by a biologically based dose-response (BBDR) sub-model composed of two modules, deterministic and stochastic (presented previously by Byczkowski and Flemming, 1996). This sub-model was governed by dose-dependent algorithms with time of exposure to free radicals t_p [h] fixed as a fraction (F_t [ratio]) of the time needed to reach the maximum effect (T_{me} [h]). For independent variable, the initial local concentrations of pro-oxidant chemical C_0 [μM] were increased stepwise between the estimated maximum "no effect" dose (C_{min} [μM]) and minimum "100% effect" dose (C_{max} [μM]) with the interval C_Δ [μM] resulting in a number of iterations "i". The initial local concentrations C_0 were captured as an array $DOSC_i$. The local, steady state concentrations of pro-oxidant chemical-derived free radicals FR_{adM} [μM] ($FR_{adM} = 10 * FR_{ad}$), at fixed time of exposure t_p [h], were captured as an array DOS_i along with initial local concentrations of pro-oxidant chemical C_0 [μM].

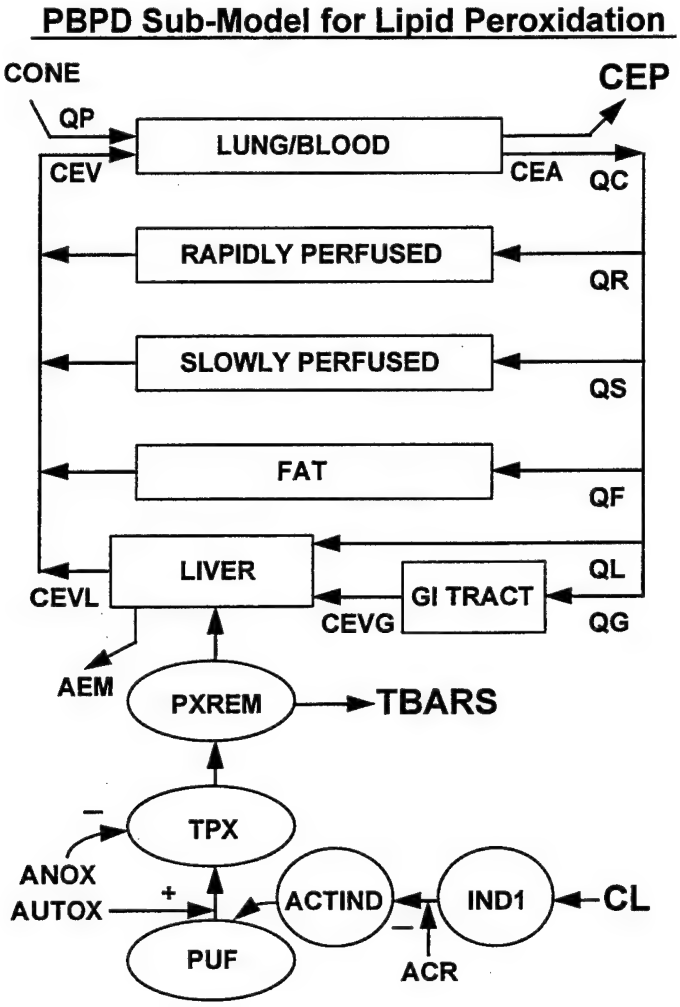

Figure 7. An interlinked biologically based pharmacodynamic (PBPD) sub-model describing lipid peroxidation combined the BBPD module for TBARS production (ovals) with the PBPD module for ethane exhalation (rectangles).

CONE - concentration of inhaled ethane [ppm]; QP - alveolar ventilation rate [L/h]; CEV - mixed venous blood ethane concentration [mg/L]; CEP - concentration of exhaled ethane [ppm]; QC - cardiac output [L/h]; CEA - concentration of ethane in arterial blood [mg/L]; QR - blood flow to rapidly perfused tissues [L/h]; QS - blood flow to slowly perfused tissues [L/h]; QF - blood flow to fat tissue [L/h]; QL - blood flow to liver tissue [L/h]; QG - blood flow through the portal vein [L/h]; CEVG - concentration of ethane in the portal vein [mg/L]; AEM - amount of metabolized ethane [mg]; CEVL - concentration of ethane in venous blood leaving the liver [mg/L]; PXREM - accumulated remaining hydroperoxides [μmol/0.1 g]; TBARS - thiobarbituric acid reactive substances [μmol/0.1 g]; TPX - accumulated total hydroperoxides [μmol/0.1 g]; ANOX - vitamin E-type antioxidants [μmol/0.1 g]; AUTOX - hydroperoxides produced by autooxidation [μmol/0.1 g]; PUF - polyunsaturated fat [μmol/0.1 g]; ACTIND - activated, free radical form of chemical inducer [μmol/0.1 g]; IND1 - internal dose of chemical inducer 1 [μmol/0.1 g]; ACR - activator (CYP) loss rate [1/h]; CL - delivered dose of pro-oxidant chemical [mg/kg].

Deterministic Module

The deterministic module estimated inhibition of uniform cellular targets (I_n [ratio]) by pro-oxidant chemical-derived free radicals (FR_{adM}) as an exponential decay function:

$$FR_{adM} + \text{CELLULAR TARGET} \xrightarrow{k_d} \text{INACTIVE TARGET}$$

it was assumed that homogenous CELLULAR TARGETS have uniform sensitivity to FR_{ad}.

$$I_n = I_0 * \exp(-k_d * FR_{adM} * t_p)$$

where I_n is a remaining activity, expressed as a fraction of remaining active cellular targets, relative to the amount before inhibition [ratio]; I_0 is the initial concentration of active cellular targets, assumed to be 100% ($I_0 = 1$. [percentage/100]); k_d is the rate constant of cellular target inactivation by free radicals [100%/μM/h]; t_p is time of exposure to free radicals [h]; and FR_{adM} are the local, steady state concentrations of pro-oxidant chemical-derived free radicals [μM]. The values of the remaining relative activity I_n were captured as an array I_{nh}:

$$I_{nh} = [I_{n1}, I_{n2}, \ldots I_{ni}].$$

Stochastic Module

The stochastic module estimated inhibition of non-uniform cellular targets (PROB [ratio]) by exposure for time t_p [h] to pro-oxidant chemical-derived free radicals (array DOS) as a 1 *minus* time-weighted fraction of a cumulative Gaussian distribution function:

$$FR_{adM} + \text{MULTIPLE TARGETS} \rightarrow \text{RANGE OF INHIBITORY RESPONSES}$$

it was assumed that non-uniform MULTIPLE TARGETS give normal distribution of the INHIBITORY RESPONSES to FR_{ad}.

$$PROB = 1 - F_t * \int_{-\infty}^{x} 1/\sqrt{2\pi} * \exp(-z^2/2) * dz$$

where $x = (DOS - M)/SD$; PROB is probability of cellular targets to remain active, relative to the amount before inhibition (expressed as a fraction of remaining active cellular targets, relative to the amount before inhibition [ratio]); DOS is array of free radical concentration values [μM], generated during exposure to the range of concentrations of pro-oxidant chemical (between maximum "no effect" and minimum "100% effect" doses); F_t is as a fraction [ratio] of the time needed to reach the maximum effect ($F_t = t_p/T_{me}$); M is mean of the cumulative Gaussian distribution of free

radical concentration values [μM]; SD is standard deviation of the cumulative Gaussian distribution of free radical concentration values [μM]; and z is a variable of integration.

PARAMETRIZATION AND CALIBRATION OF SUB-MODELS WITH DATA

PBPK Sub-Model for Internal Dose of Pro-Oxidant Chemical

Chemical-dependent parameters for TCE PBPK module in B6C3F1 mice (confirmed with data from Fisher et al., 1991) were presented previously by Das et al. (1994), and those parameters for CCl_4 (confirmed with data from Sanzgiri et al., 1995; Gallo et al., 1993; Gargas et al., 1986; and Paustenbach et al., 1986; 1988), scaled to B6C3F1 mice, were presented previously by Seckel and Byczkowski (1996). These parameters, optimized with SIMUSOLV®, are listed in Table 1. The animal-specific PBPK modeling parameters were as recommended by ILSI, RSI (1994) for mice.

TABLE 1. CHEMICAL-SPECIFIC PHARMACOKINETIC PARAMETERS FOR TCE AND CCl_4 IN B6C3F1 MICE

Parameter	Description	TCE	CCl_4
	Partition coefficients [ratio]		
PBC	Blood/air	13.4[e]	4.52[a]
PLC	Liver/blood	2.03[e]	3.14[a]
PFC	Fat/blood	41.3[e]	79.4[a]
PRC	Rapidly perfused tissue/blood	2.03[e]	3.14[a]
PSC	Slowly perfused tissue/blood	1.0[e]	2.43[b]
	Molecular weight [g/mol]		
MW		131.5	153.82
	Metabolism constants		
VMAXC	Maximum velocity [mg/hr/kg]	33.0[e]	0.65[c]
KM	Michaelis-Menten constant [mg/L]	0.25[e]	0.25[c]
KFC	1st order rate constant [1/hr/kg]	2.4[e]	0.0[c]
	Absorption rate [1/hr]		
KAIP	First order i.p. uptake	1.0[d]	1.45[d]
	Pharmacokinetic transfer constants fitted [1/hr]		
k10	Micro-constant	0.03[d]	0.3[d]
α	Macro-constant	0.01[d]	1.5[d]
β	Macro-constant	2.0[d]	1.6[d]

[a] from Gargas (1988).
[b] from Evans et al. (1994).
[c] from Gargas et al. (1986)
[d] from Seckel and Byczkowski (1996).
[e] from Das et al. (1994).

Classic PK Module for Intraperitoneal Dosing of Pro-Oxidant Chemicals

The pharmacokinetic micro- and macro-constants [1/h] were fitted to data from our laboratory obtained with B6C3F1 mice treated i.p. with TCE and CCl_4 (Seckel and Byczkowski, 1996). The pharmacokinetic transfer constants for classic PK module are listed in Table 1.

BBPD Module for Activation of Pro-Oxidant Chemical and Free Radical Concentration

Two algorithms describing the relationship between steady-state concentration of free radicals and local TCE concentration were tested, the square root algorithm (assuming that two free radicals are formed from one molecule of TCE, as described above) and a linear algorithm (Byczkowski et al., 1996; Channel et al., 1997). The linear algorithm described the reaction in which one free radical is formed from one molecule of TCE:

$$TCE \xrightarrow{k_i} FR_{ad} \xrightarrow{k_t} \text{Nonradical products}$$

Assuming steady state concentrations of free radicals: $dFR/dt = k_i * C_{LM} - k_t * FR_{ad} = 0$,

$$FR_{ad} = k_i * C_{LM}/k_t$$

where FR_{ad} is a steady-state concentration of TCE-derived free radicals [µmol/0.1 g liver]; C_{LM} is local TCE concentration [µmol/0.1 g liver]; k_i is a rate constant of free radical formation from TCE [1/h]; and k_t is the lumped rate constant of free radical recombination and quenching by the biological system [1/h].

Quantitative measurements of FR_{ad} *in vitro* using an EPR-spin trapping method failed to confirm either algorithm (Figure 8). Despite a relatively large variability in time-dependent measurements of TBARS produced in liver slices incubated with TCE (Figure 9), the dose-dependent data were much better fitted with the square root algorithm (Figure 10, curve B) than with the linear algorithm (Figure 10, curve A). Thus, the quantitative measurements of TBARS *in vitro* confirmed an adequate description of the relationship between concentration of free radicals and local TCE concentration by the square root algorithm (Byczkowski et al., 1996; Channel et al., 1997).

BBPD Sub-Model for Lipid Peroxidation

As the square root algorithm and the time-dependent activator degradation equation were introduced into the BBPD module for lipid peroxidation in the liver (originally calibrated as a linear algorithm with the experimental data from precision-cut mouse liver slices with TBOOH and $BrCCl_3$, Byczkowski et al., 1996), the modeling parameters had to be recalculated and optimized

with SIMUSOLV® software. All optimized parameters added or changed from those originally published by Byczkowski et al. (1996) are listed in Table 2. The chemical-specific parameters (factors ACTDGF and PTIND) were estimated and optimized for a range of concentrations for TCE (0.4 -5.6 μmol/0.1 g liver) and CCl_4 (0.5 - 7.6 μmol/0.1 g liver).

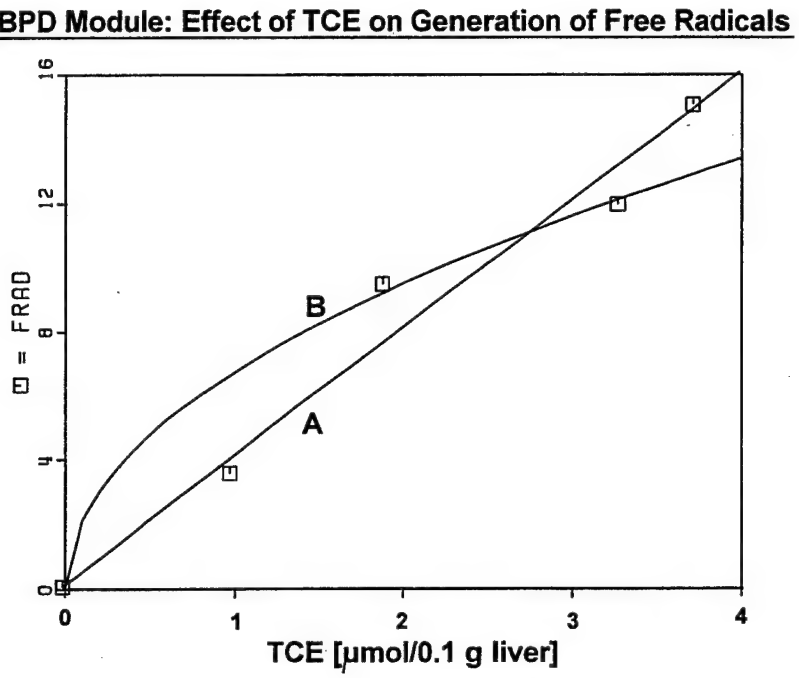

Figure 8. Calibration of the algorithm describing concentration of free radicals under steady-state conditions (FRAD [μmol/g]) with experimental data from Steel-Goodwin et al. (1995) for free radical generation by different concentrations of TCE [μmol/0.1 g liver] in mouse liver slices using an EPR/spin-trapping method.

FRAD -concentration of PBN-reactive free radicals [μmol/g liver]. The squares represent actual average experimental data points (after subtraction of physiological background levels of free radicals produced in the absence of TCE). The continuous lines are computer-generated simulations involving: A - linear algorithm; B - square root algorithm.

Since the original BBPD sub-model for lipid peroxidation was calibrated with $BrCCl_3$ (Tappel et al., 1989; Byczkowski et al., 1996), we have used the same well known pro-oxidant chemical to check if it will lead to a measurable lipid peroxidation at comparable local concentrations both *in vitro* and *in vivo*.

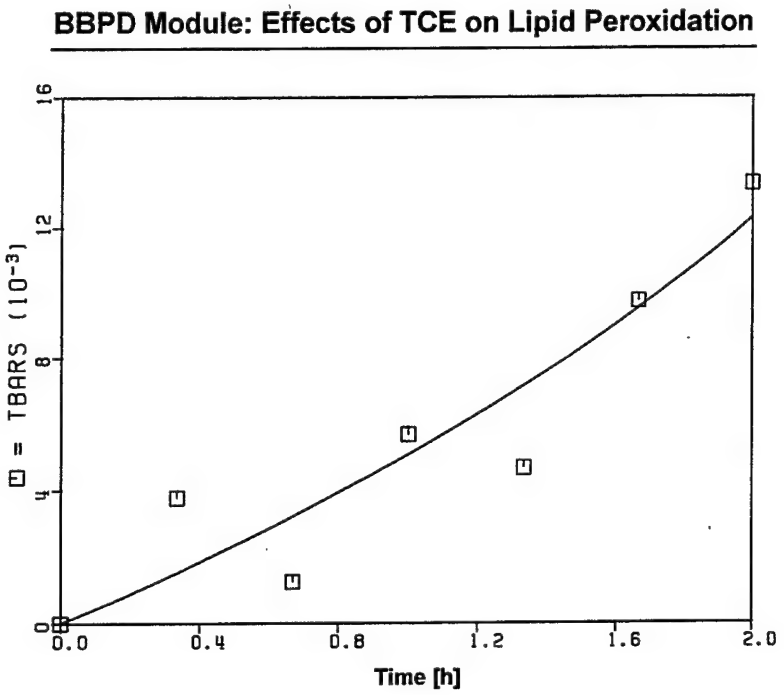

Figure 9. Results of time-dependent simulation of lipid peroxidation in mouse liver slices induced by 1 mM TCE. TBARS - thiobarbituric acid reactive substance x 10^{-3} [mmol/0.1 g liver]. Small squares depict average experimental data from our laboratory (n=4) described by Byczkowski et al. (1996). The continuous lines depict computer simulations with BBPD sub-model involving the square root algorithm and parameters optimized by SIMUSOLV® software (listed in Table 2), amount of TBARS at time=0 was subtracted from the data.

TABLE 2. PHARMACODYNAMIC PARAMETERS FOR TCE AND CCl_4 IN B6C3F1 MICE

Parameter	Description	Optimized numerical value
	Factors [1/μmol]	
ACTDGF1	Activator degradation factor 1 (TCE)	0.0014
ACTDGF2	Activator degradation factor 2 (CCl_4)	1.75
PTIND1	Potency of inducer 1 (TCE)	250.
PTIND2	Potency of inducer 2 (CCl_4)	4408.
	Rate constants [1/h]	
AUTOXF	Autooxidation rate	0.00013
PXREDF	Hydroperoxide reduction rate	0.17
ACR	Activator degradation rate	0.025
INDLF	Inducer loss rate	0.0001

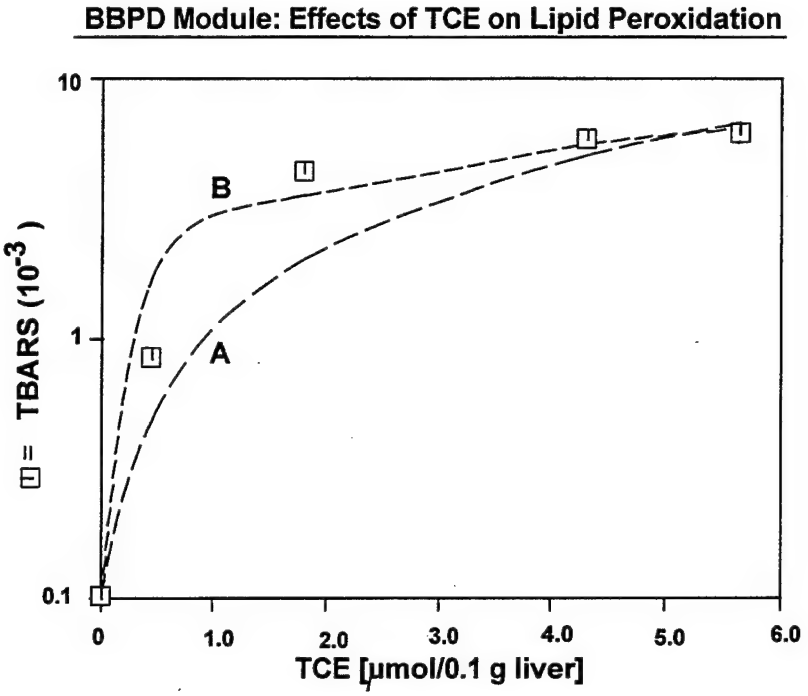

Figure 10. The results of dose-dependent simulations of lipid peroxidation in mouse liver slices for 0.5 h induced by different concentrations of TCE [µmol/0.1 g liver].
TBARS - thiobarbituric acid reactive substance x 10^{-3} [mmole/0.1 g liver]. Small squares depict average experimental data from our laboratory (n=4). Lines depict computer simulations with BBPD sub-model involving: A - linear algorithm (PTIND1=6.9); B - square root algorithm (PTIND1=250). The other parameters were optimized by SIMUSOLV® software. Amounts of TBARS in untreated controls were subtracted from the data (Byczkowski et al.,1996).

Bromotrichloromethane stimulated TBARS generation by precision-cut mouse liver slices *in vitro* (Figure 11). The lowest measurable effect was noticed at 0.1 mM $BrCCl_3$ in the medium. Considering its partition coefficients (medium/air = 2, and liver/air = 29), the 100 µM $BrCCl_3$ could produce an initial concentration of 0.145 µmol/0.1 g liver. The dose-response curves had a characteristic sigmoidal shape with a plateau reached at about 1 mM $BrCCl_3$, when incubated for 0.5 h, and at about 0.5 mM $BrCCl_3$ when incubated for 1 h. A prolonged incubation (above 1 h) with higher than 0.5 mM concentrations of $BrCCl_3$ failed to increase further the rate of TBARS generation by liver slices (results not shown here).

Figure 12 shows the results of measurement of ethane exhalation by mice in a closed gas chamber. The treatment with $BrCCl_3$ at a dose above 0.025 g/kg resulted in increased ethane exhalation measured 1h after the exposure. Twice as high dose was required to produce a significant increase in ethane exhalation after 0.5 h from the exposure. Again, the dose-response curves had a sigmoidal shape.

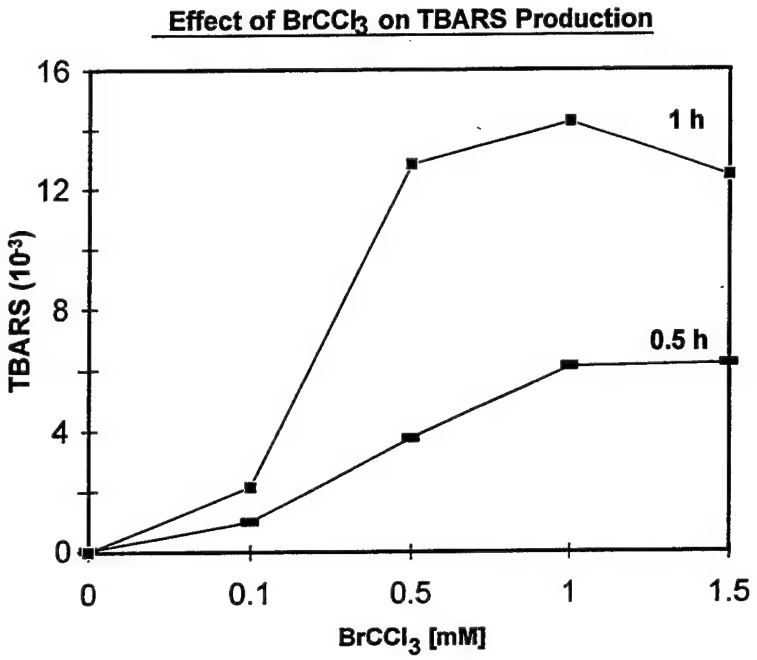

Figure 11. Effects of different doses of $BrCCl_3$ (concentration in the medium [mM]) on production of thiobarbituric acid reactive substances (TBARS - thiobarbituric acid reactive substance x 10^{-3} [mmole/0.1 g liver]) by mouse liver slices incubated for either 0.5 or 1 h in the presence of inducer.

The respective background values were subtracted from data points. Background production of TBARS in controls were respectively: 0.0226 μmole/g liver (± 0.0025 S.D., n=4) at 0.5 h, and 0.0303 μmole/g liver (±0.0035 S.D., n=4) at 1 h. Data points were significantly different from the corresponding controls (at $p \leq 0.05$, n=4) by Student's t-test.

Figure 13 shows actual time courses of stimulated ethane exhalation by mice treated with four different doses of $BrCCl_3$ (0.025, 0.05, 0.1, and 1.0 g/kg). The reliable ethane quantification threshold was 0.025 ppm There was no significant difference between ethane exhalation (followed for up to 2 h) in mice before and after i.p. injection of 0.2 mL of mineral oil only (by one-way Anova at $p \geq 0.05$).

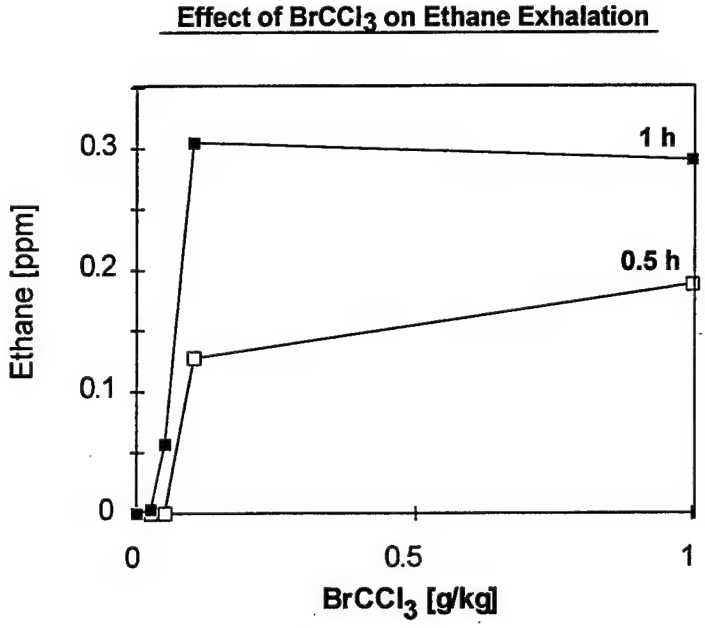

Figure 12. Effects of different doses of $BrCCl_3$ (injected i.p. [g/kg]) on ethane exhalation by five mice during either 0.5 or 1 h from the exposure to inducer (Ethane - concentration in the chamber [ppm]).

The respective physiological ethane exhalation values (background) from the same group of five mice, measured before treatment, were subtracted from the data points (respectively, 0.0435 ppm [±0.022 S.D., n=5] at 0.5 h, and 0.0447 ppm [±0.020 S.D., n=4] at 1 h).

Verification of BBPD Sub-Model for Lipid Peroxidation in vitro

The BBPD module of lipid peroxidation sub-model was further verified with *in vitro* effects of CCl_4 on the generation of TBARS by precision-cut mouse liver slices (Figure 14). The parameters were optimized with SIMUSOLV® to satisfy all set (time- and dose-dependent) of experimental data.

Verification of BBPD Sub-Model for Lipid Peroxidation in vivo

Based on the "upside down" PBPK model for ethane distribution (input in the liver, output in the lung), a PBPD module for ethane exhalation was constructed, assuming that the production of reactive free radical metabolites of xenobiotics takes place in the liver (Figure 7). At first, the module was calibrated with data from mice *in vivo*, inhaling a known concentration of ethane in a closed gas chamber (Figure 15 presented previously by Seckel and Byczkowski, 1996). These calibrations allowed us to verify partition coefficients of ethane and to estimate metabolism constants (V_{mexc}, K_{em}, and K_{efc}). Pharmacokinetic parameters for ethane exhalation module are listed in Table 3.

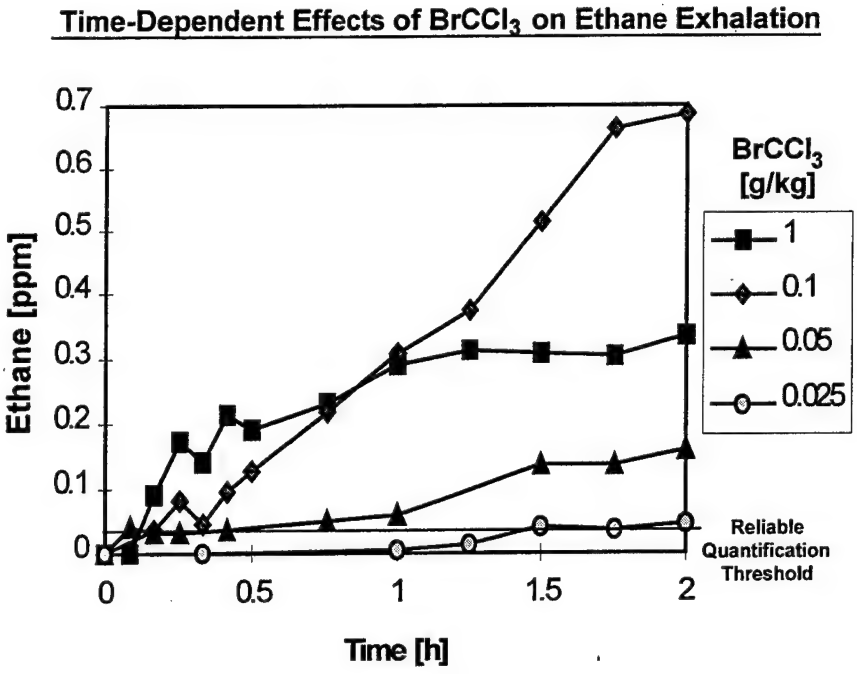

Figure 13. Time-course of effects of four different doses of $BrCCl_3$ (injected i.p. [g/kg]) on ethane exhalation (concentration in the chamber [ppm]) by five mice.
The respective physiological ethane exhalation values (background) from the same group of five mice, measured before treatment, were subtracted from the data points. The horizontal line depicts a reliable detection level of ethane by the method used (detectibility threshold + 2 SD). The ethane exhalation time courses after exposure to 0.05 (after 1 h but not 0.5 h), 0.1 and 1.0 g $BrCCl_3$/kg were significantly different from the corresponding control curves before treatment (by one-way Anova at $p \leq 0.05$). Other details are the same as in Figure 12.

Next, the PBPD sub-model, including the module for ethane exhalation, was tested *versus* experimental data from mice treated *in vivo* with TCE (Figure 16). The square root algorithm was included in the BBPD module for free radical concentration and the PBPD sub-model simulated time-dependent effects of different doses of TCE on ethane exhalation in B6C3F1 mice *in vivo* (Figure 16). The reliable ethane quantification threshold was 0.025 ppm.

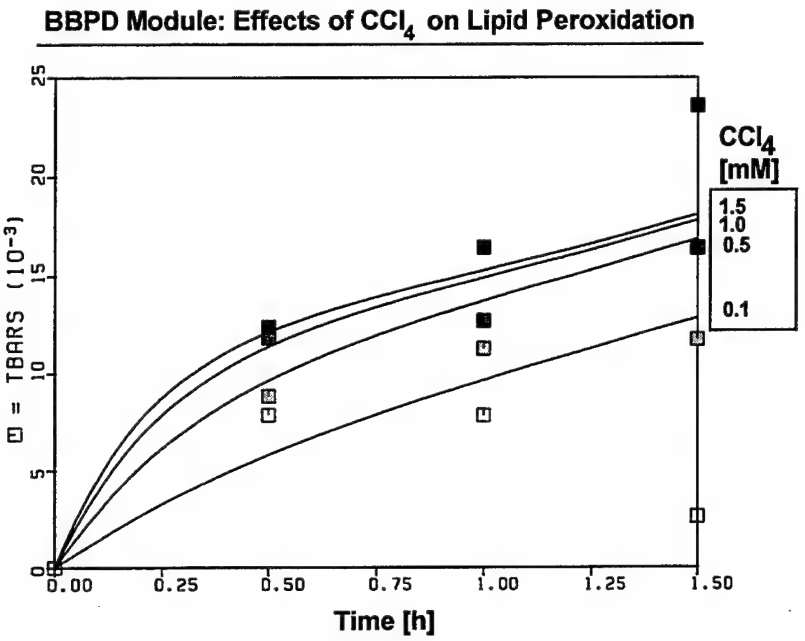

Figure 14. Time-dependent effects of four concentrations of CCl_4 (□-0.1, ▨-0.5, ■-1.0, and ■-1.5 mM) on TBARS generation by precision-cut mouse liver slices *in vitro*. Lines are computer-generated simulations by the lipid peroxidation sub-model (optimized parameters: PTIND1=4408; ACR=0.025; other parameters the same as in Table 2).

TABLE 3. PHARMACOKINETIC PARAMETERS FOR ETHANE EXHALATION IN B6C3F1 MICE

Parameter	Description	Numerical value
	Partition coefficients [ratio]	
PLA	Liver/air	0.828
PGA	Gut/air	0.996
PFA	Fat/air	2.444
PSA	Slowly perfused tissue/air	0.979
PRA	Richly perfused tissue/air	0.996
PEB	Blood/air	1.305
	Molecular weight [g/mol]	
MW		30.0
	Optimized metabolism constants	
VMEXC	Maximum velocity [mg/hr/kg]	0.286
KEM	Michaelis-Menten constant [mg/L]	0.51
KEFC	1st order rate constant [1/hr/kg]	2.786
EFFE	Efficiency of ethane generation [molar ratio]	0.001

Data presented previously by Seckel and Byczkowski (1996).

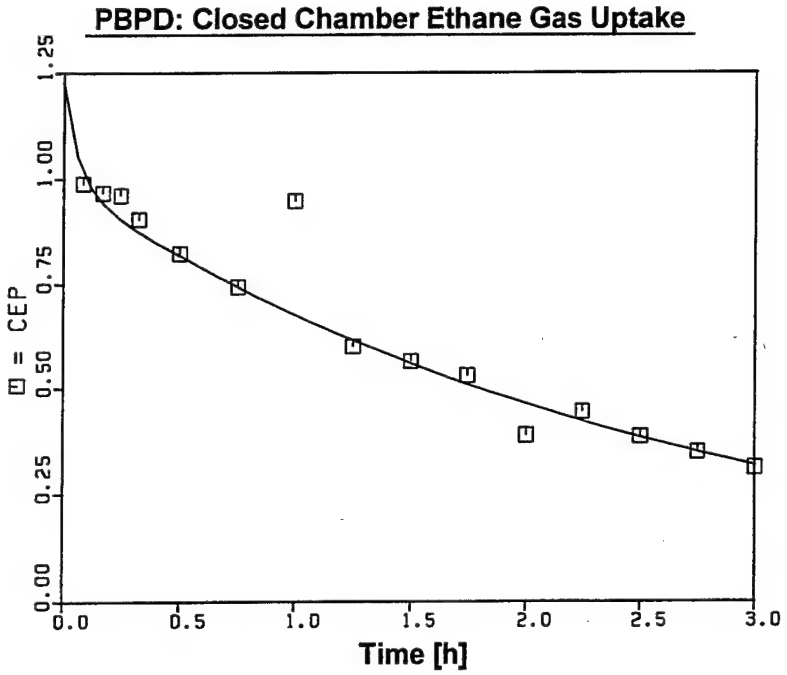

Figure 15. The results of PBPD sub-model simulations of our experimental data from mice inhaling ethane in a closed chamber (initial concentration of ethane 1 ppm).
CEP - Concentration of ethane in a closed chamber [ppm]; Time - [h]. Symbols depict experimental data collected from the closed chamber (four animals per time-point); continuous line is the PBPD model simulation (Seckel and Byczkowski, 1996).

At this step, the yield of ethane generation from lipid hydroperoxides was estimated (EF_{fe} = 0.001 [molar ratio]) by comparing the simulated molar amounts of ethane *in vivo* (Figure 16) with TBARS *in vitro* (Figure 10), produced in response to the same total cumulated dose (area under the concentration curve, AUC) of TCE in the liver.

Finally, the calibrated PBPD sub-model was verified with our data for ethane exhalation, induced by four different doses of carbon tetrachloride (CCl_4-specific parameters were taken from our *in vitro* calibration, Figure 14). At this verification step, the parameters estimated during the *in vivo* calibration with TCE were not further adjusted. Figure 17 shows the time-dependent effects of four different doses of CCl_4 on ethane exhalation along with the computer-generated simulations by the BBPD sub-model. The dose-dependent effects of CCl_4 on ethane exhalation and the computer-generated simulations at three different times from treatment are presented in Figure 18.

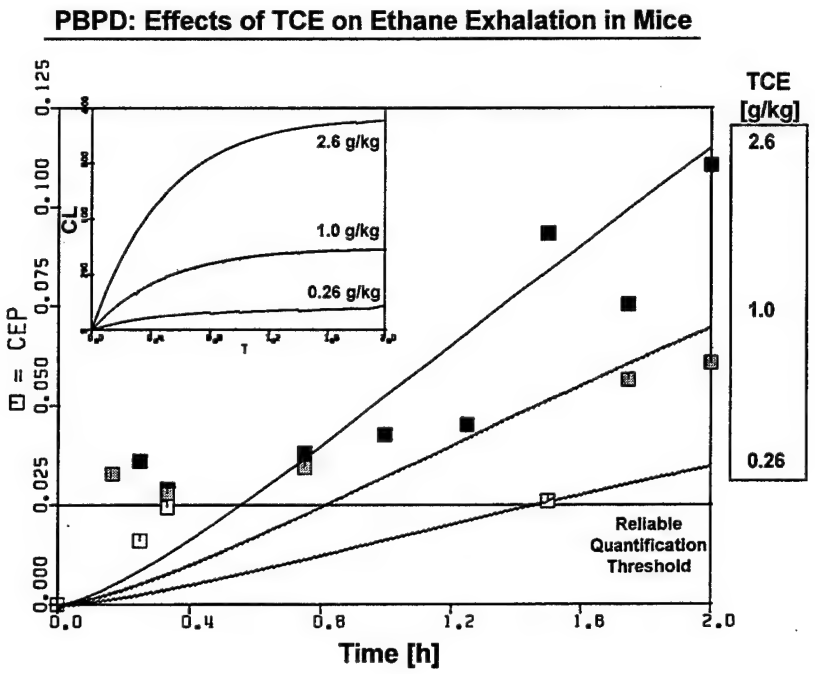

Figure 16. The results of PBPD model simulations of our experimental data from mice treated i.p. with three different doses of TCE (□-0.26,▩-1.0, and ■-2.6 g/kg) and exhaling ethane in a closed chamber (Byczkowski et al., 1996).

CEP - concentration of ethane in a closed chamber [ppm]; Time - [h]. Symbols depict experimental data collected from the closed chamber (five animals per time-point) with the respective physiological ethane exhalation values (background) from the same group of five mice, measured before treatment, subtracted from the data points. Lines are the PBPD model simulations. The horizontal line depicts a reliable ethane quantification threshold by the method used (detectibility threshold + 2 S.D.). Inset shows PBPK sub-model simulations of local TCE concentrations in the liver. CL - local concentration [mg/kg liver]; T - time [h].

BBDR Sub-Model for Cellular Target Inhibition

Two modules, composing the BBDR sub-model for cellular target inhibition by pro-oxidant chemical-derived free radicals, were based on either deterministic or stochastic equation, respectively, and were calibrated with *in vitro* data from the literature (Byczkowski and Flemming, 1996).

Deterministic Module

The deterministic BBDR module was calibrated with experimental data of Vroegop et al., (1995) for inhibition of amino acid and glucose transporters in N 18 neuronal hybridoma cell line in culture, incubated with cumene hydroperoxide (Figure 19 A) or hydrogen peroxide (Figure 19 B),

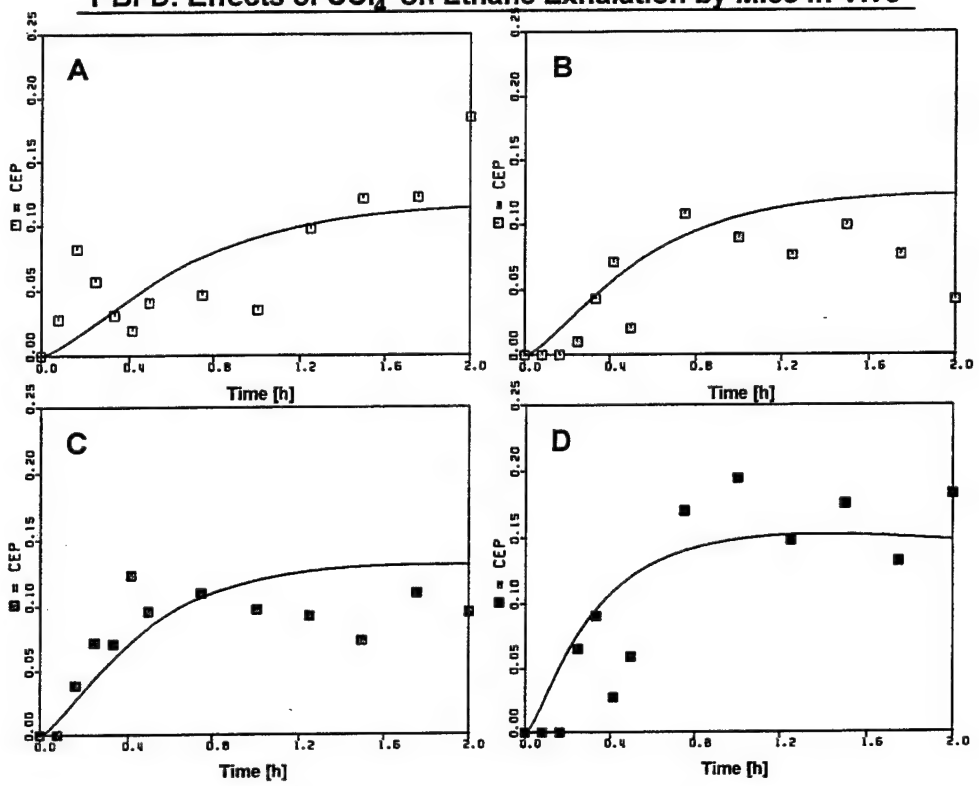

Figure 17. Time-dependent effects of four different doses of CCl_4 i.p. on the concentration of ethane exhaled by mice in a closed gas chamber *in vivo* (A. □-0.075, B.▨-0.15, C.▩-0.3, and D. ■-1.5 g/kg).

Lines are computer-generated simulations by the ethane exhalation BBPD sub-model (parameters that describe lipid peroxidation were the same as in Table 3). The respective physiological ethane exhalation values (background) from the same groups of five mice, measured before treatment, were subtracted from the data points. The reliable ethane quantification threshold by the method used was 0.025 p.p.m. (detectibility threshold + 2 SD).

respectively, Heffetz et al. (1990), and Hecht and Zick (1992), for inhibition of protein tyrosine phosphatase (PTyrPase) in rat hepatoma cells in culture incubated with hydrogen peroxide (Figure 19 C) or vanadate (Figure 19 D), respectively. The rate constant for quenching of free radicals by all biological systems investigated (k_t [1/μM/h]) was estimated as 200.0 [1/μM/h] and was fixed during all simulations. Rate constants of free radical formation (k_i [1/μM/h]) were chemical-specific and rate constants of cellular target inhibition [1/μM/h] were biological system-specific, and they were optimized with SIMUSOLV® software. Initial concentrations of active targets were assumed to be 100% in uninhibited biological systems before incubation with pro-oxidant chemicals (I_0 = 1.0 [%/100]). Timing parameters [h] were dependent on experimental setup. The

final simulation parameters are listed in Table 4, as presented previously by Byczkowski and Flemming (1996).

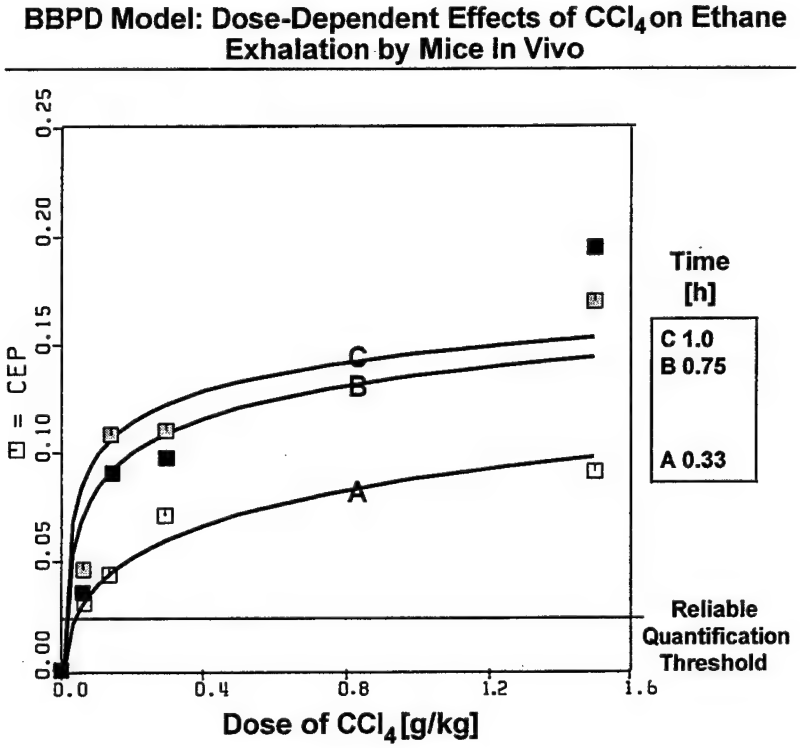

Figure 18. Dose-dependent effects of CCl_4 i.p. on the concentration of ethane exhaled by mice in a closed gas chamber *in vivo,* measured at three different times from treatment (□-0.33,■-0.75, and ■-1.0 h).

Lines (A, B, and C) are computer-generated simulations by the ethane exhalation BBPD sub-model (parameters that describe lipid peroxidation were the same as in Table 3). The respective physiological ethane exhalation values (background) from the same groups of five mice, measured before treatment, were subtracted from the data points. The reliable ethane quantification threshold by the method used was 0.025 ppm (detectibility threshold + 2 SD).

Stochastic Module

The stochastic BBDR module was calibrated with experimental data of Vroegop et al. (1995) for inhibition of amino acid transporter and mitochondrial activity in N 18 neuronal hybridoma cell line in culture, incubated with 6-OH dopamine (Figure 20 A, C) or hydrogen peroxide (Figure 20 B, D), respectively. Optimized simulation parameters are listed in Table 4, as presented previously by Byczkowski and Flemming (1996).

Some data from the literature covered a dose-response characteristics of the wide range of pro-oxidant chemical concentrations, especially when the response kinetics was slow. For such data sets, to discriminate between the targeted and random hit mechanisms using the BBDR sub-model,

it was necessary to express the pro-oxidant chemical concentrations on a logarithmic scale rather than on a linear one (Figure 21).

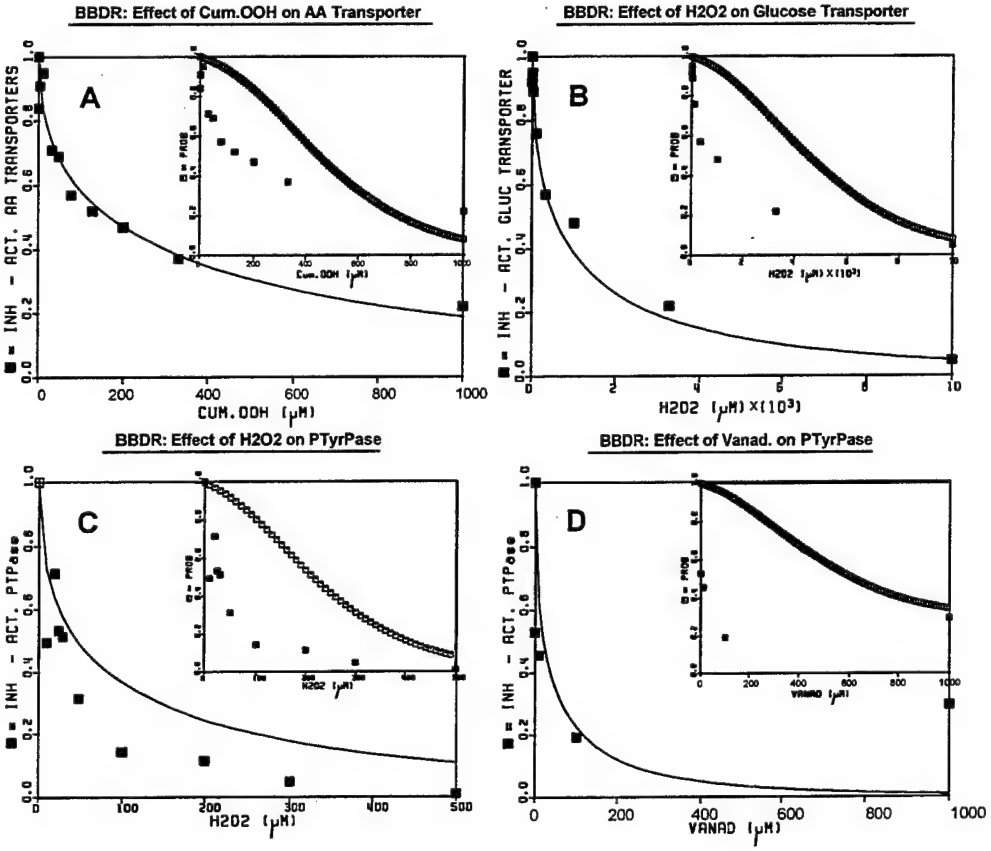

Figure 19. Calibration of the deterministic BBDR module with *in vitro* data for inhibition of cellular targets by free radicals generated by pro-oxidant chemicals. Lines are computer-generated simulations by the deterministic BBDR module. Black squares depict data from the literature. Insets show, for comparison, simulations by the stochastic BBDR module (curves depicted by empty squares) with the same data (black squares). Optimized parameters are listed in Table 4.

A. Effects of different concentrations of cumene hydroperoxide (Cum.OOH [μM]) on activity of amino acid (AA) transporter in N 18 neuronal hybridoma cell line in culture (INH [ratio]) after 1 h (*plus* 1 h preincubation with Cum.OOH; data points from Vroegop et al., 1995). B. Effects of different concentrations of hydrogen peroxide (H_2O_2 [μM]) on activity of glucose transporter (Gluc) in N 18 neuronal hybridoma cell line in culture (INH [ratio]), after 1 h (*plus* 1 h preincubation with H_2O_2; data points from Vroegop et al., 1995). C. Effects of different concentrations of hydrogen peroxide (H_2O_2 [μM]) on activity of protein tyrosine phosphatase (PTyrPase) in rat hepatoma cells in culture (INH [ratio]) after 5 min (*plus* 20 min preincubation with H_2O_2; data points from Heffetz et al., 1990). D. Effects of different concentrations of vanadate (Vanad [μM]) on activity of protein tyrosine phosphatase (PTyrPase) in rat hepatoma cells in culture (INH [ratio]), after 8 min (*plus* 0.5 h preincubation with vanadate; data from Hecht and Zick, 1992).

TABLE 4. PARAMETERS FOR THE BIOLOGICALLY BASED PHARMACODYNAMIC MODEL DESCRIBING THE INHIBITION OF CELLULAR TARGETS BY CHEMICALLY GENERATED FREE RADICALS

Parameter	Description	Numerical value
	Rate constants of FR formation [1/μM/h]	
ki	from Cum.OOH	100.0[a]
ki	from 6OHD	200.0[a]
ki	from H_2O_2, vanadate and pervanadate	18.0[a,f]
ki	from TCE	900.0[b]
	Rate constant of FR quenching [1/μM/h]	
kt	fixed for all biological systems	200.0[c]
	Rate constants of cellular target inhibition [1/μM/h]	
kd	AA transporter	0.075[a]
kd	mitochondria	0.05[a]
kd	Gluc. transporter	0.1[a]
kd	PTyrPase	1.0[f]
	Initial concentration of active targets [%/100]	
I0	assumed value for all biological systems	1.0
	Time of pre-incubation with FR [h]	
tp	Fig 19 A - B	1.0[d]
tp	Fig. 8 B	0.333[e]
tp	Fig. 19 D	0.5[g]
tp	Fig. 19 C	0.333[h]
	Length of experiment [h]	
TSTOP	Fig. 19 A - B	2.0[d]
TSTOP	Fig. 8 B	0.333[e]
TSTOP	Fig. 19 D	0.633[g]
TSTOP	Fig. 19 C	0.42[h]

Abbreviations: Cum.OOH - cumyl hydroperoxide; 6-OHD - 6-hydroxy dopamine; TCE - trichloroethylene; FR - free radicals; AA - amino acids; Gluc. - glucose; PTyrPase - protein tyrosine phosphatase.

[a] fitted to Vroegop et al. (1995).

[b] fitted to Steel-Goodwin et al. (1995).

[c] estimated from Vroegop et al. (1995), Steel-Goodwin et al. (1995), Heffez et al. (1990), and Hecht and Zick (1992).

[d] experimental from Vroegop et al. (1995).

[e] experimental from Steel-Goodwin et al. (1995).

[f] fitted to Heffez et al. (1990) and Hecht and Zick (1992).

[g] experimental from Hecht and Zick (1992).

[h] experimental from Heffez et al. (1990).

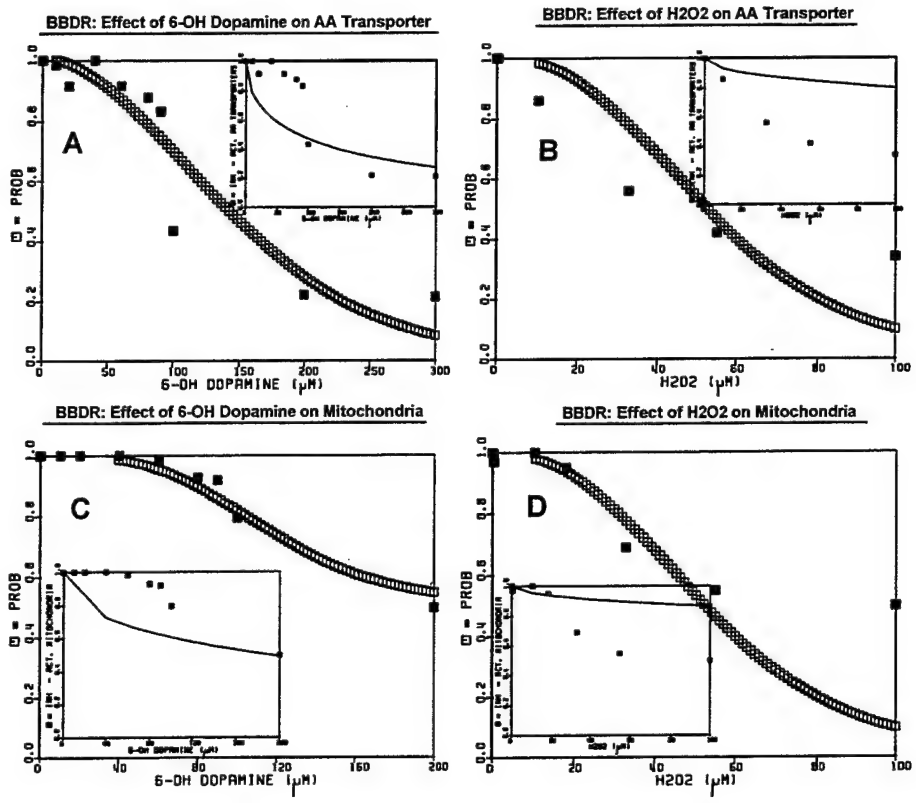

Figure 20. Calibration of the stochastic BBDR module with *in vitro* data for inhibition of cellular targets by free radicals generated by pro-oxidant chemicals. Curves depicted by empty squares are computer-generated simulations by the stochastic BBDR module. Black squares depict data from the literature. Insets show, for comparison, simulations by the deterministic BBDR module (lines) with the same data (black squares). Optimized parameters are listed in Table 4.

A. Effects of different concentrations of 6-hydroxy dopamine (6-OH Dopamine [μM]) on activity of amino acid (AA) transporter in N 18 neuronal hybridoma cell line in culture (PROB [ratio]), after 1 hour (*plus* 1 h preincubation with 6-OH dopamine; data points from Vroegop et al., 1995). B. Effects of different concentrations of hydrogen peroxide (H_2O_2 [μM]) on activity of amino acid transporter (AA) in N 18 neuronal hybridoma cell line in culture (PROB [ratio]), after 1 hour (*plus* 1 h preincubation with H_2O_2; data points from Vroegop et al., 1995). C. Effects of different concentrations of on activity of mitochondrial reduction of MTT (Mitochondria) in N 18 neuronal hybridoma cell line in culture (PROB [ratio]), after 1 hour (*plus* 1 hr preincubation with 6OHD; data points from Vroegop et al., 1995). D. Effects of different concentrations of hydrogen peroxide (H_2O_2 [μM]) on mitochondrial reduction of MTT (Mito) in N 18 neuronal hybridoma cell line in culture (PROB [ratio]), after 1 hour (*plus* 1 hr preincubation with H_2O_2; data points from Vroegop et al., 1995).

For some data of Vroegop et al. (1995), the simulations with BBDR sub-model could not distinguish between the targeted or random hit mechanisms, and both deterministic and stochastic BBDR modules gave an equal "goodness of fit" (Figure 22).

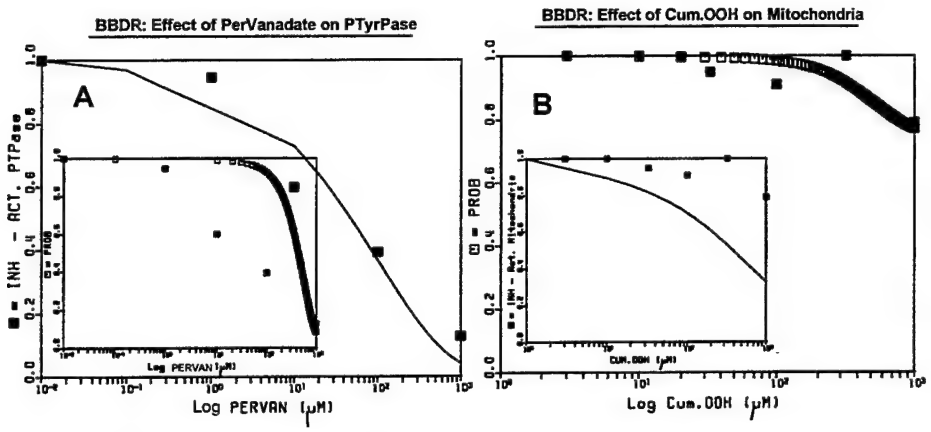

Figure 21. Calibration of the BBPD sub-model with *in vitro* data for inhibition of cellular targets by free radicals generated by pro-oxidant chemicals. Lines are computer-generated simulations by the deterministic BBDR module (A) whereas curves depicted by empty squares are computer-generated simulations by the stochastic BBDR module (B). Black squares depict data from the literature. Insets show, for comparison, simulations by either stochastic (A) or deterministic (B) BBDR modules, with the same data (black squares). Optimized parameters are listed in Table 4.

A. Effects of different concentrations of pervanadate (Pervan. [Log μM]) on the activity of protein tyrosine phosphatase (PTyrPase) in rat hepatoma cells in culture (INH [ratio]), after 15 min (*plus* 0.5 h preincubation with Pervan.; data points from Heffez et al., 1990). B. Effects of different concentrations of cumene hydroperoxide (Cum.OOH [Log μM]) on activity of mitochondrial reduction of MTT (Mitochondria) in N 18 neuronal hybridoma cell line in culture (PROB [ratio]), after 1 h (*plus* 1 h preincubation with 6OHD; data points from Vroegop et al., 1995). Optimized parameters are listed in Table 4.

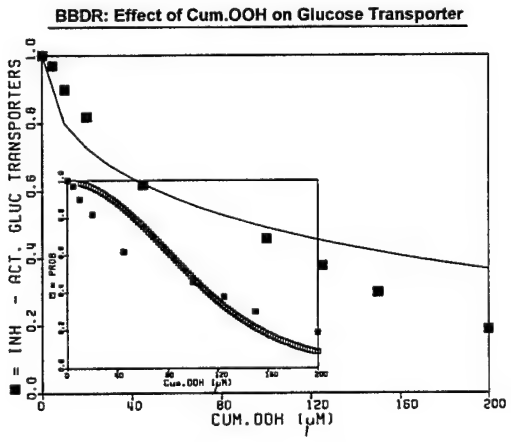

Figure 22. Calibration of the BBPD sub-model with effects of different concentrations of cumene hydroperoxide (PCONC [μM Cum.OOH]) on activity of glucose transporter (GLU) in N 18 neuronal hybridoma cell line in culture (INH [ratio]), after 1 h (*plus* 1 h pre-incubation with Cum.OOH; data points from Vroegop et al., 1995).

The continuous line is a computer-generated simulation by the deterministic BBDR module. Black squares depict data from the literature. Insets show, for comparison, a simulation by the stochastic BBDR module (the curve depicted by empty squares) with the same data (black squares). Optimized parameters are listed in Table 4.

DISCUSSION

PBPD MODEL

Several mathematical models of lipid peroxidation and free radical reactions leading to the oxidative stress were developed and described in the literature (Babbs and Steiner, 1990; Suzuki and Ford, 1994; Antunes et al., 1994; Vroegop et al., 1995). However, none of these models could be applied for dose-response characterization of pro-oxidant chemicals *in vivo*. The purpose of this modeling effort was to provide a quantitative tool, based on biochemical mechanisms, capable of predicting the biological effects of pro-oxidant chemicals (Figure 23).

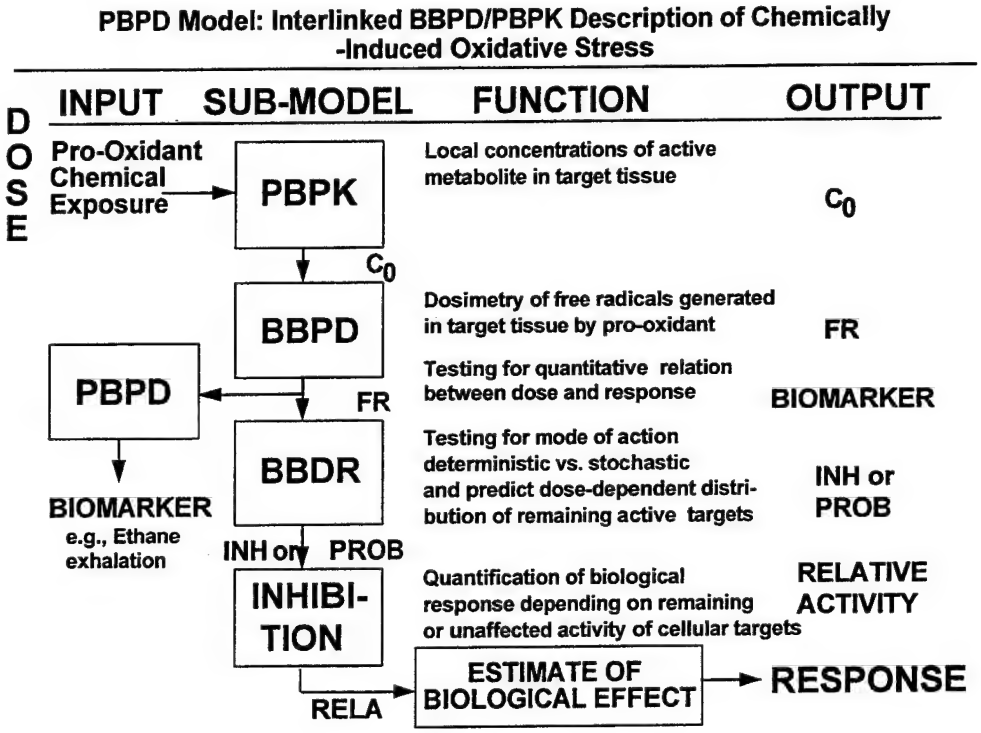

Figure 23. A scheme of PBPD model of chemically induced oxidative stress. For verification of the quantitative PBPD time- and dose-response model for pro-oxidant chemicals, a continuously responding end-point was measured as a biomarker (lipid peroxidation which generates TBARS and ethane).

PBPK - physiologically based pharmacokinetic sub-model; BBPD - biologically based pharmacodynamic sub-model; PBPD - physiologically based pharmacodynamic module; BBDR - biologically based dose-response sub-model.

The resultant PBPD model of chemically induced oxidative stress, consisting of three sub-models (PBPK/PK, BBPD, BBDR) and a PBPD module for ethane exhalation, may be used to predict time- and dose-response of biological systems, both *in vitro* and *in vivo*, to pro-oxidant chemicals, such as volatile chlorinated hydrocarbons (e.g., TCE, CCl_4, or $BrCCl_3$).

Several crucial assumptions were made during the construction of this PBPD model. The PBPK sub-model was built assuming the blood-flow limited delivery of pro-oxidant chemicals (Evans and Andersen, 1995; Kedderis, 1996). This was justified in the case of volatile chlorinated hydrocarbon solvents (Fisher et al., 1991; Gallo et al., 1993; Gargas et al., 1986; Paustenbach et al., 1988), and if needed, the sub-model may be expanded with algorithms involving "diffusion coefficients" for diffusion-limited chemicals (e.g., xenobiotics similar to dioxin; Kohn et al., 1993). The PBPK sub-model may be fitted with other sets of chemical-specific parameters and may be scaled allometrically to simulate local delivery of the pro-oxidant chemical in different animal species (Yang and Andersen, 1994). The PK module can accept pharmacokinetic macro- and micro-constants for two-compartment classical model.

The BBPD sub-model was built on a template of a previously published mathematical model for chemically induced lipid peroxidation in precision-cut liver slices (Byczkowski et al., 1996), assuming a steady-state concentration of pro-oxidant chemical-derived free radicals in the liver over time at each dose level. This assumption does not hold during the initial phase of free radical generation/mixing and during the terminal phase of free radical metabolism/quenching (Figure 24 A) and, therefore, it could not be used for rapid pulses of free radicals. On the other hand, under experimental conditions, the free radical reactions and diffusion rates are very fast (Antunes et al., 1994), so the equilibrium in the biological system is achieved almost instantaneously and, thus, the steady-state approximation gave satisfactory estimates of free radical biological effects in cellular systems (McKenna et al., 1991; Vroegop et al., 1995). Consequently, the local dose of free radicals in the liver was considered as an array (DOS) of sustained steady-state concentrations over time at each pro-oxidant chemical delivered dose (Figure 24 B) ignoring both the initial and the terminal phase (assumed a set of "zero order" functions of FR over time; Figure 24).

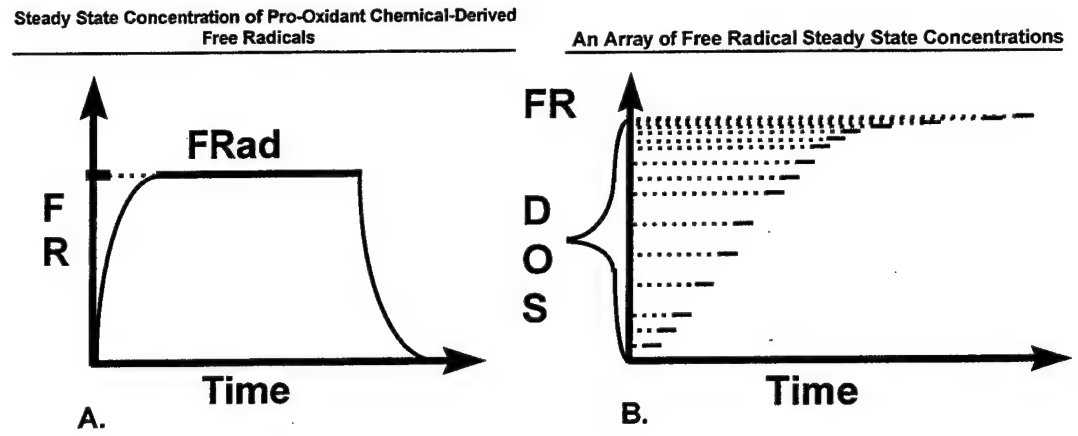

Figure 24. Representations of: A. a steady state concentration of pro-oxidant chemical-derived free radicals (FR_{ad}). B. an array (DOS) of the steady state concentrations of pro-oxidant chemical-derived free radicals (FR_{ad}).

The PBPD module was built as an "upside down" PBPK model for a volatile compound (ethane), assuming its production in the liver only, and the blood-flow limited redistribution (Seckel and Byczkowski, 1996). Obviously, other metabolically competent organs may also generate free radicals from pro-oxidant chemicals and contribute to the ethane production, but since the liver is the most active metabolically (Kulkarni and Byczkowski, 1994a), its contribution is overwhelming.

Once the maximum no-effect concentration of pro-oxidant chemical in the liver (C_{min}) and minimum 100% effective concentration (C_{max}) have been estimated (along with the time needed to accomplish the maximum effect, T_{me}) using the PBPK and BBPD sub-models, the BBDR sub-model was used to simulate and predict the dose-dependent inhibitions of cellular targets. Because in the BBDR sub-model, delivered doses of pro-oxidant chemical in the liver (expressed as initial concentrations, C_0) were set as a discrete variable (with an interval C_Δ), the corresponding steady-state concentrations of free radicals over time were returned by the model as an array (DOS; Figure 24 B). Considering the two possible modes of action of free radicals on cellular targets, deterministic or stochastic, the frequency of hitting targets depended on specificity and homogeneity of interactions (Figure 25). Thus, in the deterministic mode, a specific "shooting" of uniformly susceptible targets by free radicals in a homogenous phase gave a number of interactions (effective hits) proportional to the number of free radicals (Figure 25 A).

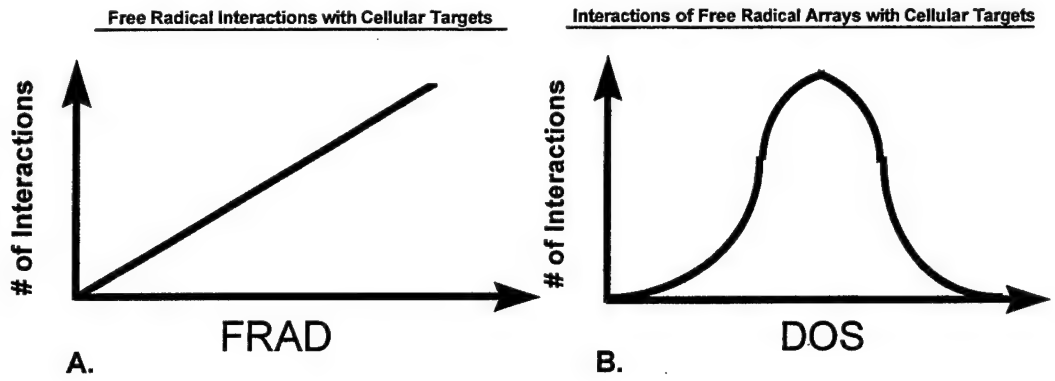

Figure 25. Representations of interaction between: A. steady state concentrations of free radicals (FR_{ad}) and homogenous cellular targets. B. arrays (DOS) of the steady-state concentrations of free radicals and heterogenous cellular targets.

On the other hand, in the stochastic mode, a random "shooting" of differently susceptible targets by free radicals in non-homogenous phases, gave a bell-shape distribution curve of the number of interactions (effective hits) over the arrays of free radicals (Figure 25 B). Assuming that this is a normal distribution, an algorithm for a 1 *minus* cumulative Gaussian distribution function was used in the stochastic module to predict the fraction of remaining active cellular targets, after Vroegop et al. (1995). These assumptions made it possible to distinguish between a specific inhibition of enzymatic or transporting cellular activities (e.g., protein tyrosine phosphatase activity by H_2O_2-derived free radicals; Figure 19 C) and a non-specific inhibition (e.g., mitochondrial reduction of MTT activity by H_2O_2-derived free radicals; Figure 20 D), based on the shape of a dose-response curve fitted to the experimental data.

OXIDATIVE STRESS AND LIPID PEROXIDATION

Pro-oxidant chemicals are bioactivated by CYP (mainly in the liver) to metabolites producing free radicals and initiating lipid peroxidation (Larson and Bull, 1992; Cojocel et al., 1989; Rosen and Rauckman, 1982; Poyer et al., 1978; Burdino et al., 1973). Our EPR spin-trapping study of mouse liver treated *in vitro* with pro-oxidant chemicals confirmed the increased production of free radicals (Steel-Goodwin et al., 1996), but an attempt to use the EPR signal as a quantitative end point to calibrate the production of free radicals from TCE turned to be unsuccessful (Figure 8). On the other hand, TBARS production in the liver was found to be a convenient quantitative end point, following the free radical generation (Figure 10) and lipid peroxidation, and thus, it was used as a biomarker for PBPD model calibrations *in vitro* (Figures 9, 11, and 14).

Riely et al., (1974) have demonstrated that chlorinated hydrocarbons, such as CCl_4, increase ethane exhalation by mice due to lipid peroxidation *in vivo*. Ethane exhalation by animals treated with CCl_4 was enhanced by pretreatment with phenobarbital and suppressed by α-tocopherol (vitamin E), and it was suggested that the formation of carbon trichloromethyl free radical ($CCl_3^{\bullet}$) by CYP in the liver was responsible for initiation of lipid peroxidation (Riely et al., 1974). Bromotrichloromethane, another pro-oxidant chemical from which CYP generates $CCl_3^{\bullet}$, increased ethane exhalation in rats, especially in vitamin E- and selenium-deficient group (Burk and Lane, 1979). However, the same authors postulated also that CCl_4- and $BrCCl_3$-induced lipid peroxidation does not necessarily correlate with liver necrosis, and may be involved at an early stage of hepatotoxicity (Burk and Lane, 1979). Since then, the ethane exhalation test was proved to be a reliable, non-invasive index of oxidative stress in experimental animals and humans (Jeejeebhoy, 1991; Kneepkens et al., 1994), and thus, we used it as a biomarker for PBPD model calibrations *in vivo* (Figures 12, 13, 16, 17, and 18).

On the other hand, despite causing lipid peroxidation as a relatively early event, oxidative stress may actually stimulate cellular proliferation, induce apoptosis, and at a very high dose of pro-oxidant chemical, it may cause necrosis (Byczkowski and Kulkarni, 1996). Some of these biological effects seemed to be mediated by latching into the cellular signal transduction process (Byczkowski and Channel, 1996). Because chemically induced oxidative stress depends on a dose of pro-oxidant chemical, it seemed essential in our study to follow effects of a range of doses of pro-oxidant chemicals on lipid peroxidation (Figures 13, 16, and 17) rather than to check only a time-course at one effective dose, as some other authors have done (Riely et al., 1974; Burk and Lane, 1979).

Comparison of Pro-Oxidant Chemical Concentrations *in vitro* vs. *in vivo*:

Since the original mathematical model for lipid peroxidation was calibrated with $BrCCl_3$ *in vitro* (Tappel et al., 1989), we used the same compound to compare a feasibility of measuring the biomarkers in our biological systems both *in vitro* (Figure 11) and *in vivo* (Figure 12), with a similar range of the pro-oxidant chemical dosage. Assuming that about 99% of the 1 g/kg of $BrCCl_3$ injected i.p., at the highest dose level, will eventually pass through the liver *in vivo*, the total cumulated internal dose (AUC) was estimated as about 2 mg/0.1 g liver over 4 h (or 10 μmol/0.1 g liver/4 h), equivalent to about 2.5 μmol/0.1 g liver/h. This amount would be compatible with the initial concentration of 0.145 to 2.175 μmol/0.1 g liver used *in vitro* (Figure 11). However, even though $BrCCl_3$ partitions preferentially in the blood, its peak concentration in the liver venous blood after the highest dose used reached only about 0.2 mg/L or 1μM

concentration. Considering the liver/blood partitioning of $BrCCl_3$ (0.7), this could produce, at most, the peak concentration of 70 pmol per 0.1 g liver *in vivo*. Actual PBPK sub-model simulations (not shown here) returned the highest sustained local concentrations in mouse of 65 pmol/0.1 g liver. However, since the PBPK sub-model was not validated with experimental data for liver concentrations *in vitro* vs. *in vivo*, these estimates remain tentative. Assuming that the free radical damage to a biological system is additive, the comparison of AUC for internal dose *in vivo* with the initial pro-oxidant concentration *in vitro* seems to be justified for the assessment of biological effects (such as lipid peroxidation).

Effects of Pro-Oxidant Chemicals on Lipid Peroxidation

From our *in vitro* experiments, presented in Figure 11, it appeared that lipid peroxidation is both time- and dose-dependent phenomenon; TBARS generation increased non-linearly with both increasing concentration of $BrCCl_3$ and increasing time of incubation. However, liver slices incubated with the highest $BrCCl_3$ concentration (1.5 mM) for 1 h generated slightly less TBARS than with the lower, 1 mM concentration of $BrCCl_3$ (Figure 11). This decrease is unlikely to be caused by the necrotic action of a high dose of $BrCCl_3$ acting for a prolonged time, since the liver slices were screened for signs of necrosis after the incubation. More probable is a mechanism of CYP suicide-inhibition caused by the accumulated damage to the enzyme by $CCl_3^{\bullet}$ and/or $Br^{\bullet}$ free radicals.

Similarly, $BrCCl_3$ administered *in vivo* showed non-linear time- and dose-dependent characteristics of lipid peroxidation stimulation, measured by ethane exhalation. This appeared from the data presented in Figures 12 and 13 that the maximum no-effect dose of $BrCCl_3$ of about 0.05 g/kg, when measured half an hour after the exposure, dropped to almost 0.025 g/kg after one hour from the exposure. On the other hand, the maximum stimulation of ethane exhalation, measured 1 h after the exposure, was reached at 0.1 g of $BrCCl_3$/kg, while ten times as high a dose of $BrCCl_3$ was still not saturable when measured 0.5 h after the exposure (Figure 12). Even more dramatic differences were noted 2 h after the exposure (Figure 13); at 1g $BrCCl_3$/kg, the ethane exhalation was still at the plateau level (0.33 p.p.m.), while ten times lower a dose (0.1 g $BrCCl_3$/kg) caused twice as high stimulation of ethane exhalation (0.68 p.p.m.).

These results suggest that the extent of chemically induced oxidative stress and effects on lipid peroxidation are linked with both time and dose of $BrCCl_3$ by a non-linear function. The non-linearity may result from limited supply of antioxidants (threshold) and from accumulated over time free radical insult to the CYP enzymatic system (suicidal inhibition). Therefore,

considering biological effects and modeling *in silico* the dose-response for pro-oxidant chemicals, both independent variables (time and dose) were taken into account to assure realistic predictions and the same should be done in future risk characterizations.

Similar characterizations of the dose-response for TCE (Figures 10 and 16) led us to the estimate of an effective dose-response range of the local liver concentrations between 0.5 mM and 50 mM (or 0.05 to 5.0 μmol/0.1 g liver), and a maximum "no observable effect" dose of TCE *in vivo* (for up to 1 h) above 0.26 g/kg. These estimates suggested that TCE is about an order of magnitude less potent a pro-oxidant than $BrCCl_3$ (based on a mg of mass comparison). On the other hand, CCl_4 had a pro-oxidant potency similar to that of $BrCCl_3$ (Figures 14 and 17).

Parameters of lipid peroxidation and the feasibility of square root algorithm, which links concentration of pro-oxidant with production of free radicals, were determined in our experiments with mouse liver slices treated *in vitro* with TCE, CCl_4, and $BrCCl_3$. The calibrated algorithms and the parameters estimated *in vitro* were included in the PBPD model simulations of time- and dose-dependent effects of different doses of pro-oxidant chemicals on ethane exhalation in B6C3F1 mice *in vivo* (Figures 16 and 18 show examples of TCE and CCl_4 effects *vs* model predictions). It seems that the PBPD model described kinetics and dynamics of chemically induced lipid peroxidation relatively well, at least for TCE and CCl_4.

EFFECTS OF FREE RADICALS ON CELLULAR TARGETS

Cellular effects of oxidative stress and free radical insult to cellular targets are well described in the literature (Byczkowski and Gessner, 1988; Kulkarni and Byczkowski, 1994a; 1994b; Byczkowski and Channel, 1996; Byczkowski and Kulkarni, 1996). Depending on the biochemical mechanism, the effects may include inhibition of enzymatic activities, inhibition of cellular transporter activities, uncoupling of oxidative phosphorylation and inhibition of the respiratory chain, interference with cellular membrane receptors and signal transduction pathway, deregulation of transcription and gene expression, and damage to vital macromolecules (lipids, proteins, and DNA). Cellular mechanisms and problems associated with risk characterization of pro-oxidant chemicals were reviewed in detail in the previous report by Byczkowski and Flemming (1995). Essentially, the interaction of pro-oxidant derived free radicals with cellular targets may be either specific (uniformly susceptible targets, suspended in the same phase as free radicals) or random (differently susceptible targets, or suspended in non-homogenous phases). The specific interactions were adequately described by deterministic module of our BBDR sub-

model (Figures 19 and 21), whereas random interactions were relatively well simulated by the stochastic module (Figures 20 and 21).

Setting a Hypothesis with the PBPD Model

There is growing body of evidence that pro-oxidant chemicals and oxidative stress can interfere with cellular signal transduction pathway (Byczkowski and Channel, 1996). Chen and Chan (1993) using 3T3-L1 cells, cultured in a serum-free medium, demonstrated that pro-oxidant chemicals (e.g., orthovanadate or DMNQ) increased [^{3}H]thymidine incorporation to DNA and enhanced expression of the c-*fos* gene. The authors suggested that pro-oxidant compounds, causing oxidative stress, increased tyrosine protein phosphorylation early in the signal transduction cascade, leading to augmentation of cell proliferation (Chen et al., 1990; Chen and Chan, 1993). This effect may be accounted for by a selective effect on redox-sensitive protein tyrosine phosphatase (PTyrPase). Typically, PTyrPases contain a nucleophilic cysteinyl residue in their catalytic center (Stone and Dixon, 1994) and their enzymatic activities are rapidly inhibited by small disulfides (Ziegler, 1985). It seems that the cysteinyl residue must be kept in the reduced -SH form, therefore, thiol-directed reagents that oxidize it cause inhibition of PTyrPases (Fischer et al., 1991).

Accordingly, Mendelson et al., (1996) demonstrated that oxidative stress caused by CCl_4 in the liver, activated the *JNK* family of protein kinases and increased the AP-1 transcription factor binding to DNA. Because mitogen activated kinases (MAPK) must be kept phosphorylated to transmit this effect, it is possible, that inhibition of PTyrPase may stop deactivation of phosphatase MKP-1 which has high affinity for phosphorylated p38 as a substrate. This, in turn, may cause a rapid dephosphorylation of p38, which was down-regulated following the oxidative stress (Mendelson et al., 1996).

Since a similar subversion of signal transduction was suggested for TCE (Maronpot et al., 1995) but was never proved, it is possible that TCE-derived free radicals can affect intracellular redox potential and may lead to the inhibition of PTyrPase activity by causing oxidation of essential cysteinyl thiols. Our EPR spin trapping experiments confirmed the presence of free radicals in TCE-treated liver, but failed to reveal their identity (Steel-Goodwin et al., 1995; 1996). Assuming that the TCE-derived free radicals are well water-soluble (Gonthier and Barret, 1989; Mason, 1992; Ni et al., 1994), they should interact with PTyrPase suspended in the same phase as free radicals, in a specific way (the cysteinyl -SH residues represent uniformly susceptible targets). If this is the case, within the relevant TCE local concentrations in the liver, an

exponential inhibition of PTyrPase should be observed with a 50% inhibitory concentration around 0.5 mM (0.05 μmol TCE/0.1 g liver), as predicted by the BBDR sub-model. However, if only lipid-soluble secondary and tertiary, lipid peroxide-derived free radicals are available in the liver, they should result in a non-specific random inhibition of PTyrPase, giving a sigmoidal, dose-response with a 50% inhibitory concentration around 22.0 mM (2.2 μmol TCE/0.1 g liver; Figure 26).

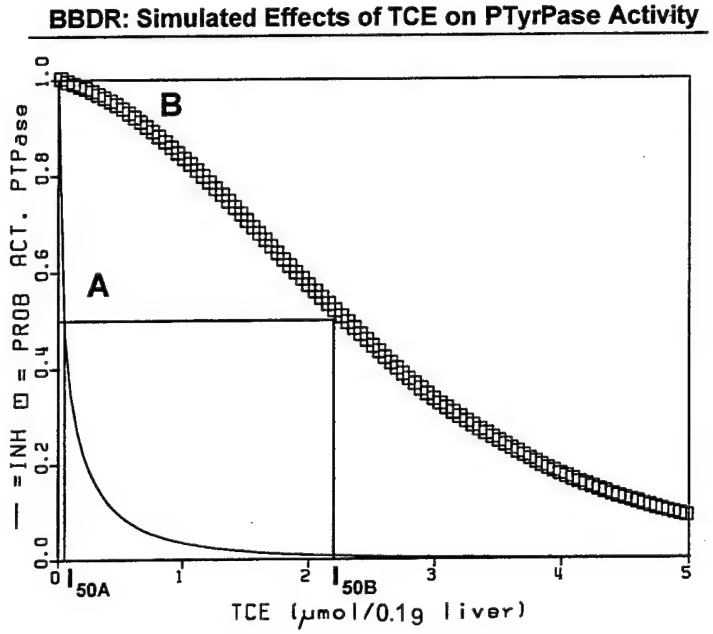

Figure 26. The results of BBDR sub-model simulations of the expected inhibition of protein tyrosine phosphatase activity in the liver of mice *in vivo* after treatment with the estimated, effective pro-oxidant range of TCE doses (resulting in the local concentrations between C_{min} = 0.05 and C_{max} = 5.0 μmol TCE/0.1 g liver; other parameters are listed in Table 4).

TCE - local concentration of TCE in the liver [μmol/0.1 g liver]. A. INH - remaining percentage of uninhibited activity by the deterministic BBDR module (x 10^2); I_{50A} - 50% inhibitory concentration (0.05 μmol TCE/0.1 g liver). B. PROB - remaining percentage of uninhibited activity by the stochastic BBDR module (x 10^2); I_{50B} - 50% inhibitory concentration (2.2 μmol TCE/0.1 g liver).

Deterministic and stochastic PBPD model theoretical simulations (unconfirmed experimentally) of the remaining percentage of the enzymatic activity of protein tyrosine phosphorylase in the liver inhibited by TCE-derived free radicals specifically (Figure 26 A) and nonspecifically (Figure 26 B) showed quite different dose-dependent characteristics and different by two orders of magnitude I_{50} values, within the relevant range of TCE concentrations. Which dose-response profile will actually occur remains to be seen, but it was possible with the aim of the

PBPD model to simulate the predicted outcome within the relevant, internal pro-oxidant dosage of TCE, and set a verifiable working hypothesis for the future experimental research.

CONCLUSION

The resultant PBPD hybrid model may be used for pharmacodynamic description of chemically-induced oxidative stress in mice, for planning the future experiments and setting the verifiable working hypotheses, and potentially may be useful for a risk characterization.

ACKNOWLEDGMENTS

The authors gratefully acknowledge the expert assistance of Maj (Dr.) S. Bachowski in parametrization of PBPK sub-model for CCl_4 with the data from literature, Maj (Dr.) L. Steel-Goodwin who performed the EPR spectroscopy analysis and TSgt R. Black, TSgt J. McCafferty, and Ms. C. Seckel who determined partition coefficients. This research was supported in part by the Department of the Air Force Environmental Initiative Program, AFOSR Work Unit 2312A202.

REFERENCES

Antunes F., A. Salvador, H.S. Marinho, and R.E. Pinto. 1994. A mathematical model for lipid peroxidation in inner mitochondrial membrane. Travaux de Laboratoire 33[suppl. T-1]:1-52.

Arterbery, V.E, W.A. Pryor, L. Jiang, S.S. Sehnert, W.M. Foster, R.A. Abrams, J.R. Williams, M.D. Wharam, Jr, and T.H. Risby. 1994. Breath ethane generation during clinical total body irradiation as a marker of oxygen-free-radical-mediated lipid peroxidation: a case study. Free Radical Biol. Med. 17:569-576.

Babbs C.F. and M.G. Steiner. 1990. Simulation of free radical reactions in biology and medicine: a new two-compartment kinetic model of intracellular lipid peroxidation. Free Radical Biol. Med. 8:471-485.

Biasi, F., M. Bosco, G. Lafranco, and G. Poli. 1995. Cytolysis does not per se induce lipid peroxidation: evidence in man. Free Radical Biol. Med. 18:909-912.

Bray, T.M. and W.J. Bettger. 1990. The physiological role of zinc as an antioxidant. Free Radical Biol. Med. 8:281-291.

Brendel, K.L, R.L. Fisher, C.L. Krumdieck, and A.J. Gandolfi. 1993. Precision-cut rat liver slices in dynamic organ culture for structure-toxicity studies. Methods Toxicol. 1A:222-226.

Brendel, K.L., A.J. Gandolfi, C.L. Krumdieck, and P.F. Smith. 1987. Tissue slicing and culture revisited. Trends Pharmacol. Sci. 8:12-15.

Buettner, G.R. 1987. Spin trapping: ESR parameters of spin adducts. Free Radicals Biol. Medicine 3: 259-303.

Burdino, E., E. Gravela, G. Ugazio, V. Vannini, and A. Calligaro. 1973. Initiation of free radical reactions and hepatotoxicity in rats poisoned with carbon tetrachloride or bromotrichloromethane. Agents Actions 4:244-253.

Burk, R.F. and J.M. Lane. 1979. Ethane production and liver necrosis in rats after administration of drugs and other chemicals. Toxicol. Appl. Pharmacol. 50:467-478.

Byczkowski, J.Z. and S.R. Channel. 1996. Chemically-induced oxidative stress and tumorigenesis: effects on signal transduction and cell proliferation. Toxic Subst. Mechan.15:101- 128.

Byczkowski, J.Z., S.R. Channel, and T.L. Pravecek. 1995. Development and experimental calibration of the mathematical model of lipid peroxidation in mouse liver slices. Tech. Report, AL/OE-TR-0179.

Byczkowski, J.Z, S.R. Channel, T.L. Pravecek, and C.R. Miller. 1996. Mathematical model for chemically induced lipid peroxidation in precision-cut liver slices: computer simulation and experimental calibration. Comp. Meth. Progr. Biomed. 50: 73-84.

Byczkowski, J.Z. and C.D. Flemming. 1995. Mathematical modeling of oxidative stress in vitro. Toxic Hazards Res. Unit Ann. Rep. No. AL/OE-TR-1996-0132.

Byczkowski, J.Z. and C.D. Flemming. 1996. Computer-aided dose-response characteristics of chemically initiated oxidative stress in vitro. 35th Annual Meeting of the Society of Toxicology, Anaheim, CA. Toxicologist 30: 240 (1227).

Byczkowski, J.Z., C.D. Flemming, C.R. Miller, W.J. Schmidt, and C.S. Seckel. 1996. Development and experimental calibration of biologically based dose-response model for oxidative stress. Society for Risk Analysis Annual Meeting, New Orleans, LA, Final Program, pp. 89, F1.03.

Byczkowski, J.Z. and T. Gessner. 1988. Biological role of superoxide ion-radical. Int. J. Biochem. 20: 569-580.

Byczkowski, J.Z. and A.P. Kulkarni. 1996. Pro-oxidant biological effects of inorganic components of petroleum: vanadium and oxidative stress. AL/OE-TR-1996-0126.

Channel, S.R., J.Z. Byczkowski, W.J. Schmidt, and C.R. Miller. 1997. Experimental verification of the mathematical model of trichloroethylene-induced lipid peroxidation in mouse liver slices. 36th SOT Annual Meeting, Cincinnati, OH. Toxicologist 36: 297 (1511).

Chen, Y. and T.M. Chan. 1993. Orthovanadate and 2,3-dimethoxy-1,4-naphtoquinone augment growth factor-induced cell proliferation and c-fos gene expression in 3T3-L1 cells. Arch. Biochem. Biophys. 305: 9-16.

Chen, Y.X., D.C. Yang, A.B. Brown, Y. Jeng, A. Tatoyan, and T.M. Chan. 1990. Activation of a membrane-associated phosphatidylinositol kinase through tyrosine-protein phosphorylation by naphtoquinones and orthovanadate. Arch. Biochem. Biophys. 238: 184-192.

Cojocel, C., W. Beuter, W. Muller, and D. Mayer. 1989. Lipid peroxidation: a possible mechanism of trichloroethylene-induced nephrotoxicity. Toxicology 55:131-141.

Comporti, M. 1985. Biology of disease, lipid peroxidation and cellular damage in toxic liver injury. Lab. Invest. 53:599-623.

Das, S.G., J.Z. Byczkowski, and J.W. Fisher. 1994. Probability analysis of TCE cancer bioassay data in the B6C3F1 mice using PBPK/PBPD modeling: a conceptual framework. Soc. for Risk Analysis Ann. Conf. and Expo., Final Program Abstracts, Baltimore, MD.

de Groot, H. and A. Littauer. 1989. Hypoxia, reactive oxygen, and cell injury. Free Radical Biol. Med. 6:541-551.

Evans, M.V. and M. Andersen. 1995. Sensitivity analysis and the design of gas uptake inhalation studies. Inhalation Toxicol. 7:1075-1094.

Evans, M.V., W.D. Crank, H.-M. Yang, and J.E. Simmons. 1994. Applications of sensitivity analysis to physiologically based pharmacokinetic model for carbon tetrachloride in rats. Toxicol. Appl. Pharm. 128: 36-44.

Finley, J.W. and M.S. Otterburn. 1993. The consequences of free radicals in foods. Toxicol. Ind. Health. 9: 77-91.

Fischer, E.H., H. Charbonneau, and N.K. Tonks. 1991. Protein tyrosine phosphatases: a diverse family of intracellular and transmembrane enzymes. Science 253:401-406.

Fisher, J.W., M.L. Gargas, B.C. Allen, and M.E. Andersen. 1991. Physiologically based pharmacokinetic modeling with trichloroethylene and its metabolite, trichloroacetic acid, in the rat and mouse. Toxicol. Appl. Pharmacol.109:183-195.

Gallo, J.M., LL. Cheung, H.J. Kim, J.V. Bruckner, and W.R. Gillespie. 1993. A physiological and system analysis hybrid pharmacokinetic model to characterize carbon tetrachloride blood concentrations following administration in different oral vehicles. J. Pharmacokinet. Biopharm. 21:551-574.

Gardner, H.W. 1989. Oxygen radical chemistry of polyunsaturated fatty acids. Free Radical Biol. Med. 7:65-86.

Gargas, M.L. 1988. Tissue solubilities and biotransformation rates of halocarbons: experimental determinations and quantitative modeling. Ph.D. Dissertation, Wright State University, Dayton, OH.

Gargas, M.L., M.E. Andersen, and H.J. Clewell III. 1986. A physiologically based simulation approach for determining metabolic constants from gas uptake data. Toxicol. Appl. Pharmacol. 86:341-352.

Gargas, M.L., R.J. Burgess, D.E. Voisard, G.H. Cason, and M.E. Andersen. 1989. Partition coefficients of low-molecular-weight volatile chemicals in various liquids and tissues. Toxicol. Appl. Pharmacol. 97:87-99.

Gonthier B.P. and L.G. Barret. 1989. In-vitro spin-trapping of free radicals produced during trichloroethylene and diethylether metabolism. Toxicol. Lett. 47:225-134.

Gower, J.D. 1988. A role for dietary lipids and antioxidants in the activation of carcinogens. Free Radical Biol. Med. 5: 95-111.

Guilbaud, R., A.C. Ricard, C. Daniel, S. Boileau, H.V. Tra, and G. Chevalier. 1994. A method to evaluate lipid peroxidation by automated analysis of exhaled pentane in human and rat breath. Toxicology Methods 4:1-11.

Haegele, A.D., S.P. Briggs, and H.J. Thompson. 1994. Antioxidant status and dietary lipid unsaturation modulate oxidative DNA damage. Free Radical Biol. Med. 16:111-115.

Hecht, D. and Y. Zick. 1992. Selective inhibition of protein tyrosine phosphatase activities by H_2O_2 and vanadate in vitro. Biochem. Biohys. Res. Comm. 188:773-779.

Heffetz, D., I. Bushkin, R. Dror, and Y. Zick. 1990. The insulinomimetic agents H_2O_2 and vanadate stimulate protein tyrosine phosphorylation in intact cells. J. Biol. Chem. 265: 2896-2902.

ILSI, RSI, International Life Sciences Institute, Risk Science Institute. 1994. Physiological Parameter Values for PBPK Models (Brown R, editor). A report prepared by ILSI, RSI under the cooperative agreement with the U.S. Environmental Protection Agency Office of Health and Environmental Assessment, Washington, DC.

Janero, D.R. 1990. Malondialdehyde and thiobarbituric acid-reactivity as diagnostic indices of lipid peroxidation and peroxidative tissue injury. Free Radical Biol. Med. 9:515-540.

Jeejeebhoy, K.N. 1991. In vivo breath alkane as an index of lipid peroxidation. Free Radical Biol. Med. 19:191-193.

Kappus, H. 1986. Overview of enzyme systems involved in bio-reduction of drugs and in redox cycling. Biochem. Pharmacol. 35:1-6.

Kazui, M., K.A. Andreoni, E.J. Norris, A.S. Klein, J.F. Burdick, C. Beattie, S.S. Sehnert, W.R. Bell, G.B. Bulkley, and T.H. Risby. 1992. Breath ethane: a specific indicator of free-radical-mediated lipid peroxidation following reperfusion of the ischemic liver. Free Radical Biol. Med. 13:509-515.

Kedderis, G.L. 1996. Hepatic blood flow limitation of the bioactivation of hazardous chemical air pollutants. Fund. Appl. Toxicol. 30:34-35.

Kehrer, J.P. 1993. Free radicals as mediators of tissue injury and disease. Crit. Rev. Toxicol. 23: 21-48.

Kneepkens, C.M., G. Lepage, and C.C. Roy. 1994. The potential of the hydrocarbon breath test as a measure of lipid peroxidation. Free Radical Biol. Med. 17:127-160.

Kohn, M.C., G.W. Lucier, G.C. Clark, C. Sewall, A.M. Tritscher, and C.J. Portier. 1993. A mechanistic model of effects of dioxin on gene expression in the rat liver. Toxicol. Appl. Pharmacol. 120:138-154.

Krumdieck, C.L., J.E. Dos Santos, and K.J. Ho. 1980. A new instrument for the rapid preparation of tissue slices. Analyt. Biochem. 104:118-123.

Kulkarni, A.P. and J.Z. Byczkowski. 1994a. Hepatotoxicity. In: Introduction to Biochemical Toxicology (Hodgson, E. and P.E.Levi, eds.), pp. 459 - 490, Appleton & Lange, Norwalk, CT.

Kulkarni, A.P. and J.Z. Byczkowski. 1994b. Effects of transition metals on biological oxidations. In: Environmental Oxidants (Nriagu, J.O., and M. Simmons, Eds.), pp. 475-496, John Eiley & Sons, Inc., New York, NY.

Larson J.L. and R.J. Bull. 1992. Metabolism and lipoperoxidative activity of trichloroacetate and dichloroacetate in rats and mice. Toxicol. Appl. Pharmacol.115:268-277.

Maronpot, R.R., C.H. Anna, T.R. Devereux, G.W. Lucier, B.E. Butterworth, and M.W. Anderson. 1995. Considerations concerning the murine hepatocarcinogenicity of selected chlorinated hydrocarbons. Prog. Clin. Biol. Res. 391:305-323.

Mason, R.P. 1992. Free radical metabolites of toxic chemicals and drugs as sources of oxidative stress. In: Biological Consequences of Oxidative Stress (Spatz, L, and A.D. Bloom, editors), pp. 23-49, Oxford University Press, New York, NY.

McKenna R., F.J. Kezdy, and D.E. Epps. 1991. Kinetic analysis of the free-radical-induced lipid peroxidation in human erythrocyte membranes: evaluation of potential antioxidants using cis-parinaric acid to monitor peroxidation. Anal. Biochem.196:443-450.

Mendelson, K.G., L.R. Contois, S.G. Tevosian, R.J. Davis, and K.E. Paulson. 1996. Independent regulation of JNK/p38 mitogen-activated protein kinases by metabolic oxidative stress in the liver. Proc. Natl. Acad. Sci. USA. 93:12908-12913.

Mitchell and Gauthier Associates, Inc. 1993. Advanced Continuous Simulation Language (ACSL). Reference Manual. Concord, MA.

Ni Y.C., T.Y. Wong, F.F. Kadlubar, and P.P. Fu. 1994. Hepatic metabolism of chloral hydrate to free radical(s) and induction of lipid peroxidation. Biochem. Biophys. Res. Comm. 204:937-943

Papas, A.M. 1993. Oil-soluble antioxidants in foods. Toxicol. Ind. Health. 9: 123-149.

Paustenbach, D.J., G.P. Carlson, J.E. Christian, and G.S. Born. 1986. A comparative study of the pharmacokinetics of carbon tetrachloride in the rat following repeated inhalation exposures of 8 and 11.5 hr/day. Fund. Appl. Toxicol. 6:484-497.

Paustenbach, D.J., H.J. Clewell III, M.L. Gargas, and M.E. Andersen. 1988. A physiologically based pharmacokinetic model for inhaled carbon tetrachloride. Toxicol. Appl. Pharmacol. 96: 191 - 211.

Poyer, J.L., R.A. Floyd, P.B. McCay, E.G. Janzen, and E.R. Davis. 1978. Spin trapping of the trichloromethyl radical produced during enzymatic NADPH oxidation in the presence of carbon tetrachloride and bromotrichloromethane. Biochim. Biophys. Acta 539:402-409.

Pratt, D.E. 1993. Antioxidants indigenous to foods. Toxicol. Ind. Health. 9: 63-75.

Refat, M., T.J. Moore, M. Kazui, T.H. Risby, J.A. Perman, and K.B. Schwartz. 1991. Utility of breath ethane as a noninvasive biomarker of vitamin E status in children. Pediatr. Res. 30:396-403.

Riely, C.A., G.A. Cohen, and M. Lieberman. 1974. Ethane evolution: a new index of lipid peroxidation. Science 183:208-210.

Roberfroid, M. and P.B. Calderon. 1994. Free Radicals and Oxidation Phenomena in Biological Systems. Marcel Dekker, Inc., New York, NY.

Rosen, G.M. and E.J. Rauckman. 1982. Carbon tetrachloride-induced lipid peroxidation: a spin trapping study. Toxicol. Lett. 10:337-344.

Sagai, M. and T. Ichinose. 1980. Age-related changes in lipid peroxidation as measured by ethane, ethylene, butane and pentane in respired gases of rats. Life Sci. 27:731-738.

Sanzgiri, U.Y., H.J. Kim, S. Muralidhara, C.E. Dallas, and J.V. Bruckner. 1995. Effect of route and pattern of exposure on the pharmacokinetics and acute hepatotoxicity of carbon tetrachloride. Toxicol. Appl. Pharmacol. 134:148-154.

Seckel, C.S. and J.Z. Byczkowski. 1996. Experimental parameters to support a pharmacodynamic model for ethane exhalation. 35th Annual Meeting of the Society of Toxicology, Anaheim, CA. Toxicologist 30: 244 (1247).

Sipes, I.G., R.L. Fisher, P.F. Smith, E.R. Stine, A.J. Gandolfi, and K. Brendel. 1987. A dynamic liver culture system: a tool for studying chemical biotransformation and toxicity. Arch. Toxicol. Suppl. 11:20-33.

Smith, C.V. 1991. Correlations and apparent contradictions in assessment of oxidant stress status in vivo. Free Radical Biol. Med. 10:217-224.

Stadtman, E.R., C.N. Oliver, P.E. Starke-Reed, and S.G. Rhee. 1993. Age-related oxidation reaction in proteins. Toxicol. Ind. Health. 9: 187-196.

Steel-Goodwin, L., T.L. Pravecek, B.L. Hancock, W.J. Schmidt, S.R. Channel, D. Bartholomew, C.T. Bishop, M.M. Ketcha, and A.J. Carmichael. 1995. Trichloroethylene: free radical studies in B6C3F1 mouse liver slices. 34th Annual Meeting of the Society of Toxicology, Baltimore, MD, Toxicologist 15:30 (161).

Steel-Goodwin, L., A.J. Carmichael, W.W. Schmidt, C. Miller, and J.Z. Byczkowski. 1996. Quantitation of free radicals in B6C3F1 mouse liver slices on exposure to four chemical carcinogens: an EPR/spin trapping study. 35-th Annual Meeting of the Society of Toxicology, Anaheim, CA. Toxicologist 30: 243 (1246).

Steiner, E.C., T.D. Rey, and P.S. McCroskey. 1990. Simusolv Reference Guide. Modeling and simulation software. The Dow Chemical Company, Midland, MI.

Stone, R.L. and J.E. Dixon. 1994. Protein-tyrosine phosphatases. J. Biol. Chem. 269: 31323-31326.

Suzuki Y.J. and G.D. Ford. 1994. Mathematical model supporting the superoxide theory of oxygen toxicity. Free Radical Biol. Med.16:63-72.

Taffe, B.G., Takahashi, N., Kensler,T.W., and R.P. Mason. 1987. Generation of free radicals from organic hydroperoxide tumor promoters in isolated mouse keratinocytes. Formation of alkyl and alkoxyl radicals from tert-butyl hydroperoxide and cumene hydroperoxide. J. Biol. Chem. 262:12143-12149.

Tappel, A.L., A.A. Tappel, and C.G. Fraga. 1989. Application of simulation modeling to lipid peroxidation process. Free Radical Biol. Med.7:361-368.

Timmins, G.S. and M.J. Davies. 1993. Free radical formation in isolated murine keratinocytes treated with organic peroxides and its modulation by antioxidants. Carcinogenesis 14:1615-1620.

Trush, M.A. and T.W. Kensler. 1991. An overview of the relationship between oxidative stress and chemical carcinogenesis. Free Radical Biol. Med. 10:201-209.

Videla, L.A., Barros S.B.M., and V.B.C. Junquiera. 1990. Lindane-induced liver oxidative stress. Free Radical Biol. Med. 9:169-179.

Vroegop, S.M., D.E. Decker, and S.E. Buxser. 1995. Localization of damage induced by reactive oxygen species in cultured cells. Free Radical Biology and Medicine 18:141-151.

Williams, G.M. 1993. Inhibition of chemical-induced experimental cancer by synthetic phenolic antioxidants. Toxicol. Ind. Health. 9: 303-308.

Willis, R.J. 1980. Possible role of endogenous toxigenic lipids in the carbon tetrachloride poisoned hepatocyte. Federation Proc. 39:3134-3137.

Yang, S.H. and M.E. Andersen. 1994. Pharmacokinetics. In: Introduction to Biochemical Toxicology (Hodgson, E. and P.E. Levi, eds.), pp. 49 -73, Appleton & Lange, Norwalk, CT.

Ziegler, D.M. 1985. Role of reversible oxidation-reduction of enzyme thiols-disulfides in metabolic regulation. Ann. Rev. Biochem. 54: 305-329.

APPENDIX: Source Codes of PBPD Model Written in ACSL®

• PBPD Sub-Model

Sub-Model for Pro-Oxidant Induced Lipid Peroxidation *.CSL FILE

```
'This PBPD sub-model predicts ethane exhalation by mice in a closed '
'chamber after dosing with CCl4, TCE and BrCCl3 based on TBARS'
'model published by Byczkowski et al., 1996; interlinked with '
'PBPK/TCPK sub-model Das et al., 1994 and Seckel and Byczkowski'
'1996. Final version 1/03/97                '

PROGRAM: PBPD FOR P-OX-INDUCED OXIDATIVE STRESS

INITIAL

LOGICAL    CC          $'Flag set to .TRUE. for closed chamber runs      '

'     Miscellaneous commands                                             '
CONSTANT   CC = .true.     $'Default to close chamber                    '
CONSTANT PBPK = 1.         $'Default to interlink with PBPK model        '
'                          to use two-compartment CPK switch PBPK=0.     '
CONSTANT   CPK= 0.         $'Switch CPK=1 to use two-compartment PK      '

 'PEROXIDATION PARAMETERS FOR LIVER [per 0.1 g of liver]                 '

 CONSTANT    PUF    =  7.0       $'[micromol/0.1 g liver]               '
 CONSTANT    PXZLUF=  12.0       $'peroxidizability of PUFA L[1/h]      '
 CONSTANT    PXZHUF=  24.0       $'peroxidizability of PUFA H[1/h]      '
 CONSTANT    ANOX1 =  0.0037     $'Vit.E antiox[mcmol/0.1g liv]         '
 CONSTANT    ACT1  =  0.0003     $'activator1[mcmol cytP450/0.1gliv]    '
 CONSTANT    GSH   =  0.6        $'glutathione [mcmol/0.1 g liver]      '
 CONSTANT    PXTTBA=  0.1        $'yield of TBARS/mol hydroperoxide     '
 CONSTANT    LPUF  =  3.         $'LA-derivative PUFA[mcmol/0.1 g]      '
 CONSTANT    HPUF  =  4.         $'HA-derivative PUFA[mcmol/0.1 g]      '
 CONSTANT    ANOX2 =  0.         $'non-Vit.E antiox[mcmol/0.1 g liv]    '
 CONSTANT    ANOX3 =  0.         $'added antioxidant[mcmol/0.1g liv]    '
 CONSTANT    EFANO1 = 1.         $'effectiveness of Vit.E               '
 CONSTANT    EFANO2 = 0.         $'effectiveness of non-Vit.E a-o       '
 CONSTANT    EFANO3 = 0.         $'effectiveness of added a-o           '
 CONSTANT    ANOXUF = 2.         $'antioxidant use factor [1/mcmol]     '
 CONSTANT    ACT2   = 0.         $'activator 2 [mcmol/0.1 g liver]      '
 CONSTANT    ACACT1 = 1.         $'activity of activator 1              '
 CONSTANT    ACACT2 = 0.         $'activity of activator 2              '
 CONSTANT    ACTDGF = 1.75       $'activator degradation fctr [1/mcmol] '
 CONSTANT    IND2   = 0.         $'inducer2[mcM chemical/0.1g liv]      '
 CONSTANT    PTIND1 = 4408.      $'potency of inducer 1 [1/mcmol]       '
 CONSTANT    PTIND2 = 0.         $'potency of inducer 2 [1/mcmol]       '
 CONSTANT    INDLF  = 0.0001     $'inducer loss factor [1/h]            '
 CONSTANT    PXRATE = 0.00029    $'peroxidation rate [mcmol/mcmol]      '
 CONSTANT    AUTOXF = 0.00013    $'autooxidation factor [1/h]           '
 CONSTANT    GPENZA = 1.         $'glutathione peroxidase[1/mcmol]      '
 CONSTANT    PXREDF = 0.17       $'hydroperoxide reduction factor [1/h] '
 CONSTANT    PHYSPX = 0.         $'physiological levels of Hperoxides   '
 CONSTANT    ANREG  = 0.0007     $'antioxidant regenerated in situ      '
 CONSTANT    ANOXR  = 0.001      $'antioxidant regeneration rate constant'
 CONSTANT    BCKGD  = 0.0        $'TBARS in control [mcm/0.1 g]         '
 CONSTANT    ACR    = 0.025      $'activator degradation rate constant  '

 'TIMING COMMANDS                                                        '
```

```
 CONSTANT    POINTS = 200.
 CINT=TSTOP/POINTS
CONSTANT  TCHNG = 4.0   $'Length of inhalation exposure to P-Ox [h]     '
CONSTANT   TINF = 0.01  $'Length of IV infusion with P-Ox [h]          '

'repeated gavage dosing                                                '
constant   DAYS=0.08333 $'Duration of simulation [DAYS] if pdays=0.    '
constant   pdays=0.     $'No-gavage days in cycle                      '

 'PARAMETERS FOR MOUSE IN VIVO                                         '

CONSTANT   KLC = .050   $'First order chamber loss [Lin fraction/h]    '
CONSTANT   KS = 100000. $'Suppression rate constant for metabolism     '
CONSTANT AVBW = 38.0    $'Average BW of mice=Tot W/n  [g]              '
 BW = AVBW/1000         $'Average body weight per mouse [kg]           '

CONSTANT   QPC = 30.00   $'Alveolar ventilation rate [l/h]             '
CONSTANT   QCC = 16.5    $'Cardiac output [l/h]                        '
 QLC = 0.24 - QGC
CONSTANT   QGC = .175  $'Fractional blood flow to gut                  '
CONSTANT   QFC = .05   $'Fractional blood flow to fat                  '
CONSTANT   QSC = .238  $'Fractional blood flow to slow                 '
CONSTANT   QRC = .472  $'Fractional blood flow to rapid                '

CONSTANT   VLC = .05   $'Fraction liver tissue                         '
CONSTANT   VGC = .033  $'Fraction gut tissue                           '
CONSTANT   VSC = .558  $'Fraction slow tissue                          '
CONSTANT   VRC = .031  $'Fraction rapid tissue                         '
CONSTANT   VFC = .1    $'Fraction fat tissue                           '

'         PARAMETERS FOR ETHANE                                        '
CONSTANT   PLA = 0.828   $'Liver/air partition coefficient             '
CONSTANT   PGA = 0.996   $'Gut/air partition coefficient               '
CONSTANT   PFA = 2.444   $'Fat/air partition coefficient               '
CONSTANT   PSA = 0.979   $'Slowly perfused tissue/air partition        '
CONSTANT   PRA = 0.996   $'Richly perfused tissue/air partition        '
CONSTANT   PEB = 1.305   $'Blood/air partition coefficient             '

PEL=PLA/PEB  $'Liver/blood partition coefficient                       '
PEG=PGA/PEB  $'Gut/blood partition coefficient                         '
PEF=PFA/PEB  $'Fat/blood partition coefficient                         '
PES=PSA/PEB  $'Slow/blood partition coefficient                        '
PER=PRA/PEB  $'Rich/blood partition coefficient                        '

CONSTANT   BACKE=0.     $'Background ethane concentration [ppm]        '
CONSTANT   MEW = 30.    $'Molecular weight Et [g/mol]
'
CONSTANT   VMEXC=0.286  $'Maximum velocity of metabolism [mg/h-1kg]    '
CONSTANT   KEM = 0.51   $'Michaelis-Menten constant [mg/L]             '
CONSTANT   KEFC= 2.786  $'First order metabolism rate constant[1/h-1kg]'
CONSTANT   NRATS= 5.    $'Number of mice [for closed chamber]          '
CONSTANT   VCHC = 0.745 $'Volume of closed chamber [L]                 '
CONSTANT   SODA =0.005  $'Volume of soda lime [L]                      '

'         PARAMETERS FOR P-Ox                                          '
CONSTANT   BAB = 0.99    $'Fraction absorbed from i.p. to portal blood '
CONSTANT   FAB = 0.0001 $'Fraction absorbed from i.p. directly to fat  '
'                        Note: (BAB + FAB) < 1.                        '

'Carbon Tetrachloride - specific constants          '
CONSTANT   PLCC = 3.14  $'Liver/blood partition coefficient            '
```

```
CONSTANT    PFCC = 79.4  $'Fat/blood partition coefficient                '
CONSTANT    PRCC =  3.14 $'Richly perfused tissue/blood partition         '
CONSTANT    PBCC =  4.52 $'Blood/air partition coefficient                '
CONSTANT    PSCC = 2.43      $'Slowly perfused tissue/blood partition     '

CONSTANT    MWCC =153.82     $'Molecular weight P-Ox [g/mol]              '
CONSTANT    DOSE = 0.        $'Dose of active P-Ox [mg/kg]                '
'Estimate of initial concentration of chemical in the liver [mg/L]       '
           CL0 = DOSEIP/VLC
CONSTANT   KAIP = 1.45         $'First order i.p. uptake [1/h]            '
CONSTANT   DOSEIP = 1500.      $'i.p. dose [mg/kg]                        '
           DIP = DOSEIP*BW     $'i.p. dose per animal [mg]                '
CONSTANT   PDOSEC= 0.          $'Oral dose [mg/kg]                        '
           DOSEC = PDOSEC*BW   $'p.o. dose per animal [mg]                '
CONSTANT   KAC = 1.            $'Oral uptake rate [1/hr]
'
CONSTANT   IVDOSC = 0.         $'i.v. dose [mg/kg]
'
CONSTANT   CONCC =0.           $'Inhaled concentration [ppm]              '

'Metabolic constants for CCl4 '
CONSTANT VMAXCC=0.65 $'Maximum velocity of metabolism [mg/h-1kg]         '
CONSTANT   KMC = 0.25 $'Michaelis-Menten constant CCl4 [mg/L]            '
CONSTANT   KFCC= 0.0  $'First order metabolism rate constant [1/h-1kg]   '

'Pharmacokinetic transfer constants fitted                               '
CONSTANT    k10 = 0.3   $'Pharmacokinetic transfer micro-constant [1/h]  '
CONSTANT   alpha= 1.5   $'Pharmacokinetic macro-constant [1/h]           '
CONSTANT    beta= 1.6   $'Pharmacokinetic macro-constant [1/h]           '

CONSTANT   EFFE =0.001  $'Efficiency of ethane generation [molar ratio]  '

'    Inhalation P-Ox Exposure definition                                 '
IF (CC) RATS = NRATS                  $'Closed chamber simulation        '
IF (CC) KL = KLC

IF (.NOT.CC) RATS = 0.                $'Open chamber simulation          '
IF (.NOT.CC) KL = 0.
'Turn off chamber losses so concentration remains constant               '

AI0C = CONCC*VCH*MWCC/24450.  $'Initial amount of P-Ox in chamber [mg]   '

'         PARAMETERS FOR CLOSED CHAMBER                                  '
CONE= BACKE
VCH = VCHC-(RATS*BW)-SODA     $'Net chamber volume [L]                   '
AEI0 = CONE*VCH*MEW/24450.    $'Initial amount of E in chamber [mg]      '

 '                  INITIALIZATION                                       '
 'RESETS INITIAL CONDITIONS BEFORE PEROXIDATION                          '
 CONSTANT ACTLOS=0.           $'activator loss                           '
 CONSTANT AUTOX =0.           $'autooxidation                            '
 CONSTANT PXREDG=0.           $'Hydroperoxides red. by GSH peroxidase'
 CONSTANT PXLUF =0.00199      $'L-Hydroperoxides formed                  '
 CONSTANT PXHUF =0.0053       $'H-Hydroperoxides formed                  '
 CONSTANT PXREM =0.           $'accumulated remaining Hydroperoxides '
 CONSTANT TPX   =0.           $'accumulated total Hydroperoxides formed'
 CONSTANT ILR   =0.           $'rate of inducer loss = 0.                '
 CONSTANT   CL = 0.           $'no inducer                               '
 'Reset output arrays at initialization                                  '
 ETH = 0.
 CONC= 0.
```

```
'     Scaled parameters for mouse                                          '

       QC = QCC*BW**0.74
       QP = QPC*BW**0.74
       QL = QLC*QC
       QG = QGC*QC
       QF = QFC*QC
       QS = 0.24*QC-QF
       QR = 0.76*QC-QL-QG
       QLB= QL+QG
       VL = VLC*BW
       VG = VGC*BW
       VF = VFC*BW
       VS = 0.82*BW-VF
       VR = 0.101*BW-VL-VG
     VMEX = VMEXC*BW**0.7
      KEF = KEFC/BW**0.3
      VEK = VMEXC/KEM
   VMAXC4 = VMAXCC*BW**0.7
     KFC4 = KFCC/BW**0.3


INTEGER DAY

'     Repeated gavage dosing with P-Ox                                     '
      tstop= (days+PDAYS)*24.
       CINT= tstop/points
        DAY=-1.  $'TO START GAVAGE ON MONDAY -1, TUES 0, WEDN 1, ETC       '

END                           $'End of Initial                             '

DYNAMIC

'     GAV = FEED MICE p.o. with P-Ox YES=1, NO=0.                          '
DISCRETE CAT1
       INTERVAL CAT = 24.        $'EXECUTE CAT1 EVERY 24 hr                 '
                DAY=DAY+1
       IF(DAY.GT.DAYS) GOTO OUT
       IF(MOD(DAY,7).GE.5) GOTO OUT
                GAV = 1.         $'GAVAGE = YES                             '
       SCHEDULE CAT2 .AT. T+0.01  $'SCHEDULE END OF GAVAGE                  '
                OUT.. CONTINUE
END    $'END OF CAT1                                                        '

DISCRETE CAT2
                GAV = 0.         $'GAVAGE = NO                              '
END    $'END OF CAT2                                                        '

 ALGORITHM IALG = 2              $'Gear stiff method                        '
DERIVATIVE
'-------------------------------------------------------------------------'
'             <<<<MODULE LOCAL DOSE OF P-Ox>>>>                           '

'Estimate of actual conc. of chemical in the liver CL(C)[mg/L] by two-     '
'compartment open-system classic pharmacodynamic CPK sub-model as CL.      '
'Alternatively, CL(C) is calculated continuously by PBPK sub-model as      '
'CLC'
'- - - - - - - - - - - - - - - - - - - - - - - - - - - - - - - - - - - - -'
'                   <<<<SUB-MODEL CPK>>>>                                '

      CL = CL0*k10*(exp(-beta*t)-exp(-alpha*t))/(alpha - beta)
```

```
'- - - - - - - - - - - - - - - - - - - - - - - - - - - - - - - - -'
'                  <<<<SUB-MODEL PBPK FOR P-Ox>>>>                  '

'Includes code for suppression of metabolism                          '
IVRC = IVDOSC*BW/TINF

'    i.p. dosing with P-Ox                                              '
 RMRIP = -KAIP*MRIP $'Rate of change of amount in i.p. cavity [mg/h]   '
  MRIP = INTEG(RMRIP,DIP) $'Amount of toxicant in i.p. cavity [mg]      '

'  AIP = amount of P-Ox absorbed from i.p.                              '
  RAIP = KAIP*MRIP  $'Rate absorption from i.p. cavity [mg/h]           '
   AIP = DIP - MRIP  $'Amount of toxicant absorbed from i.p. [mg]       '

'      CIC = Concentration in inhaled air [mg/L]                        '
    CIZONE = RSW((T.LT.TCHNG).OR.CC,1.,0.)
      RAIC = RATS*QP*(CAC/PBCC-CIC) - (KLC*AIC)
       AIC = INTEG(RAIC,AIOC)
       CIC = AIC/VCH*CIZONE
        CP = CIC*24450./MWCC

'   Repeated gavage dosing with P-Ox                                    '

'      MRC = Amount remaining in stomach [mg]                           '
      RMRC = gav*dosec/tinf - raoc
       MRC = integ(rmrc,0.)

'        AOC = total mass input from stomach                            '
        RAOC = kac*mrc
         AOC = integ(raoc,0.)

'       AGC = Amount in gut [mg]                                        '
        RAGC = QG*(CAC-CVGC)     $'This is in addition to RAOC          '
         AGC = INTEG(RAGC,0.)
        CVGC = AGC/(VG*PRCC)
         CGC = AGC/VG

'      CAC = Concentration in arterial blood [mg/L]                     '
       CAC = (QC*CVC+QP*CIC)/(QC+(QP/PBCC))
     AUCBC = INTEG(CAC,0.)

'      AXC = Amount exhaled [mg]                                        '
       CXC = CAC/PBCC
    CXPPMC = (0.7*CXC+0.3*CIC)*24450./MWCC
      RAXC = QP*CXC
       AXC = INTEG(RAXC, 0.)

'      ASC = Amount in slowly perfused tissues [mg]                     '
      RASC = QS*(CAC-CVSC)
       ASC = INTEG(RASC,0.)
      CVSC = ASC/(VS*PSCC)
       CSC = ASC/VS

'      ARC = Amount in rapidly perfused tissues [mg]                    '
      RARC = QR*(CAC-CVRC)
       ARC = INTEG(RARC,0.)
      CVRC = ARC/(VR*PRCC)
       CRC = ARC/VR

'      AFC = Amount in fat tissue [mg]                                  '
```

```
      RAFC = QF*(CAC-CVFC) + (FAB*RAIP)
       AFC = INTEG(RAFC,0.)
      CVFC = AFC/(VF*PFCC)
       CFC = AFC/VF

'       ALC = Amount in liver tissue [mg]                                    '
       RALC = QL*(CAC-CVLC)+QG*(CVGC-CVLC)+raoc-RAMC+(BAB*RAIP)
        ALC = INTEG(RALC,0.)
       CVLC = ALC/(VL*PLCC)
        CLC = ALC/VL

'      AMC = Amount metabolized [mg]                                         '
      RAMC = (VMAXC4*CVLC)/(KMC+CVLC) + KFC4*CVLC*VL
       AMC = INTEG(RAMC, 0.)
       ambc= amc/bw

'-----------------------------------------------------                      '
'      IVC = Intravenous infusion rate [mg/hr]                               '
       IVC = IVRC*(1.-step(tinf))

'      CVC = Mixed venous blood concentration P-Ox [mg/L]                    '
CVC=(QF*CVFC+(QL+QG)*CVLC+QS*CVSC+QR*CVRC+IVC+RAIP*(1-(BAB+FAB)))/QC

'   CTMASS = mass balance of P-Ox [mg]                                       '
    CTMASS = AFC+ALC+ASC+ARC+AMC+AXC+AGC
    cbal   = aoc-ctmass     $'gavage, repeated; mass bal'
      cball=   mrc-ctmass
'   CDOSEX = Net amount P-Ox absorbed [mg]                                   '
    CDOSEX = AIC+AOC+IVC*TINF+AIP
    BWCC = CDOSEX/bw
    MOLCC= BWcc/MWCC       $'Milimoles P-Ox absorbed [mmoles/kg]             '

'^^^^END OF PBPK SUB-MODEL FOR P-Ox^^^^^^^^^^^^^^^^^^^^^^^^^^^^^^^^^^^^^^^^'

'- - - - - - - - - - - - -LINK - - - - - - - - - - - - - - - - - - -'
'    Link with local concentration of P-Ox:                                  '
'Switch interlinking with PBPK or CPK yields normalized concentration        '
'in liver, compatible with slices [mcromole/0.1 g]
'
    IND1 = (CL*CPK + CLC*PBPK)/(MWCC*10)    $'MWCC * 10 = 1538.2             '

A=CL/(MWCC*10)
B=CLC/(MWCC*10)
AUCA = INTEG(A,0)
AUCB = INTEG(B,0)
PROCEDURAL
if (IND1.LE.0.) IND1=0.0  $'Prevents from attempt SQRT negative value'
END                       $'End of procedural                                '
 '- - - - - - - - - - - - - - - - - - - - - - - - - - - - - - - - - - - - '

 '             <<<<MODULE LIPID PEROXIDATION>>>>                           '

PROCEDURAL
IF (IND1.GE.CL0) IND1 = CL0/(MWCC * 10)
IF (LPUFRE.LE.0) LPUFRE = 0.
IF (HPUFRE.LE.0) HPUFRE = 0.
IF (ACTLOS.GE.ACTEF)  ACTLOS = ACTEF
IF (ANOXRE.LE.1.e-10) ANOXRE = 1.e-10
IF (GSHREM.LE.0) GSHREM = 0.
IF (INDLOS.GE.INDEF)  INDLOS = INDEF
IF (PXREDA.GE.TPX) PXREDA = TPX
```

```
END     $'End of procedural                                                    '

'****************BBPB SUB-MODEL FOR LIPID PEROXIDATION**********'
'-------------------------------------------------------------'
 '#s Corresponding to equations in Byczkowski et al. (1996)     '
 'This part has been calibrated in vitro in mouse liver slices  '
'-------------------------------------------------------------'
 '1. Remaining polyunsaturated fatty acids [micromol/0.1gliv]   '

 LPUFRE = LPUF - PXLUFA - AUTOXA/2
 HPUFRE = HPUF - PXHUFA - AUTOXA/2

 '2. Effective activator [micromoe/0.1 g liver]                 '

 ACTEF =  ACT1*ACACT1 + ACT2*ACACT2

 '3. Activator loss [micromole/0.1 g liver]                     '

 ACTLOS = ACTEF*ACTDGF*TPX

 '4. Remaining activator [micromole/0.1 g liver]                '

 ACTREM = (ACTEF - ACTLOS)*exp(-ACR*INDREM*t)

 '5. Effective inducer [micromole/0.1 g liver]                  '

 INDEF = SQRT(IND1*PTIND1) + IND2*PTIND2

 '6. Remaining inducer [micromole/0.1g liv]                     '

 INDREM = INDEF - INDLOS

 '6.a. Inducer loss rate [micromol/0.1 g liver/hr]              '

 ILR = INDEF*INDLF

 '7. Activated inducer [micromol/0.1 g liver]                   '

 ACTIND = INDREM*ACTREM

 '8. Effective antioxidant [micromol/0.1g liver]                '

 ANOXEF = ANOX1*EFANO1 + ANOX2*EFANO2 + ANOX3*EFANO3

 '9. Remaining antioxidant [mcromol/0.1 g]                      '

 ANOXRE = ANOXEF - ANOXEF*TPX*ANOXUF + ANREG*exp(-ANOXR*t)

 '10.Hydroperoxides formed by action of activated inducer on    '
 '    PUFA [micromol/0.1 g liver/hr]                            '

 PXLUF = LPUFRE*PXZLUF*ACTIND*PXRATE/ANOXRE
 PXHUF = HPUFRE*PXZHUF*ACTIND*PXRATE/ANOXRE

 '12.Autooxidation [micromole/0.1 g liver/hr]                   '

 AUTOX = (LPUFRE + HPUFRE)*AUTOXF*TPX/ANOXRE

 '14.Accumulated total hydroperoxides formed [mcmol/0.1 g liver]'
```

```
TPX = AUTOXA + PXLUFA + PXHUFA + PHYSPX

'15.Remaining glutathione [micromol/0.1 g liver]                '

GSHREM = GSH - PXREDA

'16.Hydroperoxides reduced by glutathione peroxidase           '
'   [micromol/0.1 g liver/hr]                                  '

PXREDG = PXREM*GPENZA*GSHREM*PXREDF

'18.Accumulated remaining hydroperoxides [micromole/0.1 g liv.]'
'

PXREM = TPX - PXREDA

'19.Amount of TBARS from accumulated remaining hydroperoxides  '
' [micromol/0.1 g liver]                                       '

TBARS = PXREM*PXTTBA + BCKGD

'   Inducer lost over time [micromol/0.1 g liver]              '

INDLOS = INTEG(ILR,0.)

'11.Accumulated hydroperoxides formed by action of activated   '
'   inducer on PUFA [micromole/0.1 g liver]                    '

PXLUFA = INTEG(PXLUF, 0.)

PXHUFA = INTEG(PXHUF, 0.)

'13.Accumulated autooxidation [micromol/0.1 g liver]           '

AUTOXA = INTEG(AUTOX, 0.)

'17.Accumulated hydroperoxides reduced by glutathione          '
'   [micromole/0.1 g liver]                                    '

PXREDA = INTEG(PXREDG, 0.)
'- - - - - - - - - - - - - - - - - - - - - - - - - - - - - - - '
'^^^^^End of BBPD Sub-model for lipid peroxidation^^^^^^^^^^^^^^^'

'- - - - - - - - - - - - - -LINK- - - - - - - - - - - - - - - '
'Link with Accumulated Remaining Hydroperoxides produced in the liver  '

'Assumed lipid peroxidation in the liver only, evoked by P-Ox
concentration'
'Lipid peroxidation is driven by hydroperoxides generated by free      '
'radicals depending on SQRT of local concentration of P-Ox in liver    '

ETH = PXREM*EFFE   $'Molar Amount of ethane produced [mcM/0.1 g liver]'

'Rate of evolution of ethane produced in the liver [mg E/hr/mouse]     '

                      REOX=(ETH*VL*300)/(t+1e-12)
'REOX = f(SQRT(RPOX))'
'300=MEW/1000/0.0001 over time prevented to start from dividing by 0   '
'- - - - - - - - - - - - - - - - - - - - - - - - - - - - - - - - - - - '

'           <<<<MODULE ETHANE EXHALATION>>>>                          '
```

```
'This part has been calibrated in mice in vivo                          '

'****PBPD SUB-MODEL FOR ETHANE*****************************************'
'      CEI = Concentration in inhaled air (mg/L)                        '
      REAI = RATS*QP*(CEA/PEB-CEI)-(KL*AEI)
       AEI = INTEG(REAI,AEI0)                          $ 'Chamber       '
       CEI = AEI/VCH                                   $ 'With N mice   '
       CEP = CEI*24450./MEW     $'concentration in closed chamber       '

'-------------------------------------------------                       '
'      CEA = Concentration in arterial blood [mg/L]                     '
       CEA = (QC*CEV+QP*CEI)/(QC+(QP/PEB))

'      AEX = Amount exhaled per mouse [mg]                              '
       CEX = CEA/PEB
    CXEPM = (0.7*CEX+0.3*CEI)*24450./MEW
      REAX = QP*CEX
       AEX = INTEG(REAX,0.)

'      AES = Amount in slowly perfused tissues per mouse [mg]           '
      REAS = QS*(CEA-CEVS)
       AES = INTEG(REAS,0.)
      CEVS = AES/(VS*PES)
       CES = AES/VS

'      AER = Amount in rapidly perfused tissues per mouse [mg]          '
      REAR = QR*(CEA-CEVR)
       AER = INTEG(REAR,0.)
      CEVR = AER/(VR*PER)
       CER = AER/VR

'      AEF = Amount in fat tissue per mouse [mg]                        '
      REAF = QF*(CEA-CEVF)
       AEF = INTEG(REAF,0.)
      CEVF = AEF/(VF*PEF)
       CEF = AEF/VF

'      AEG = Amount in gut tissue per mouse [mg]                        '
      REAG = QG*(CEA-CEVG)
       AEG = INTEG(REAG,0.)
      CEVG = AEG/(VG*PEG)
       CEG = AEG/VG

'      AEL = Amount in liver tissue per mouse [mg]                      '
      REAL = QL*(CEA-CEVL)+QG*(CEVG-CEVL)-REAM+REOX
       AEL = INTEG(REAL,0.)
      CEVL = AEL/(VL*PEL)
       CEL = AEL/VL

'      AEM = Amount metabolized per mouse w/suppression (KS) [mg]       '
      REAM = (VMEX*CEVL)/(KEM+CEVL*(1+CEVL/KS)) + KEF*CEVL*VL $'[mg/h] '

       AEM = INTEG(REAM,0.)                          $'Amount [mg]      '

'      CEV = Mixed venous blood concentration per mouse [mg/L]          '
       CEV = (QF*CEVF+ (QL+QG)*CEVL+ QS*CEVS+ QR*CEVR)/QC

'AMOUNT INHALED PER MOUSE                                               '
       REINH = QP*CEI
       AEINH = INTEG(REINH,0)
```

```
'TMESS = MASS BALANCE PER MOUSE                                              '
       TMESS = (AES+AER+AEF+AEM+AEL+AEX+AEG)
       BEL = AEINH - TMESS
'^^^^END OF SUB-MODEL FOR ETHANE^^^^^^^^^^^^^^^^^^^^^^^^^^^^^^^^^^^^^^^^^^^^'
'-------------------------------------------------------------------------'
 TERMT(T.GE.TSTOP)            $'Termination at TSTOP                        '

END                           $'End of derivative                          '
END                           $'End of dynamic                             '
'^^^^^^^^^^^^^^^^^^^^^^^^^^^^^^^^^^^^^^^^^^^^^^^^^^^^^^^^^^^^^^^^^^^^^^^^^^'
TERMINAL                     $'Resets parameters to initial values'
ACTREM = ACTEF
INDREM = INDEF
ANOXRE = ANOXEF
'Save arrays of dependent variable'
 ETH = CEP
CONC = Ind1
 END                          $'End of terminal                            '
'-------------------------------------------------------------------------'
^^^^END OF PBPD SUB-MODEL FOR P-OX-INDUCED LIPID PEROXIDATION^^^^'

END                           $'End of program                             '
*************************************************************************
```

- **Command files for CCl_4 and TCE**

PBPD Sub-Model *.CMD FILE for CCl_4

```
'ETHANE.CMD'
'GAS UPTAKE/EXHALATION DATA FOR ETHANE IN MICE'

PREPAR T,'ALL'
SET GRDCPL=.F.    $'Turns off grid lines'

PROCED CONDIT
'TABLE 3: CONDITIONS FOR MICE'
SET KLC=0.05, KS=100000.,POINTS=300.
SET PLA=0.8285, PGA=0.996, PFA=2.444, PRA=0.996
SET PSA=0.979, PEB=1.305, EFFE=0.001
SET MEW=30., AVBW=31.
SET VMEXC=0.286, KEM=0.51, KEFC=2.786
SET NRATS=5, VCHC=0.745, SODA=0.005
SET QPC=30.0, QCC=16.5
DISPLAY QPC,QCC,VMEXC,KEM,KEFC,PEB,PLA,PGA,PFA,PSA
END

PROCED FIG15
'Ethane Uptake from Closed Chamber 1 ppm'
SET TITLE = 'ETHANE UPTAKE'
SET BACKE=1.227, DOSEIP=0.
SET KLC=.05, KS=100000.,
SET PLA=0.8285, PGA=0.996, PFA=2.444, PRA=0.996
SET PSA=0.979, PEB=1.305
SET MEW=30., DAYS=0.125
SET VMEXC=0.286, KEM=0.51, KEFC=2.786
SET NRATS=4, VCHC=0.745, SODA=0.005
SET QPC=30.0, QCC=16.5, AVBW=31.

DATA
T              CEP
0.0             .       INITIAL
```

```
0.08300         0.988875
0.17000         0.966695
0.25000         0.961003
0.33000         0.903836
0.50000         0.822943
0.75000         0.743472
1.00000         0.946910
1.25000         0.599756
1.50000         0.564610
1.75000         0.530173
2.00000         0.387864
2.25000         0.443700
2.50000         0.384679
2.75000         0.348181
3.00000         0.311571

END $'END OF DATA'
START
PLOT CEP
END

PROCED CONDCCL
'TABLE 1&2: CHEMICAL-SPECIFIC CONDITIONS FOR LIPID PEROXIDATION BY CCl4'
SET PTIND1=4408., ACR=0.025,
SET k10=0.3,alpha=1.5,beta=1.6,KAIP=1.45
SET ACTDGF=1.75, INDLF=0.0001,MWCC=153.8
SET ANREG=0.0007, ANOXR=0.001
END

PROCED FIG17A
'Ethane Exhalation after CCl4 0.075 g/kg'
SET TITLE = 'ETHANE EXHALATION AFTER CCl4'
PREPAR t,'ALL',CL
SET DAYS=0.083333, NRWITG=.F.
SET BACKE=0.,POINTS=300,AVBW=32.82
SET DOSEIP=75.

'[h]             [ppm]'
DATA
T               CEP
0.              0.
0.0833          0.027758
0.166667        0.081802
0.25            0.057029
0.333333        0.030957
0.416667        0.019462
0.5             0.04063
0.75            0.046445
1.              0.035008
1.25            0.097736
1.5             0.120978
1.75            0.121889
2.              0.184791
END $'END OF DATA'
START

PLOT CEP,'lo'=0.,'hi'=0.25,'xhi'=2.2
END         $'End of file'

PROCED FIG17B
'Ethane Exhalation after CCl4 0.15 g/kg'
```

```
SET TITLE = 'ETHANE EXHALATION AFTER CCl4'
PREPAR t,'ALL',CL
SET DAYS=0.083333, NRWITG=.F.,
SET BACKE=0.,POINTS=200,AVBW=32.56
SET DOSEIP=150.

'[h]          [ppm]'
DATA
T             CEP
0.            0.
0.0833        0.
0.166667      0.
0.25          0.010312
0.333333      0.043063
0.416667      0.071015
0.5           0.020494
0.75          0.107916
1.            0.089671
1.25          0.076225
1.5           0.099269
1.75          0.076916
2.            0.042414
END $'END OF DATA'
START

PLOT CEP,'lo'=0.,'hi'=0.25,'xhi'=2.2
END         $'End of file'

PROCED FIG17C
'Ethane Exhalation after CCl4 0.3 g/kg'
SET TITLE = 'ETHANE EXHALATION AFTER CCl4'
PREPAR t,'ALL',CL
SET DAYS=0.083333, NRWITG=.F.,
SET BACKE=0.,POINTS=200,AVBW=38.
SET DOSEIP=300.

'[h]          [ppm]'
DATA
T             CEP
0.            0.
0.0833        0.
0.166667      0.038776
0.25          0.072132
0.333333      0.070974
0.416667      0.123789
0.5           0.096211
0.75          0.109947
1.            0.097474
1.25          0.092724
1.5           0.073632
1.75          0.110104
2.            0.095158
END $'END OF DATA'
START

PLOT CEP,'lo'=0.,'hi'=0.25,'xhi'=2.2
END         $'End of file'

PROCED FIG17D
'Ethane Exhalation after CCl4 1.5 g/kg'
SET TITLE = 'ETHANE EXHALATION AFTER CCl4'
```

```
PREPAR t,'ALL',CL
SET DAYS=0.083333, NRWITG=.F.,
SET BACKE=0.,POINTS=300,AVBW=31.8
SET DOSEIP=1500.

'[h]          [ppm]'
DATA
T           CEP
0.          0.
0.0833      0.
0.166667    0.
0.25        0.065464
0.333333    0.090988
0.416667    0.027442
0.5         0.059182
0.75        0.170162
1.          0.194608
1.25        0.148473
1.5         0.175496
1.75        0.132515
2.          0.182836
END $'END OF DATA'
START

PLOT CEP,'lo'=0.,'hi'=0.25,'xhi'=2.2
END         $'End of file'

PROCED FIG18
'Ethane Exhalation after CCl4 1.5, 0.3, 0.15, 0.075 g/kg'
SET TITLE = 'ETHANE EXHALATION AFTER CCl4'
PREPAR /clear t,CEP
SET DAYS=0.083333, NRWITG=.T.,FTSPLT=.T.
SET BACKE=0., POINTS=300.
SET AVBW=35.
SET NRATS=5,
SET DOSEIP=75.
START

SET DOSEIP=150.
START

SET DOSEIP=300.
START

SET DOSEIP=1500.

'[h]         [ppm]'
DATA
T           CEP
0.          0.          INITIAL
0.0833      0.
0.166667    0.
0.25        0.065464
0.333333    0.090988
0.416667    0.027442
0.5         0.059182
0.75        0.170162
1.          0.194608
1.25        0.148473
1.5         0.175496
1.75        0.132515
```

```
2.          0.182836
0.           0.                INITIAL
0.0833       0.
0.166667     0.038776
0.25         0.072132
0.333333     0.070974
0.416667     0.123789
0.5          0.096211
0.75         0.109947
1.           0.097474
1.25         0.092724
1.5          0.073632
1.75         0.110104
2.           0.095158
0.           0.                INITIAL
0.0833       0.
0.166667     0.
0.25         0.010312
0.333333     0.043063
0.416667     0.071015
0.5          0.020494
0.75         0.107916
1.           0.089671
1.25         0.076225
1.5          0.099269
1.75         0.076916
2.           0.042414
0.             0.              INITIAL
0.0833         0.027758
0.166667       0.081802
0.25           0.057029
0.333333       0.030957
0.416667       0.019462
0.5            0.04063
0.75           0.046445
1.             0.035008
1.25           0.097736
1.5            0.120978
1.75           0.121889
2.             0.184791
END $'END OF DATA'
START

PLOT CEP,'lo'=0.,'hi'=0.25,'xhi'=2.2
END         $'End of file'

**************************************************************************
```

PBPD Sub-Model *.CMD FILE for TCE

```
PROCED FIG16
SET TITLE='MICE ETHANE AFTER TCE:2.6,1,0.26g/kg'
SET TSTOP=2., NRWITG=.t.,
PREPAR t,'all'
SET k10=0.03, alpha=0.01, beta=2.0, EFFE=0.001,
SET PBCC=13.4, PLCC=2.03, PFCC=41.3,PRCC=2.03, PSCC=1.
SET MWCC=131.5, VMAXCC=33., KMC=0.25, KFCC=2.4
SET ACTDGF=0.0014, PTIND1=250, KAIP=1., DOSE=2600.,
START
```

```
SET DOSE=1000.
START

SET DOSE=260.

'[h]    [ppm]'
DATA
T        CEP
0.       0.000001    INITIAL
0.25     0.036148
0.333    0.027971
0.75     0.038132
1.       0.042805
1.25     0.045230
1.5      0.093413
1.75     0.075427
2.       0.110495
0.       0.000001    INITIAL
0.1667   0.032907
0.25     0.016053
0.3333   0.026683
1.5      0.026005
1.75     0.056478
2.       0.060730
0.       0.000001   INITIAL
0.75     0.034561

END      $'end of data'
START

PLOT CEP, CLC, 'xhi'=2.
END      $'end of file'
**************************************************************************
```

- **BBDR Sub-Model**

Deterministic and stochastic modules *.CSL FILE

```
PROGRAM: FREE RADICAL DOSE RESPONSE
'A program that calculates amount of free radicals from initial  '
'local concentration of P-Ox and estimates their cellular effect '
'based on Vroegop et al. 1995. Final version for SIMUSOLV 1/10/97'

==       OPEN(UNIT=41,STATUS='NEW',FILE='GRAPHG.FIG')
        WRITE(41,10)
10..FORMAT(' PROC NDATA'/ ' DATA'/ ' PCONC       PROB')

INITIAL              $'Pre-execution section of program          '
CONSTANT ki =0.001   $'rate constant of free radical formation   '
CONSTANT kt =0.002   $'rate constant of free radical recombination'
                     '   ki            kt                       '
                     'C ---> FR + FR ---> Nonradical products     '
'assuming early phase C=C0, and the steady state condition:      '
'dFR/dt = ki*C0 - kt*FR*FR = 0. (const. ki, kt [1/uM*h])         '
CONSTANT kd = 0.075 $'rate constant of receptor inactivation     '
                     '                kd                       '
                     'FR + RECEPTOR ---> RECEPTOR Inactive       '
'assuming first order process for receptor inactivation and      '
'uniform sensitivity fo FR with rate constant kd [100%/uM*h]     '

CONSTANT I0 = 1.     $'Initial concentration of receptors [%*E-2]'
```

```
CONSTANT tp = 1.          $'Time of receptors exposure to FR [h]    '
CONSTANT a  = 0.075       $'Receptor population response constant   '
CONSTANT TSTOP = 2.       $'Length of experiment [h]                '
CONSTANT TME= 1.          $'Time to maximum effect [h]              '
CONSTANT POINTS= 1.       $'Number of communication intervals       '
         Ft = tp/TME      $'Fraction of max time [ratio]            '
'Parameters for dose-response simulation                            '

CONSTANT   CMIN = 100.  $'Starting concentration [uM]               '
CONSTANT   CMAX = 1000. $'Final concentration [uM]                  '
CONSTANT  CDELT = 100.  $'Concentration interval [uM]               '

'Miscellaneous parameters                                          '
 INTEGER I,ND
 CINT = TSTOP/POINTS    $'Interval for saving data to *.RRR file '
 REAL DOS(1000),PROB(1000),DOSC(1000)
'arrays of data saved for plotting PROBability vs DOSe             '
'Initialize variables for dose-response calculation               '
PCONC=0. $  FRad=0. $  Inh=1.0
C0 = CMIN-CDELT
ND = INT((CMAX - CMIN)/CDELT) + 1
I = 1

'Start of dose-response loop                                       '
RESTRT..C0=C0+cdelt
END  $'End of INITIAL section                                      '
'------------------------------------------------------------------'

DYNAMIC $'Beginning of execution section of program                '

'------------------------------------------------------------------'

  FR = SQRT(ki*C0/kt)       $'Concentration of free radicals [uM] '

'^^^^^^^^^^^^^^^^^^^^^^^^DETERMINISTIC MODULE^^^^^^^^^^^^^^^^^^^^^^^^'
  In = I0 * exp(-kd*FR*tp) $'Amount of active receptors remaining'
                            'after exposure to FR for time = tp   '

  TERMT(T.GE.TSTOP)  $'Stop simulation when T >= TSTOP             '
'------------------------------------------------------------------'

END       $'End of dynamic section                                 '

TERMINAL  $'Post-execution section of program                      '

PCONC = C0                  $'Save current concentration [uM]      '
 FRad = FR                  $'Save conc. of free radicals [uM]     '
 Inh  = In                  $'Relative amount of active receptors  '
 DOS(I) = FRad              $'Save I-th FR concentration to array  '
 DOSC(I)=PCONC              $'Save I-th chemical conc. to array    '
 I = I + 1
CALL LOGD(.FALSE.)
IF (C0.lt.cmax) goto restrt    $'Restart to initial unless done   '

'^^^^^^^^^^^^^^^^^^^^^^^^STOCHASTIC MODULE^^^^^^^^^^^^^^^^^^^^^^^^'
'**********************START FORTRAN SUBROUTINE**********************'

PROCEDURAL(PROB = ND,DOS,Ft)
   CALL OMPHI(ND,DOS,PROB,Ft)
 END                        $'End of procedural'
```

```
PROCEDURAL(DOSC,PROB)
       DO 20 K = 1,ND
          WRITE(41,30) DOSC(K),PROB(K)
20..CONTINUE
30..FORMAT( F9.3,2X,F6.4)
       WRITE(41,40)
40..FORMAT('  END')
END
END       $'End of terminal section'
END       $'End of program'

      SUBROUTINE OMPHI(ND,D1,PROB,Ft)
C
C     OMPHI FINDS 1 - CUMMULATIVE GAUSSIAN DISTRIBUTION.
C
      INTEGER I,ND,NDMAX
      PARAMETER(NDMAX=1000)
      REAL M,SD,D,S1,S2,N,Ft,PROB(NDMAX),D1(NDMAX)
C
C     VARIABLE    TYPE    DESCRIPTION
C        I        INTEGER INDEX VARIABLE
C        ND       INTEGER NUMBER OF DOSES
C       NDMAX     INTEGER MAX NUMBER OF DOSES
C        Ft       REAL    FRACTION OF TIME TO MAX EFFECT
C        M        REAL    MEAN OF DOSE
C        SD       REAL    STANDARD DEVIATION OF DOSE
C        D        REAL    DOSE VALUE
C        D1       REAL    ARRAY OF DOSE VALUES
C        PROB     REAL    ARRAY OF RESULTS OF 1 - CUM. GAUSS. DIST.
C
C     CALCULATES THE MEAN AND STANDARD DEVIATION OF DOSE.
C
      S1 = 0.0
      S2 = 0.0
      DO 10 I = 1,ND
         D = D1(I)
         S1 = S1 + D
         S2 = S2 + D*D
   10 CONTINUE
      N = FLOAT(ND)
      M = S1/N
      SD = SQRT((S2 - S1*S1/N)/(N - 1))
C
C     FINDS AND OUTPUTS THE PROBABILITY OF CUMMULATIVE GAUSSIAN.
C
      DO 20 I = 1,ND
         D = D1(I)
         PROB(I) = 1.0 - Ft * PHI(M,SD,D)
   20 CONTINUE
      RETURN
      END
      FUNCTION PHI(M,SD,D)
C
C     PHI FINDS THE CUMMULATIVE GAUSSIAN DISTRIBUTION USING THE
C     ERROR FUNCTION AND THE COMPLEMENTARY ERROR FUNCTION.
C
      REAL M,SD,D,X
C
C     VARIABLE     TYPE     DESCRIPTION
C         M        REAL     INPUT MEAN OF DOSE(D)
C        SD        REAL     INPUT STANDARD DEVIATION OF DOSE(D)
```

```
C          D         REAL      INPUT DOSE
C          X         REAL      INTERNAL VARIABLE
C
      X = (D - M)/SD
      X = X/SQRT(2.0)
      IF (X .GE. 0.0) THEN
         PHI = (1.0 + ERF(X))/2.0
      ELSE
         PHI = ERFC(-X)/2.0
      ENDIF
      RETURN
      END
      FUNCTION erf(x)
C
C     ERF FINDS THE ERROR FUNCTION.
C
C     USES gammp
C
      REAL erf,x,gammp
      if(x.lt.0.)then
        erf=-gammp(.5,x**2)
      else
        erf=gammp(.5,x**2)
      endif
      return
      END
      FUNCTION gammp(a,x)
C
C     GAMMP FINDS THE INCOMPLETE GAMMA FUNCTION P(a,x).
C
      REAL a,gammp,x
C
C     USES gcf,gser
C
      REAL gammcf,gamser,gln
      if(x.lt.0..or.a.le.0.)pause 'bad arguments in gammp'
      if(x.lt.a+1.)then
        call gser(gamser,a,x,gln)
        gammp=gamser
      else
        call gcf(gammcf,a,x,gln)
        gammp=1.-gammcf
      endif
      return
      END
      SUBROUTINE gcf(gammcf,a,x,gln)
C
C     GCF RETURNS THE INCOMPLETE GAMMA FUNCTION Q(a,x) EVALUATED
C     BY ITS CONTINUED FRACTION REPRESENTATION AS GAMMCF.  IT
C     ALSO RETURNS lnGAMMA(a) AS GLN.
C
      INTEGER ITMAX
      REAL a,gammcf,gln,x,EPS,FPMIN
      PARAMETER (ITMAX=100,EPS=3.e-7,FPMIN=1.e-30)
C
C     USES gammln
C
      INTEGER i
      REAL an,b,c,d,del,h,gammln
      gln=gammln(a)
      b=x+1.-a
```

```
      ---
      c=1./FPMIN
      d=1./b
      h=d
      do 11 i=1,ITMAX
        an=-i*(i-a)
        b=b+2.
        d=an*d+b
        if(abs(d).lt.FPMIN)d=FPMIN
        c=b+an/c
        if(abs(c).lt.FPMIN)c=FPMIN
        d=1./d
        del=d*c
        h=h*del
        if(abs(del-1.).lt.EPS)goto 1
11    continue
      pause 'a too large, ITMAX too small in gcf'
1     gammcf=exp(-x+a*log(x)-gln)*h
      return
      END
      SUBROUTINE gser(gamser,a,x,gln)
C
C     GSER RETURNS THE INCOMPLETE GAMMA FUNCTION P(a,x) EVALUATED
C     BY ITS SERIES REPRESENTATION AS GAMSER. IT ALSO RETURNS
C     lnGAMMA(a) AS GLN.
C
      INTEGER ITMAX,n
      REAL a,gamser,gln,x,EPS,ap,del,sum,gammln
      PARAMETER (ITMAX=100,EPS=3.e-7)
C
C     USES gammln
C
      gln=gammln(a)
      if(x.le.0.)then
        if(x.lt.0.)pause 'x < 0 in gser'
        gamser=0.
        return
      endif
      ap=a
      sum=1./a
      del=sum
      do 11 n=1,ITMAX
        ap=ap+1.
        del=del*x/ap
        sum=sum+del
        if(abs(del).lt.abs(sum)*EPS)goto 1
11    continue
      pause 'a too large, ITMAX too small in gser'
1     gamser=sum*exp(-x+a*log(x)-gln)
      return
      END
      FUNCTION gammln(xx)
C
C     GAMMLN RETURNS THE VALUE ln[GAMMA(xx)] FOR xx > 0.
C
      REAL gammln,xx
      INTEGER j
      DOUBLE PRECISION ser,stp,tmp,x,y,cof(6)
      SAVE cof,stp
      DATA cof,stp/76.18009172947146d0,-86.50532032941677d0,
     *24.01409824083091d0,-1.231739572450155d0,
     *.1208650973866179d-2,
```

```
      ---
     *-.5395239384953d-5,2.5066282746310005d0/
      x=xx
      y=x
      tmp=x+5.5d0
      tmp=(x+0.5d0)*log(tmp)-tmp
      ser=1.000000000190015d0
      do 11 j=1,6
        y=y+1.d0
        ser=ser+cof(j)/y
11    continue
      gammln=tmp+log(stp*ser/x)
      return
      END
      FUNCTION erfc(x)
C
C     ERFC FINDS COMPLIMENTARY ERROR FUNCTION.
C
      REAL erfc,x
C
C     USES gammp,gammq
C
      REAL gammp,gammq
      if(x.lt.0.)then
        erfc=1.+gammp(.5,x**2)
      else
        erfc=gammq(.5,x**2)
      endif
      return
      END
      FUNCTION gammq(a,x)
C
C     GAMMQ RETURNS THE INCOMPLETE GAMMA FUNCTION Q(a,x) = 1 -
C     P(a,x).
C
      REAL a,gammq,x
C
C     USES gcf,gser
C
      REAL gammcf,gamser,gln
      if(x.lt.0..or.a.le.0.)pause 'bad arguments in gammq'
      if(x.lt.a+1.)then
        call gser(gamser,a,x,gln)
        gammq=1.-gamser
      else
        call gcf(gammcf,a,x,gln)
        gammq=gammcf
      endif
      return
      END
*******************************************************************************
```

- **Command files and graphics for deterministic and stochastic modules**

BBDR Sub-Model *.CMD FILES

```
'^^^^^^^^^^^^^^^^^^^^DATA FROM LITERATURE^^^^^^^^^^^^^^^^^^^^^^'

'-----------------Steel-Goodwin et al., (1995)---------------'
PROCED FIG8
'kinetics of FRAD production from TCE in precision cut'
'mouse liver slices'
PREPAR 'CLEAR',Pconc, FRad
```

```
SET TITLE = 'BBPD Module: Effect of TCE on Generation of Free Radicals'
SET ki=900,kt=200,cmin=1.,cdelt=1.,cmax=40.,tp=0.333
SET TSTOP=0.333,NRWITG=.T., TME=0.333
'data normalized to physiological background=0.'

'uM/g      uM/g'
DATA
Pconc      FRad
0.         0.
9.85       3.5
18.9       9.4
32.8      11.9
37.15     15.
END            $'end of data'
START
PLOT FRAD,'TAG'='- FR CONCENTR. (um/g)','XTAG'='  - TCE (um/g)'
END            $'end of Linda'

'------------------Vroegop, et al. (1995)--------------------'
PROCED FIG19A
'effect of cumene hydroperoxide on amino acid'
'transport 1 = 19000 cpm'
SET TITLE = 'BBDR: Effect of Cum.OOH on AA Transporter'
PREPAR 'CLEAR',Pconc,Inh
SET cmin=10.,cdelt=10.,cmax=1000.,TP=1.,TSTOP=2.
SET NRWITG=.T.,ki=100,kt=200,kd=0.075, TME=1.

'uM        % Control'
DATA
Pconc      Inh
0.         1.
1.         0.84
3.3        0.91
10.        0.95
33.        0.71
50.        0.69
80.        0.57
130.       0.52
200.       0.47
330.       0.37
1000.      0.22
END              $'end of data'
START
PLOT Inh,'lo'=0., 'TAG'=' - ACT. AA TRANSPORTERS' ...
     'XTAG' = ' - CUM.OOH (uM)'
END              $'end of CHDOSEAA'

PROCED FIG19B
'effect of H2O2 on glucose'
'transporter 1 = 25250 cpm'
SET TITLE = 'BBDR: Effect of H2O2 on Glucose Transporter'
PREPAR 'CLEAR',Pconc,Inh
SET cmin=100.,cdelt=100.,cmax=10000.,TP=1.,TSTOP=2.
SET NRWITG=.T.,ki=18,kt=200,kd=0.1, TME=1.

'uM        % Control'
DATA
Pconc      Inh
0.         1.
3.3        0.92
10.        0.95
```

```
33.       0.89
100.      0.76
330.      0.57
1000.     0.48
3300.     0.22
10000.    0.05
33000.    0.04
END               $'end of data'
START
PLOT Inh,'lo'=0., 'TAG'=' - ACT. GLUC TRANSPORTERS' ...
     'xhi'=10000,'XTAG' = ' - H2O2 (uM)'
END               $'end of H2O2DG'

'--------------Heffetz et al. (1990)--------------------------'
PROCED FIG19C
'effect of H2O2 on protein Tyr phosphatase'
'Tyr Pase activity measured as [32P] remaining'
'in [32P]poly-(Glu,Tyr)'
SET TITLE = 'BBDR: Effect of H2O2 on PTyrPase'
PREPAR 'CLEAR',Pconc,Inh
SET cmin=0.01,cdelt=10.,cmax=500.,TP=0.3333,TSTOP=0.42
SET NRWITG=.T.,ki=18,kt=200,kd=1.,TME=0.3333

'mM       % Control'
DATA
Pconc     Inh
0.          1.
10.       0.4953
20.       0.7143
25.       0.5333
30.       0.5143
50.       0.3143
100.      0.1430
200.      0.1143
300.      0.0476
500.      0.00952
END               $'end of data'
START
PLOT Inh,'lo'=0.,'TAG'=' - ACT. PTPase'...
     'XTAG' = ' - H2O2 (uM)'
END               $'end of H2O2PTP'

'--------------Hecht and Zick (1992)--------------------------'
PROCED FIG19D
'effect of vanadate on protein Tyr phosphatase'
'Tyr Pase activity measured as [32P] remaining'
'in [32P]poly-(Glu,Tyr)'
SET TITLE = 'BBDR: Effect of Vanad. on PTyrPase'
PREPAR 'CLEAR',Pconc,Inh
SET cmin=0.1,cdelt=10.,cmax=1000.,TP=0.5,TSTOP=0.633
SET NRWITG=.T.,ki=18,kt=200,kd=1.,TME=0.7

'uM       % Control'
DATA
Pconc     Inh
0.        1.
1.        0.529
10.       0.456
100.      0.191
1000.     0.294
END               $'end of data'
```

```
START
PLOT Inh,'lo'=0.,'xlo'=0.,'TAG'=' - ACT. PTPase'...
     'XTAG' = ' - VANAD (uM)'
END                $'end of VANADTP'

 '------------------Vroegop, et al. (1995)--------------------'
PROCED FIG20A
'effect of 6-OH dopamine on amino acid transport 1 = 5600 cpm'
PREPAR 'CLEAR',Pconc,Inh
SET TITLE = 'BBDR: Effects of 6-OH Dopamine on AA Transporter'
SET TP=1.,TSTOP=2.,ki=200,kd=0.075,cmin=10.,cdelt=3.,cmax=300.
SET NRWITG=.T.,Kt=200,TME=1.
'uM        % Control'
DATA
Pconc      Inh
0.         1.
10.        1.
20.        0.916
40.        1.
60.        0.916
80.        0.8779
90.        0.8321
100.       0.4351
200.       0.2214
300.       0.2137
END                $'end of data'
START
PLOT Inh,'lo'=0., 'TAG'=' - ACT. AA TRANSPORTERS' ...
     'XTAG' = ' - 6-OH DOPAMINE (uM)'
END                $'end of 6OHDAA'

PROCED FIG20B
'effect of H2O2 on amino acid transport 1 = 6350 cpm'
SET TITLE = 'BBDR: Effect of H2O2 on AA Transporter'
PREPAR 'CLEAR',Pconc,Inh
SET cmin=10.,cdelt=1.,cmax=100.,TP=1.,TSTOP=2.
SET NRWITG=.T.,ki=18,kt=200,kd=0.075, TME=1.

'uM        % Control'
DATA
Pconc      Inh
0.         1.
0.33       1.0
10.        0.86
33.        0.56
55.        0.42
100.       0.34
END                $'end of data'
START
PLOT Inh,'lo'=0., 'TAG'=' - ACT. AA TRANSPORTERS' ...
     'XTAG' = ' - H2O2 (uM)'
END                $'end of H2O2DAA'

PROCED FIG20C
'effect of 6-OH dopamine on mitochondria staining 1 = 0.51 OD'
SET TITLE = 'BBDR: Effect of 6-OH Dopamine on Mitochondria'
PREPAR 'CLEAR',Pconc,Inh
SET kd=0.05,cmin=40.,cdelt=2.,cmax=200.,TP=1.,TSTOP=2.
SET NRWITG=.T.,ki=200,kt=200, TME=2.04

'uM        % Control'
```

```
DATA
Pconc      Inh
0.          1.
10.         1.0
20.         1.0
40.         1.0
60.         0.982
80.         0.927
90.         0.918
100.        0.795
200.        0.498
300.        0.502
500.        0.466
END                 $'end of data'
START
PLOT Inh,'lo'=0., 'TAG'=' - ACT. MITOCHONDRIA' ...
     'XTAG' = ' - 6-OH DOPAMINE (uM)'
END                 $'end of 6OHDMIT'

PROCED FIG20D
'effect of H2O2 on mitochondria staining 1 = 0.49 OD'
SET TITLE = 'BBDR: Effect of H2O2 on Mitochondria'
PREPAR 'CLEAR',Pconc,Inh
SET cmin=10.,cdelt=1.,cmax=100.,TP=1.,TSTOP=2.
SET NRWITG=.T.,ki=18,kt=200,kd=0.05, TME=1.

'uM        % Control'
DATA
Pconc      Inh
0.          1.
0.33        0.97
10.         1.
18.         0.95
33.         0.69
55.         0.55
100.        0.50
END               $'end of data'
START
PLOT Inh,'lo'=0., 'TAG'=' - ACT. MITOCHONDRIA' ...
     'XTAG' = ' - H2O2 (uM)'
END               $'end of H2O2DM'

'--------------Heffetz et al. (1990)-------------------------'
PROCED FIG21A
'effect of pervanadate on protein Tyr phosphatase'
'in the presence of 2 mM H2O2'
'Tyr Pase activity measured as [32P] remaining'
'in [32P]poly-(Glu,Tyr)'
SET TITLE = 'BBDR: Effect of PerVanadate on PTyrPase'
PREPAR 'CLEAR',Pconc,Inh
SET cmin=0.1,cdelt=10.,cmax=1000.,TP=0.333,TSTOP=0.42
SET NRWITG=.T.,ki=18,kt=200,kd=1.,TME=0.333

'uM        % Control'
DATA
Pconc      Inh
0.01   1.
1.          0.9467
10.         0.6
100.        0.3933
1000.       0.1267
```

```
END                $'end of data'
START
PLOT Inh,'lo'=0.,'xlog','xlo'=0.01,'TAG'=' - ACT. PTPase'...
     'XTAG' = ' - PERVAN (uM)'
END                $'end of VANADTP'

'------------------Vroegop, et al. (1995)--------------------'
PROCED FIG21B
'effect of CumOOH on mitochondria staining 1 = 0.49 OD'
SET TITLE = 'BBDR: Effect of Cum.OOH on Mitochondria'
PREPAR 'CLEAR',Pconc,Inh
SET cmin=10.,cdelt=10.,cmax=1000.,TP=1.,TSTOP=2.
SET NRWITG=.T.,ki=100,kt=200,kd=0.05, TME=4.

'uM        % Control'
DATA
Pconc      Inh
0.         1.
3.         1.0
10.        1.
33.        0.95
100.       0.91
330.       1.0
1000.      0.79
END                $'end of data'
START
PLOT Inh,'lo'=0., 'TAG'=' - ACT. MITOCHONDRIA' ...
     'xlog','xlo'=1,'XTAG' = ' - Log CUM.OOH (uM)'
END                $'end of CHDMIT'

PROCED FIG22
'effect of cumene hydroperoxide on glucose'
'transporter 1 = 18300 cpm'
SET TITLE = 'BBDR: Effect of Cum.OOH on Glucose Transporter'
PREPAR 'CLEAR',Pconc,Inh
SET cmin=10.,cdelt=2.,cmax=200.,TP=1.,TSTOP=2.
SET NRWITG=.T.,ki=100,kt=200,kd=0.1, TME=1.

'uM        % Control'
DATA
Pconc      Inh
0.         1.
4.5        0.97
10.        0.90
20.        0.82
45.        0.62
100.       0.46
125.       0.38
150.       0.30
200.       0.19
END                $'end of data'
START
PLOT Inh,'lo'=0., 'TAG'=' - ACT. GLUC TRANSPORTERS' ...
     'XTAG' = ' - CUM.OOH (uM)'
END                $'end of CHDG'

'--------------------Theoretical simulation---------------------'
PROCED FIG26A
'theoretical BBDR deterministic simulation with the range of TCE'
'local doses corresponding to ethane exhalation experiments      '
SET TITLE = 'BBDR: Simulated Effects of TCE on PTyrPase Activity'
```

```
PREPAR 'CLEAR',PCONC, Inh
SET cmin=0.5,cdelt=0.5,cmax=50.,TP=0.5,TSTOP=0.633,TME=0.5
SET NRWITG=.T., ki=900., kt=200., kd=1.
START

'SET TME=1.'
'START'

'SET TME=2.'
'START'
PLOT Inh,'char'=' ','lo'=0.,'tag'='- % ACT. PTPase'...
      'xhi'=50.,'xtag'='- TCE (um/g)'
END          $'end of TCEPTP'

*************************************************************************
```

BBDR Stochastic Array Graphics *.CSL FILE

```
PROGRAM: PLOT FOR GRAFGAUS
'Program allows to plot GRAPHG.CMD files created by GRAFGAUS    '
'Final version 8/28/95                                          '

INITIAL
variable N = 0.    $'defines independent variable N = PCONC      '
CONSTANT Nmax=100.$'defines the maximum PCONC value in plot      '
CONSTANT CINT= 1. $'reports at every whole unit of PCONC         '
CONSTANT FRAD= 0. $'sham value for another independent variable'
END

DYNAMIC
PCONC = N
PROB = 0.          $'sham values for dependent variables        '
ACT = 0.
END

TERMT (N.GE.Nmax)  $'Stop at maximum dose                        '
END
*************************************************************************
```

Output of stochastic module, created by *BBDR Sub-Model: BBDR Array Graphics *.CMD FILE

```
'FIG 19 A'
PROC NDATA
prepar pconc,prob
set title='BBDR: Effect of Cum.OOH on AA Transporter'
set Nmax=1000.
DATA
PCONC        PROB
     0.         1.       INITIAL
  10.000   0.9927
  20.000   0.9883
  30.000   0.9834
  40.000   0.9781
```

50.000	0.9723
60.000	0.9659
70.000	0.9591
80.000	0.9517
90.000	0.9439
100.000	0.9356
110.000	0.9269
120.000	0.9177
130.000	0.9082
140.000	0.8982
150.000	0.8879
160.000	0.8772
170.000	0.8661
180.000	0.8548
190.000	0.8431
200.000	0.8312
210.000	0.8190
220.000	0.8066
230.000	0.7940
240.000	0.7813
250.000	0.7683
260.000	0.7552
270.000	0.7419
280.000	0.7286
290.000	0.7152
300.000	0.7017
310.000	0.6881
320.000	0.6745
330.000	0.6609
340.000	0.6472
350.000	0.6336
360.000	0.6200
370.000	0.6065
380.000	0.5930
390.000	0.5796
400.000	0.5662
410.000	0.5530
420.000	0.5398
430.000	0.5268
440.000	0.5139
450.000	0.5011
460.000	0.4885
470.000	0.4760
480.000	0.4636
490.000	0.4514
500.000	0.4394
510.000	0.4276
520.000	0.4159
530.000	0.4045
540.000	0.3932
550.000	0.3821
560.000	0.3712
570.000	0.3605
580.000	0.3500

```
 590.000   0.3397
 600.000   0.3296
 610.000   0.3197
 620.000   0.3100
 630.000   0.3005
 640.000   0.2913
 650.000   0.2822
 660.000   0.2734
 670.000   0.2647
 680.000   0.2562
 690.000   0.2480
 700.000   0.2400
 710.000   0.2321
 720.000   0.2245
 730.000   0.2170
 740.000   0.2098
 750.000   0.2027
 760.000   0.1958
 770.000   0.1891
 780.000   0.1826
 790.000   0.1763
 800.000   0.1702
 810.000   0.1642
 820.000   0.1584
 830.000   0.1528
 840.000   0.1473
 850.000   0.1420
 860.000   0.1369
 870.000   0.1319
 880.000   0.1271
 890.000   0.1224
 900.000   0.1179
 910.000   0.1135
 920.000   0.1093
 930.000   0.1052
 940.000   0.1012
 950.000   0.0974
 960.000   0.0937
 970.000   0.0901
 980.000   0.0866
 990.000   0.0833
1000.000   0.0800
 END    $'end of data'
 START
 PLOT PROB,'lo'=0,'hi'=1,'xhi'=1000,'xtag'=' -CUM.OOH (uM)'
 END    $'END of file'

'FIG 19 B'
PROC NDATA
prepar pconc,prob
set title='BBDR: Effect of H2O2 on Glucose Transporter'
set Nmax=10000.
DATA
PCONC        PROB
```

0.	1.	INITIAL
100.000	0.9927	
200.000	0.9883	
300.000	0.9834	
400.000	0.9781	
500.000	0.9723	
600.000	0.9659	
700.000	0.9591	
800.000	0.9517	
900.000	0.9439	
1000.000	0.9356	
1100.000	0.9269	
1200.000	0.9177	
1300.000	0.9082	
1400.000	0.8982	
1500.000	0.8879	
1600.000	0.8772	
1700.000	0.8661	
1800.000	0.8548	
1900.000	0.8431	
2000.000	0.8312	
2100.000	0.8190	
2200.000	0.8066	
2300.000	0.7940	
2400.000	0.7813	
2500.000	0.7683	
2600.000	0.7552	
2700.000	0.7419	
2800.000	0.7286	
2900.000	0.7152	
3000.000	0.7016	
3100.000	0.6881	
3200.000	0.6745	
3300.000	0.6609	
3400.000	0.6472	
3500.000	0.6336	
3600.000	0.6200	
3700.000	0.6065	
3800.000	0.5930	
3900.000	0.5796	
4000.000	0.5662	
4100.000	0.5530	
4200.000	0.5398	
4300.000	0.5268	
4400.000	0.5139	
4500.000	0.5011	
4600.000	0.4885	
4700.000	0.4760	
4800.000	0.4636	
4900.000	0.4514	
5000.000	0.4394	
5100.000	0.4276	
5200.000	0.4159	
5300.000	0.4045	

```
5400.000  0.3932
5500.000  0.3821
5600.000  0.3712
5700.000  0.3605
5800.000  0.3500
5900.000  0.3397
6000.000  0.3296
6100.000  0.3197
6200.000  0.3100
6300.000  0.3005
6400.000  0.2913
6500.000  0.2822
6600.000  0.2734
6700.000  0.2647
6800.000  0.2562
6900.000  0.2480
7000.000  0.2400
7100.000  0.2321
7200.000  0.2245
7300.000  0.2170
7400.000  0.2098
7500.000  0.2027
7600.000  0.1958
7700.000  0.1891
7800.000  0.1826
7900.000  0.1763
8000.000  0.1702
8100.000  0.1642
8200.000  0.1584
8300.000  0.1528
8400.000  0.1473
8500.000  0.1420
8600.000  0.1369
8700.000  0.1319
8800.000  0.1271
8900.000  0.1224
9000.000  0.1179
9100.000  0.1135
9200.000  0.1093
9300.000  0.1052
9400.000  0.1012
9500.000  0.0974
9600.000  0.0937
9700.000  0.0901
9800.000  0.0866
9900.000  0.0833

10000.000 0.0800
 END  $'End of data'
 START
 PLOT PROB,'lo'=0,'hi'=1,'xhi'=10000,...
      'xtag'=' -H2O2 (uM)'
 END  $'END of file'
```

```
'FIG 19 C'
PROC NDATA
prepar pconc,prob
set title='BBDR: Effect of H2O2 on PTyrPase'
set Nmax=500.
DATA
PCONC        PROB
      0.       1.      INITIAL
   0.010   0.9959
  10.010   0.9817
  20.010   0.9680
  30.010   0.9525
  40.010   0.9353
  50.010   0.9163
  60.010   0.8958
  70.010   0.8740
  80.010   0.8509
  90.010   0.8269
 100.010   0.8020
 110.010   0.7764
 120.010   0.7503
 130.010   0.7238
 140.010   0.6970
 150.010   0.6702
 160.010   0.6434
 170.010   0.6167
 180.010   0.5902
 190.010   0.5641
 200.010   0.5384
 210.010   0.5131
 220.010   0.4884
 230.010   0.4643
 240.010   0.4409
 250.010   0.4181
 260.010   0.3960
 270.010   0.3747
 280.010   0.3541
 290.010   0.3343
 300.010   0.3153
 310.010   0.2971
 320.010   0.2796
 330.010   0.2629
 340.010   0.2470
 350.010   0.2318
 360.010   0.2174
 370.010   0.2037
 380.010   0.1906
 390.010   0.1783
 400.010   0.1666
 410.010   0.1556
 420.010   0.1452
 430.010   0.1354
 440.010   0.1261
 450.010   0.1174
```

```
 460.010   0.1093
 470.010   0.1016
 480.010   0.0944
 490.010   0.0876
 END      $'End of data'
 START
 PLOT PROB,'lo'=0,'hi'=1.,'xhi'=500,'xtag'=' -H2O2 (uM)'
 END    $'End of file'

'FIG 19 D'
PROC NDATA
prepar pconc,prob
set title='BBDR: Effect of Vanad. on PTyrPase'
set Nmax=1000.
DATA
PCONC        PROB
   0.          1.        INITIAL
   0.100    0.9976
  10.100    0.9930
  20.100    0.9890
  30.100    0.9848
  40.100    0.9803
  50.100    0.9754
  60.100    0.9702
  70.100    0.9646
  80.100    0.9587
  90.100    0.9525
 100.100    0.9460
 110.100    0.9391
 120.100    0.9320
 130.100    0.9246
 140.100    0.9170
 150.100    0.9091
 160.100    0.9011
 170.100    0.8928
 180.100    0.8843
 190.100    0.8756
 200.100    0.8668
 210.100    0.8578
 220.100    0.8487
 230.100    0.8395
 240.100    0.8302
 250.100    0.8207
 260.100    0.8113
 270.100    0.8017
 280.100    0.7921
 290.100    0.7825
 300.100    0.7728
 310.100    0.7631
 320.100    0.7535
 330.100    0.7438
 340.100    0.7342
 350.100    0.7246
 360.100    0.7150
```

370.100	0.7055
380.100	0.6960
390.100	0.6866
400.100	0.6773
410.100	0.6680
420.100	0.6588
430.100	0.6498
440.100	0.6408
450.100	0.6319
460.100	0.6232
470.100	0.6145
480.100	0.6060
490.100	0.5976
500.100	0.5893
510.100	0.5811
520.100	0.5731
530.100	0.5652
540.100	0.5574
550.100	0.5498
560.100	0.5423
570.100	0.5350
580.100	0.5278
590.100	0.5207
600.100	0.5138
610.100	0.5070
620.100	0.5004
630.100	0.4939
640.100	0.4875
650.100	0.4813
660.100	0.4753
670.100	0.4694
680.100	0.4636
690.100	0.4579
700.100	0.4524
710.100	0.4471
720.100	0.4419
730.100	0.4368
740.100	0.4318
750.100	0.4270
760.100	0.4223
770.100	0.4177
780.100	0.4132
790.100	0.4089
800.100	0.4047
810.100	0.4006
820.100	0.3967
830.100	0.3928
840.100	0.3891
850.100	0.3854
860.100	0.3819
870.100	0.3785
880.100	0.3752
890.100	0.3720
900.100	0.3689

```
 910.100   0.3658
 920.100   0.3629
 930.100   0.3601
 940.100   0.3574
 950.100   0.3547
 960.100   0.3521
 970.100   0.3497
 980.100   0.3473
 990.100   0.3450
 END      $'END of data'
 START
 PLOT PROB,'lo'=0,'hi'=1,'xtag'=' -VANAD (uM)'
 END     $'end of file'

'FIG 20 A'
PROC NDATA
Prepar Pconc,Prob
Set title='BBDR: Effect of 6-OH Dopamine on AA Transporter'
Set Nmax=300.
DATA
PCONC        PROB
   0.0     1.  INITIAL
  10.000   0.9849
  20.000   0.9670
  30.000   0.9437
  40.000   0.9154
  50.000   0.8825
  60.000   0.8459
  70.000   0.8060
  80.000   0.7639
  90.000   0.7200
 100.000   0.6752
 110.000   0.6301
 120.000   0.5853
 130.000   0.5412
 140.000   0.4982
 150.000   0.4568
 160.000   0.4172
 170.000   0.3796
 180.000   0.3442
 190.000   0.3109
 200.000   0.2800
 210.000   0.2513
 220.000   0.2249
 230.000   0.2007
 240.000   0.1786
 250.000   0.1585
 260.000   0.1402
 270.000   0.1238
 280.000   0.1090
 290.000   0.0958
 300.000   0.0840
 END       $'End of Data'
 START
```

```
 PLOT PROB,'lo'=0,'hi'=1.,'tag'=' -Act. AA Transp'...
     'xhi'=300, 'xtag'=' - 6-OH DOPAMINE (uM)'
END        $'End of File'

'FIG 20 B'
PROC NDATA
prepar pconc,prob
set title='BBDR: Effect of H2O2 on AA Transporter'
set nmax=100.
DATA
PCONC        PROB
   0.       1.      INITIAL
  10.000   0.9816
  11.000   0.9776
  12.000   0.9732
  13.000   0.9683
  14.000   0.9629
  15.000   0.9570
  16.000   0.9506
  17.000   0.9437
  18.000   0.9362
  19.000   0.9283
  20.000   0.9199
  21.000   0.9110
  22.000   0.9016
  23.000   0.8917
  24.000   0.8814
  25.000   0.8706
  26.000   0.8594
  27.000   0.8478
  28.000   0.8358
  29.000   0.8234
  30.000   0.8107
  31.000   0.7977
  32.000   0.7843
  33.000   0.7707
  34.000   0.7568
  35.000   0.7427
  36.000   0.7284
  37.000   0.7139
  38.000   0.6993
  39.000   0.6845
  40.000   0.6696
  41.000   0.6547
  42.000   0.6396
  43.000   0.6246
  44.000   0.6095
  45.000   0.5944
  46.000   0.5794
  47.000   0.5644
  48.000   0.5494
  49.000   0.5346
  50.000   0.5198
  51.000   0.5052
```

```
 52.000  0.4907
 53.000  0.4764
 54.000  0.4622
 55.000  0.4482
 56.000  0.4344
 57.000  0.4208
 58.000  0.4074
 59.000  0.3943
 60.000  0.3813
 61.000  0.3686
 62.000  0.3562
 63.000  0.3440
 64.000  0.3320
 65.000  0.3203
 66.000  0.3089
 67.000  0.2977
 68.000  0.2868
 69.000  0.2762
 70.000  0.2658
 71.000  0.2557
 72.000  0.2459
 73.000  0.2364
 74.000  0.2271
 75.000  0.2181
 76.000  0.2094
 77.000  0.2009
 78.000  0.1927
 79.000  0.1848
 80.000  0.1771
 81.000  0.1696
 82.000  0.1624
 83.000  0.1555
 84.000  0.1488
 85.000  0.1423
 86.000  0.1360
 87.000  0.1300
 88.000  0.1242
 89.000  0.1186
 90.000  0.1133
 91.000  0.1081
 92.000  0.1031
 93.000  0.0983
 94.000  0.0937
 95.000  0.0893
 96.000  0.0851
 97.000  0.0810
 98.000  0.0772
 99.000  0.0734
100.000  0.0699
END   $'End of data'
START
PLOT PROB,'lo'=0,'hi'=1.,'xhi'=100
END  $'END of file'
```

```
'FIG 20 C'
PROC NDATA
prepar pconc, prob
set title='BBDR: Effect of 6-OH Dopamine on Mitochondria'
SET NMAX=200.
DATA
PCONC       PROB
    0.        1.      INITIAL
  40.000  0.9826
  50.000  0.9672
  60.000  0.9455
  70.000  0.9178
  80.000  0.8852
  90.000  0.8489
 100.000  0.8106
 110.000  0.7720
 120.000  0.7344
 130.000  0.6990
 140.000  0.6667
 150.000  0.6379
 160.000  0.6129
 170.000  0.5917
 180.000  0.5740
 190.000  0.5595
 200.000  0.5478
 END
 START
 PLOT PROB,'lo'=0.,'hi'=1.,'tag'=' -ACT Mito'...
      'xhi'=200., 'xtag'=' -6-OH DOPAMINE (uM)'
 END

'FIG 20 D'
PROC NDATA
prepar pconc,prob
set title='BBDR: Effect of H202 on Mitochondria'
set Nmax=100.
DATA
PCONC       PROB
   0.     1.     INITIAL
  10.000  0.9608
  20.000  0.8800
  30.000  0.7663
  40.000  0.6362
  50.000  0.5061
  60.000  0.3874
  70.000  0.2867
  80.000  0.2059
  90.000  0.1439
 100.000  0.0982
 END    $'end of data'
  START
  PLOT PROB,'lo'=0.,'hi'=1.,'xhi'=100,'xtag'=' -H2O2 (uM)'
  END  $'END of file'
```

```
'FIG 21 A'
PROC NDATA
prepar pconc,prob
set title='BBDR: Effect of PerVanadate on PTyrPase'
set Nmax=1000
DATA
PCONC       PROB
   0.01     1.          INITIAL
   0.100    0.9966
  10.100    0.9902
  20.100    0.9846
  30.100    0.9788
  40.100    0.9724
  50.100    0.9656
  60.100    0.9583
  70.100    0.9505
  80.100    0.9422
  90.100    0.9335
 100.100    0.9244
 110.100    0.9148
 120.100    0.9048
 130.100    0.8945
 140.100    0.8838
 150.100    0.8728
 160.100    0.8615
 170.100    0.8499
 180.100    0.8380
 190.100    0.8258
 200.100    0.8135
 210.100    0.8009
 220.100    0.7882
 230.100    0.7753
 240.100    0.7622
 250.100    0.7490
 260.100    0.7358
 270.100    0.7224
 280.100    0.7090
 290.100    0.6955
 300.100    0.6819
 310.100    0.6684
 320.100    0.6549
 330.100    0.6413
 340.100    0.6278
 350.100    0.6144
 360.100    0.6010
 370.100    0.5877
 380.100    0.5744
 390.100    0.5612
 400.100    0.5482
 410.100    0.5352
 420.100    0.5224
 430.100    0.5097
 440.100    0.4971
 450.100    0.4847
```

460.100	0.4724
470.100	0.4603
480.100	0.4484
490.100	0.4366
500.100	0.4250
510.100	0.4135
520.100	0.4023
530.100	0.3912
540.100	0.3804
550.100	0.3697
560.100	0.3592
570.100	0.3489
580.100	0.3389
590.100	0.3290
600.100	0.3193
610.100	0.3098
620.100	0.3005
630.100	0.2914
640.100	0.2826
650.100	0.2739
660.100	0.2654
670.100	0.2571
680.100	0.2490
690.100	0.2411
700.100	0.2334
710.100	0.2259
720.100	0.2186
730.100	0.2115
740.100	0.2045
750.100	0.1978
760.100	0.1912
770.100	0.1848
780.100	0.1785
790.100	0.1725
800.100	0.1666
810.100	0.1609
820.100	0.1553
830.100	0.1499
840.100	0.1447
850.100	0.1396
860.100	0.1347
870.100	0.1299
880.100	0.1253
890.100	0.1208
900.100	0.1164
910.100	0.1122
920.100	0.1081
930.100	0.1041
940.100	0.1003
950.100	0.0966
960.100	0.0930
970.100	0.0895
980.100	0.0862
990.100	0.0829

```
 END    $'END of data'
 START
 PLOT PROB,'lo'=0.,'hi'=1,'xlog','xlo'=0.01,...
      'xtag'=' -Log PerVan (uM)'
 END   $'End of file'

'FIG 21 B'
PROC NDATA
prepar pconc,prob
set title='BBDR: Effect of Cum.OOH on Mitochondria'
set Nmax=1000.
DATA
PCONC        PROB
   0.1     1.       INITIAL
  10.000   0.9982
  20.000   0.9971
  30.000   0.9959
  40.000   0.9945
  50.000   0.9931
  60.000   0.9915
  70.000   0.9898
  80.000   0.9879
  90.000   0.9860
 100.000   0.9839
 110.000   0.9817
 120.000   0.9794
 130.000   0.9770
 140.000   0.9745
 150.000   0.9720
 160.000   0.9693
 170.000   0.9665
 180.000   0.9637
 190.000   0.9608
 200.000   0.9578
 210.000   0.9548
 220.000   0.9517
 230.000   0.9485
 240.000   0.9453
 250.000   0.9421
 260.000   0.9388
 270.000   0.9355
 280.000   0.9321
 290.000   0.9288
 300.000   0.9254
 310.000   0.9220
 320.000   0.9186
 330.000   0.9152
 340.000   0.9118
 350.000   0.9084
 360.000   0.9050
 370.000   0.9016
 380.000   0.8983
 390.000   0.8949
 400.000   0.8916
```

410.000	0.8882
420.000	0.8850
430.000	0.8817
440.000	0.8785
450.000	0.8753
460.000	0.8721
470.000	0.8690
480.000	0.8659
490.000	0.8629
500.000	0.8599
510.000	0.8569
520.000	0.8540
530.000	0.8511
540.000	0.8483
550.000	0.8455
560.000	0.8428
570.000	0.8401
580.000	0.8375
590.000	0.8349
600.000	0.8324
610.000	0.8299
620.000	0.8275
630.000	0.8251
640.000	0.8228
650.000	0.8206
660.000	0.8183
670.000	0.8162
680.000	0.8141
690.000	0.8120
700.000	0.8100
710.000	0.8080
720.000	0.8061
730.000	0.8043
740.000	0.8024
750.000	0.8007
760.000	0.7990
770.000	0.7973
780.000	0.7957
790.000	0.7941
800.000	0.7925
810.000	0.7911
820.000	0.7896
830.000	0.7882
840.000	0.7868
850.000	0.7855
860.000	0.7842
870.000	0.7830
880.000	0.7818
890.000	0.7806
900.000	0.7795
910.000	0.7784
920.000	0.7773
930.000	0.7763
940.000	0.7753

```
 950.000   0.7743
 960.000   0.7734
 970.000   0.7725
 980.000   0.7717
 990.000   0.7708
1000.000   0.7700
 END      $'END of data'
 START
 PLOT PROB,'lo'=0.,'hi'=1.,'xlog','xlo'=1.,...
      'xtag'=' -Log Cum.OOH (uM)'
END    $'End of file'

'FIG 22'
PROC NDATA
prepar pconc,prob
set title='BBDR: Effect of Cum.OOH on Glucose Transporter'
set Nmax=200.
DATA
PCONC        PROB
   0.      1.        INITIAL
  10.000   0.9792
  20.000   0.9487
  30.000   0.9068
  40.000   0.8553
  50.000   0.7963
  60.000   0.7323
  70.000   0.6656
  80.000   0.5984
  90.000   0.5325
 100.000   0.4692
 110.000   0.4098
 120.000   0.3548
 130.000   0.3048
 140.000   0.2598
 150.000   0.2200
 160.000   0.1850
 170.000   0.1546
 180.000   0.1284
 190.000   0.1061
 200.000   0.0872
 END    $'END of data'
 START
 PLOT PROB,'lo'=0,'hi'=1.,'xtag'=' -Cum.OOH (uM)'
 END       $'END of file'

'FIG 26 B'
PROC NDATA
PREPAR pconc,prob
set title='BBDR: Simulated Effects of TCE on PTyrPase Activity'
set Nmax=50
DATA
PCONC        PROB
   0.500   0.9927
   1.000   0.9883
```

1.500	0.9834
2.000	0.9781
2.500	0.9723
3.000	0.9659
3.500	0.9591
4.000	0.9517
4.500	0.9439
5.000	0.9356
5.500	0.9269
6.000	0.9177
6.500	0.9082
7.000	0.8982
7.500	0.8879
8.000	0.8772
8.500	0.8661
9.000	0.8548
9.500	0.8431
10.000	0.8312
10.500	0.8190
11.000	0.8066
11.500	0.7940
12.000	0.7813
12.500	0.7683
13.000	0.7552
13.500	0.7419
14.000	0.7286
14.500	0.7152
15.000	0.7016
15.500	0.6881
16.000	0.6745
16.500	0.6609
17.000	0.6472
17.500	0.6336
18.000	0.6200
18.500	0.6065
19.000	0.5930
19.500	0.5796
20.000	0.5662
20.500	0.5530
21.000	0.5398
21.500	0.5268
22.000	0.5139
22.500	0.5011
23.000	0.4885
23.500	0.4760
24.000	0.4636
24.500	0.4514
25.000	0.4394
25.500	0.4276
26.000	0.4159
26.500	0.4045
27.000	0.3932
27.500	0.3821
28.000	0.3712

```
  28.500  0.3605
  29.000  0.3500
  29.500  0.3397
  30.000  0.3296
  30.500  0.3197
  31.000  0.3100
  31.500  0.3005
  32.000  0.2913
  32.500  0.2822
  33.000  0.2734
  33.500  0.2647
  34.000  0.2562
  34.500  0.2480
  35.000  0.2400
  35.500  0.2321
  36.000  0.2245
  36.500  0.2170
  37.000  0.2098
  37.500  0.2027
  38.000  0.1958
  38.500  0.1891
  39.000  0.1826
  39.500  0.1763
  40.000  0.1702
  40.500  0.1642
  41.000  0.1584
  41.500  0.1528
  42.000  0.1473
  42.500  0.1420
  43.000  0.1369
  43.500  0.1319
  44.000  0.1271
  44.500  0.1224
  45.000  0.1179
  45.500  0.1135
  46.000  0.1093
  46.500  0.1052
  47.000  0.1012
  47.500  0.0974
  48.000  0.0937
  48.500  0.0901
  49.000  0.0866
  49.500  0.0833
  50.000  0.0800
 END $'End of data'
  START
PLOT PROB,'lo'=0.,'hi'=1.,'xi'=500,'xtag'='-TCE (umol/g liver)'
  END  $'End of file'
**************************************************************************
```